Ollscoil na Gaillimhe
University of Galway

Provided by the author(s) and University of Galway in accordance with publisher policies. Please cite the published version when available.

Title	Properties of electrode-attached biofilms for application to microbial fuel cells
Author(s)	Jana, Partha sarathi
Publication Date	2015-03-26
Item record	http://hdl.handle.net/10379/4926

Downloaded 2024-04-17T16:00:19Z

Some rights reserved. For more information, please see the item record link above.

PROPERTIES OF ELECTRODE-ATTACHED BIOFILMS FOR APPLICATION TO MICROBIAL FUEL CELLS

Thesis Submitted to

National University of Ireland, Galway

For the award of the degree

of

Doctor of Philosophy

by

Partha Sarathi Jana

Under the Guidance of

Prof. Dónal Leech

SCHOOL OF CHEMISTRY

NATIONAL UNIVERSITY OF IRELAND GALWAY

March 2015

Acknowledgments

The research presented in this thesis has been carried out at the Biomolecular Electronics Research Laboratory, School of Chemistry, National University of Ireland Galway. The journey would not have been possible without support and encouragement of a lot of people.

First and foremost, I would like to express my deep sense of gratitude to my supervisor Prof. Dónal Leech, whose expertise; understanding, enthusiasm and patience guided me throughout the course of research. Without his encouragements and selfless help, I could never finish my doctoral work. I could not have imagined having a better advisor and mentor for my Ph.D study.

The second person whom I am very grateful to Prof. Vincent O' Flaherty for his scientific advice and constant support throughout my Ph.D.

My sincere thanks to Dr. Krishna Katuri, Dr. Paul Kavanagh and Dr. Florence Abram for their advice and help during several stages of this research.

I thank the School of Chemistry for their support and Head of the School Prof. Paul Murphy for his scientific support.

I would also like to thank my family for the support they provided me through my entire life and in particular, I must acknowledge my wife, Simrat, without whose love, encouragement and editing assistance, I would not have finished this thesis.

Furthermore, I am thankful to my past and present fellow lab mates: Saravanan, Domhnall, Peter, Rakesh, Isioma who helped me in various stages of my work.

Date 26/03/2015

(Partha Sarathi Jana)

DECLARATION

The thesis entitled ‘PROPERTIES OF ELECTRODE-ATTACHED BIOFILMS FOR APPLICATION TO MICROBIAL FUEL CELLS’ is my own research and has not been submitted for another degree, either at National University of Ireland, Galway or elsewhere.

Signed: Partha Sarathi Jana ----------

(Partha Sarathi Jana)

Symbols and Abbreviations

°C	Degree Celsius
AEM	Anion exchange membrane
APHA	American Public Health Association
BOD	Biochemical oxygen demand
CE	Coulombic efficiency
CEM	Cation exchange membranes
Cm	Centimetre
cm^2	Square centimeter
COD	Chemical oxygen demand
DO	Dissolved oxygen
Do	Oxygen diffusion coefficient
E_0	Standard redox potential
EDX	Energy dispersive x-ray analysis
F	Faraday's constant
g/L	Gram per liter
H	Hour
HRT	Hydraulic retention time
I	Current
Kg	Kilogram
kJ	Kilo joule
kW/m^3	Kilowatt per cubic metre
kΩ	Kilo ohm
mA	Milli ampere
MFC	Microbial fuel cell
mg/L	Milligram per litre
mL	Millilitre
mM	Milli mole
Mol	Mole
ms/cm	Milli siemen/centimeter
mV	Millivolt
mW	Milliwatt

mW/m^2	Milliwatt per square metre
NADH	Nicotinamide adenine dinucleotide
NADPH	Nicotinamide adenine dinucleotide phosphate
OLR	Organic loading rate
P	Power
PEM	Proton exchange membrane
Pt	Platinum
SEM	Scanning electron microscopy
SHE	Standard hydrogen electrode
SLR	Sludge loading rate Time
TS	Total solids
UASB	Up flow anaerobic sludge blanket
V	Voltage
VFA	Volatile Fatty Acid
VS	Volatile solids
VSS	Volatile suspended solids
W/m^3	Watt per cubic metre
Ω	Ohm

Glossary of terms

BOD	Biochemical oxygen demand (BOD) is the amount of dissolved oxygen needed by aerobic biological organisms in a body of water to break down organic material present in a given water sample at certain temperature over a specific time period.
Bioelectricity	Electric potentials and currents produced by living organisms.
COD	Chemical oxygen demand (COD) is a measure of the capacity of water to consume oxygen during the decomposition of organic matter and the oxidation of inorganic chemicals such as ammonia and nitrite.
EAB	The main feature of electroactive bacteria (EAB) is the ability to transfer electron from the microbial cell to an electrode
Genomics	The branch of molecular biology concerned with the structure, function, evolution, and mapping of genomes.
Log phase	The period of growth of a population of cells (as of a microorganism) in a culture medium during which numbers increase exponentially.
OLR	Organic loading rate is defined as the application of soluble and particulate organic matter. It is typically expressed on an area basis as Kg of BOD per unit area, such as Kg $BOD_5/m^3/day$.
Proteome	The proteome is the entire set of proteins expressed by a genome.
Seed sludge	Seed sludge refers to a mass of sludge that contains populations of microorganisms.
SS	Suspended solids (SS) refer to small solid particles which remain in suspension in water as a colloid or due to the motion of the water.
VSS	A volatile suspended solid (VSS) is a water quality measure obtained from the loss on ignition of total suspended solids.

Publications

- P. Jana, K. Katuri, P. Kavanagh, A. Kumar, D. Leech. (2014) 'Charge transport in films of Geobacter sulfurreducens on graphite electrodes as a function of film thickness' Physical Chemistry Chemical Physics'
- P. S. Jana, M. M. Ghangrekar, D. Leech. 'Comparison of performance of an earthen plate and nafion as membrane separators in dual chamber microbial fuel cells', Envir. Eng. & Management J.
- Quantitative proteomic approach to examine *Geobacter sulfurreducens* in microbial fuel cells……. in preparation.

Conference

- Partha Sarathi Jana, Krishna Katuri and Donal Leech 'A comparison of membranes in a continuous microbial fuel cell operation' 3rd International Microbial Fuel Cell Conference, Leeuwarden, 2011, The Netherlands.
- Partha Sarathi Jana, Nigel O'Donoghue, Dónal Leech., 'A comparison study of proton exchange membrane alternative and wastewater treatment at low temperature in continuous microbial fuel cell operation' Electrochem 2012, Dublin, Ireland
- P. Jana, P. Kavanagh, R. Sapireddy, K. Katuri, A. Kumar, D. Leech. 'Biofilm formation on graphite anode surfaces for application to microbial electrochemical cells' 2013, Ryan Institute Research Day, Galway, Ireland.
- P. Jana, P. Kavanagh, D. Leech, K. Katuri, S. Rengaraj, D. MacAodha,V. O'Flaherty. 'Surfaces for the formation of biofilms in microbial fuel cells' Smart Surface 2012, Dublin, Ireland.

Research Visit during the Doctoral program

Exchange research visitor to the Department of Chemistry at University of Rennes (France) Dr. Frédéric Barrière to work on Improvisation of microbial fuel cells performance by electrode modification through reduction of specific aryl diazonium salts.

TABLE OF CONTENTS

Abstract

Energy, in any form, plays the most important role in the modern world. We have been dependent on conventional energy sources such as coal and petroleum product for quite a long time. Therefore, there is an alarming need for more environmentally sustainable alternative energy resources. This thesis focuses on studies of microbial fuel cells (MFC). MFC devices use electro active bacteria to oxidize organic substrates degrading wastes and generating electricity. In the present study the effect of bacterial biofilms thickness, charge transport and power generation was studied in single chamber electrochemical cell using acetate as an electron donor. The thicker biofilms display higher charge transport diffusion co-efficient than that in thinner films, as increased film porosity of these films improves ion transport, required to maintain electro-neutrality upon electrolysis. Quartz crystal microbalance (QCM) technique was used to understand the effect of initial electro active bacterial attachment and deposition on gold electrode. It was observed that the viscoelastic properties of the biofilm increased as function of time leading to the better current generation. An attempt has been made to produce low cost MFC from the earthen plate, without involving any costly membrane. The material of the earthen plate used is found to be effective for ion transfer. The earthen plate separator is 99 % cheaper than the Nafion membrane, showing promise as an alternate separator for application to MFC technology. The proteomics analysis of *Geobacter sulfurreducens* growth on carbon cloth electrodes versus planktonic cells revealed different protein expression depending on the nature the of terminal electron acceptor. The majority of the proteins are localized in the cell membrane and involved in energy metabolism, binding and transport functional categories. In the present study the effect of influent chemical oxygen demand (COD) concentration (2000-4000 mg/L) and feed temperature (15 ºC – 32 ºC) on COD removal efficiency and power generation was studied in dual chambered MFC treating synthetic and real dairy wastewater. The results demonstrate the feasibility of novel MFC configuration for an effective wastewater treatment technology which ensures better reliable effluent quality.

Chapter 1

Introduction

1.1 Background

Global energy demand is increasing as an effect of mushrooming population and, with energy generation mostly dependent on conventional energy resources. Eighty five percent of energy demand is fulfilled by fossil fuel resources such as coal and petroleum (http://www.energy4me.org). Environmental pollution and global warming are associated aftermaths of the exploitation of fossil fuels to support in transport and energy sectors. There is thus an alarming need for environmentally sustainable alternative energy resources. Renewable energy sources such as biomass, wind, solar, and hydropower can provide energy and are more environmentally sustainable.

In addition to increased energy requirements, increased global urbanization and industrialization generates increased water demand and wastewater degradation issues. Conventional sewage treatment systems such as those based on activated sludge processes have a requirement for oxygen and energy supply (White, 2008). Alternative treatment technologies which are less energy intensive, yet still efficient and sustainable are sought. In the past two decades, high rate anaerobic processes are increasingly applied for the treatment of domestic as well as industrial wastewaters. Although energy can be recovered in the form of methane gas during anaerobic

treatment of wastewater, utilization of methane is not attractive while treating small quantities of low strength wastewater (Listowski *et al*., 2011). Therefore, alternatives for simultaneous wastewater treatment and clean energy production are much desired.

Biomass is one of the proposed future energy sources. However, biomass energy is currently used through combustion, which is a source of stationary air pollutants which threatens human and ecological health (Holdren *et al*., 2000). A means to capture the energy value in biomass without combustion would provide energy without causing local pollution problems. For example, microorganisms can channel electrons from biomass molecules, and generate energy in forms that can readily be used by human society. The different forms of energy that can be recovered from organic matter through bacteria-mediated reactions are: methanogenesis to produce CH_4, fermentation to recover ethanol, hydrogenesis to produce H_2, and microbial fuel cells (MFCs) for production of electricity. Among these alternatives, MFCs are attractive because they can generate electricity directly without combustion. Due to their potential advantages, MFCs have gained much attention in recent years (Kim *et al*., 2005; Logan, 2005; Lovley, 2006b; Rabaey & Verstraete, 2005; Scott & Murano, 2007).

1.2 Microbial fuel cell (MFC)

Microbial fuel cell technology generates electricity from organic compounds that may be sourced from organic waste, through the catalytic activity of microorganisms such as bacteria. Certain bacteria, collectively known as electrochemically active bacteria (EAB), electrogens or anode respiring bacteria (ARB), have been shown to be capable of transferring electrons to solid (i.e. electrode) acceptors. The MFC based technology therefore converts the energy stored in chemical bonds of organic compounds to electrical energy, through the catalytic reactions by microorganisms. MFCs can also be used in wastewater treatment facilities to break-down organic matter, while generating electricity (Logan *et al*., 2006a; Lovley, 2006a; Rabaey & Verstraete, 2005; Schaetzle *et al*., 2008).

They have been studied for application as biosensors, such as systems for biological oxygen demand monitoring (Kim *et al*., 2003; Moon *et al*., 2004). In earlier studies, (Heilmann & Logan, 2006; Kim *et al*., 2004; Logan *et al*., 2005; Oh & Logan, 2006) the amount of power generated in MFCs was very low, but in the past few years there have been reports of MFCs with capacity to generate higher power (Fan *et al*., 2012). Microbial power generation technology is still in its infancy but shows great promise as a novel method to simultaneously accomplish wastewater treatment and electricity generation. Currently, real-world applications of MFCs are limited because of their low power density level and high cost (Foley *et al*., 2010; Rabaey & Verstraete, 2005). Efforts are being made to improve the performance and reduce the construction and operational costs of MFCs. The economic sustainability or low cost is one of the key factors influencing future implementation of this technology. The integrative cost of electricity generation and wastewater treatment would be lower than the conventional costs of power generation (Rabaey & Verstraete, 2005). Thus, amalgamating the wastewater treatment technology with power generation would both a challenging and rewarding engineering task.

1.3 Working principle of MFC

Conventionally a MFC consists of two compartments, one containing an anode and the other a cathode, both separated by an ion-exchange membrane (Gil *et al*., 2003). Microbes in the anodic chamber of an MFC oxidize organic matter and generate electrons and protons. The anode acts as an electron acceptor, in the absence of any other soluble electron acceptor (i.e. oxygen) and these electrons are transported to the cathode through an external circuit (Figure 1). Usually, electrons reaching the cathode combine with protons that diffuse from the anodic chamber through an ion-exchange membrane, (a proton exchange membrane, PEM) and oxygen provided from air to form water (Bond *et al*., 2002; Min & Logan, 2004). Production of electric current is made possible by keeping microbes separated from oxygen other than the anode and this requires an anaerobic anodic chamber (Du *et al*., 2007).

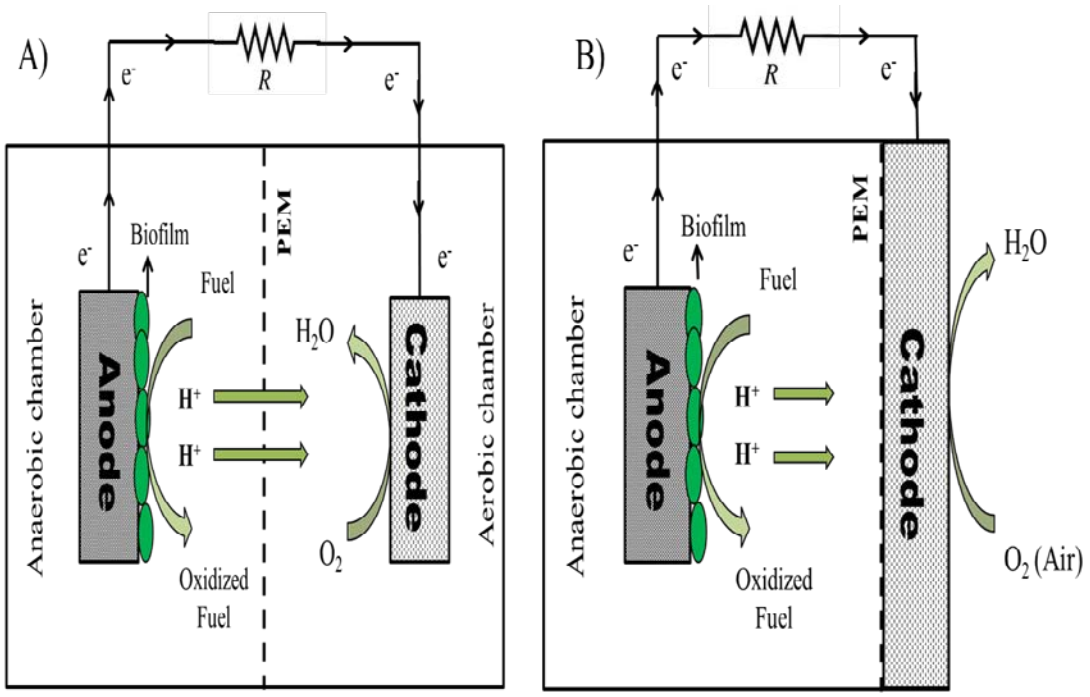

Figure 1.1 Schematic diagram of (A) dual chambered and (B) single chambered microbial fuel cell with PEM.

Inside the anaerobic anode chamber, organic substrate is oxidized by electrogenic bacteria which produce electrons and protons that are passed on to terminal electron acceptor through an electron transport chain. Electrons are shuttled from bacterial cell to solid anode surface through electron shuttling mediator, direct electron transfer via outer membrane bound cytochrome or additional mechanism, such as that proposed through conductive pilli, via physical adherence of the bacterial cell to the anode (Reguera *et al.*, 2006) and self-exchange by which electrons are conducted in a bucket-brigade manner by a sequence of bimolecular electron transfer reactions between adjacent redox protein (Strycharz-Glaven *et al.*, 2011).

Typical electrode reactions in MFC compartments are as follows.

If acetate is used as a model organic substrate:

Anode reaction: $CH_3COOH + 2H_2O \rightarrow 2CO_2 + 8H^+ + 8e^-$

Cathode reaction: $2O_2 + 8e^- + 8H^+ \rightarrow 4H_2O$

Thermodynamically capable of generating $\Delta G = -583$ kJ/mol

If sucrose is used as a model organic substrate

Anode reaction: $C_{12}H_{22}O_{11} + 13H_2O \rightarrow 12CO_2 + 48H^+ + 48e^-$

Cathode reaction: $48H^+ + 48e^- + 12O_2 \rightarrow 24H_2O$

Overall reaction: $C_6H_{12}O_6 + 6\ O_2 \rightarrow 6\ CO_2 + 6\ H_2O$ + Electrical energy

Thermodynamically capable of generating ΔG – 2840 kJ/mol

The overall reaction is the breakdown of the substrate into carbon dioxide and water with electricity as a by-product.

Bacteria are prokaryotic cells of around 0.5 to 1.5 µm in size. Generally bacteria can be rod, spherical or spiral shaped. The understanding of bacterial metabolism is an important part of understanding operational mechanisms of MFC technology. The electricity production in MFC strongly depends on bacterial activity and the oxidation reaction in the anode chamber. In MFC anodes, electrogenic bacteria oxidize the organic substrate through catabolic processes for both generations of energy and extra electrons and protons for MFC application (Du *et al*., 2007). Electrons are removed from primary donor and transferred to the terminal electron acceptor within a bacterial cell through a series of electron carrier proteins and cofactors, such as NADH dehydrogenase, ubiquinone or cytochromes. The energy released during the electron transport permits bacteria to push protons to the periplasm.

Electrons produced from the oxidation of substrate in an MFC anode chamber are proposed to be transferred to the solid electrode by several mechanisms discussed below.

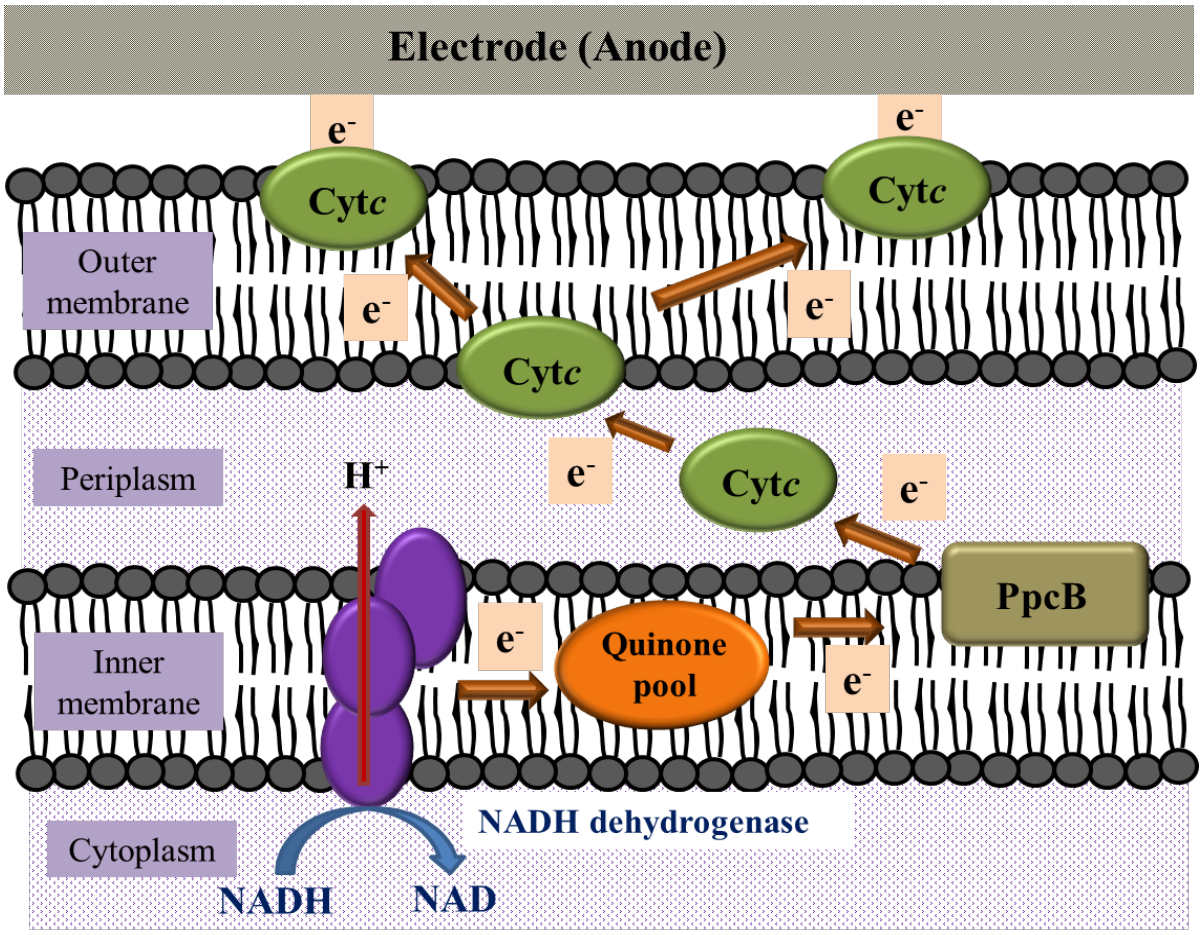

Figure 1.2 Summary of DET mechanisms proposed to be involved in the electron transport from bacterial cells to the solid anode in a microbial fuel cell.

1.3.1 Direct electron transfer (DET)

Different type of bacteria have the capabilities to transfer electrons beyond the cell surface (Sydow *et al*., 2014) collectively known as EAB. Cultures of EAB, such as *Geobacter sp, Rhodoferax sp* and *Shewanella sp* have been studied in microbial fuel cells. For DET to occur it is assumed that bacteria become physically attached to the solid electrode and transfer electrons without the requirement of any diffusional redox species. In recent years, use of electroanalytical and spectro-electrochemical techniques, often in combination with genetic engineering,

immunohistochemical staining, or NMR, has helped elucidate the role of electron transferring species (cytochromes, pili) in current production by *Geobacter sulfurreducens* (GS) biofilms on anodes. For example, genomic analysis of GS has identified coding sequences for periplasmic cytochromes, membrane cytochromes and other outer membrane proteins that can contribute to extracellular electron transport and DET to electrodes. DET relies on the existence of at least a single cell layer on the electrode surface (Rabaey *et al*., 2011).

1.3.2 Mediated electron transfer

Electrons can be transferred from the bacteria through metabolites of endogenous redox molecules by the bacteria which are capable of acting as electron shuttles between the bacteria and the electrode (Logan *et al*., 2006b). The endogenous redox mediators are produced by bacteria in metabolic pathways and include molecules such as soluble quinones, flavin (Marsili *et al*., 2008; von Canstein *et al*., 2008), pyocyanin (Rabaey *et al*., 2004a) and 2-amino-3-carboxy-1,4-naphthoquinone, ACNQ (Newman, 2001). Synthetic exogenous mediators such as neutral red (Park & Zeikus, 2000), methylene blue, thionine, meldola's blue (Ieropoulos *et al*., 2005b), 2-hydroxy-1,4-naphthoquinone (HNQ) (Allen & Bennetto, 1993) and Fe(III)EDTA (Vega & Fernández, 1987) have been used to shuttle electrons between terminal respiratory enzymes of bacteria and solid electrode surfaces (Hasan *et al*., 2013; Park & Zeikus, 2000; Pasco *et al*., 2005). These mediators can divert electrons from the electron transport chain by entering outer cell membranes, becoming reduced, and then leaving in reduced state to transport electrons to the solid electrode (Bennetto *et al*., 1983). MFCs operating on endogenous mediators are proposed to have more commercial potential, as addition of exogenous mediators is expensive and they can be toxic to bacteria (Liu *et al*., 2012).

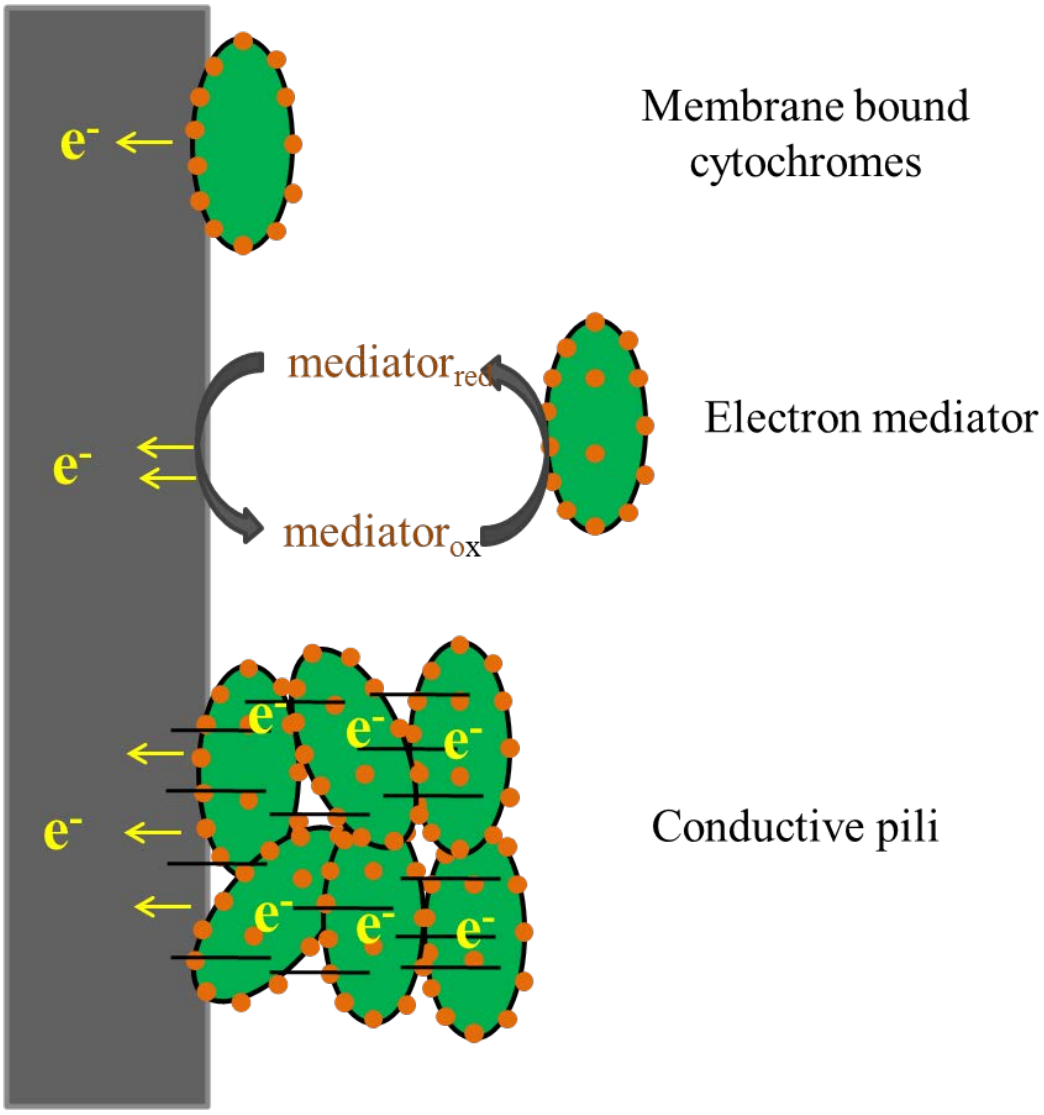

Figure 1.3 Different methods for extracellular electron transfer to an anode acting as an electron acceptor in a microbial fuel cell

1.3.3 Microbial biofilms

Bacterial attachment is the initial and an important step during biofilm formation (Kreth *et al.*, 2004; Otto & Silhavy, 2002). Bacterial attachment is dependent on physiological factors, surface properties, hydrodynamic effects and the

physiochemical properties of the cell (Marcus *et al*., 2012). Biofilms are very important in wastewater treatment processes, soil and plant ecology (Olsson *et al*., 2008). In the case of microbial fuel cell technology, the electrical current generated by an anodic biofilm containing EAB typically increases with the amount of active biomass attached to the electrode (Reguera *et al*., 2006). The mechanism of coordination among cells and cellular components during transport of electrons through a thick biofilm and at the anode/biofilm interface remains unresolved (Bond *et al*., 2012). Little has been reported on how film thickness can affect how rapid charge is transported through bacterial biofilms on solid electrodes, and how this contributes to catalytic current generation.

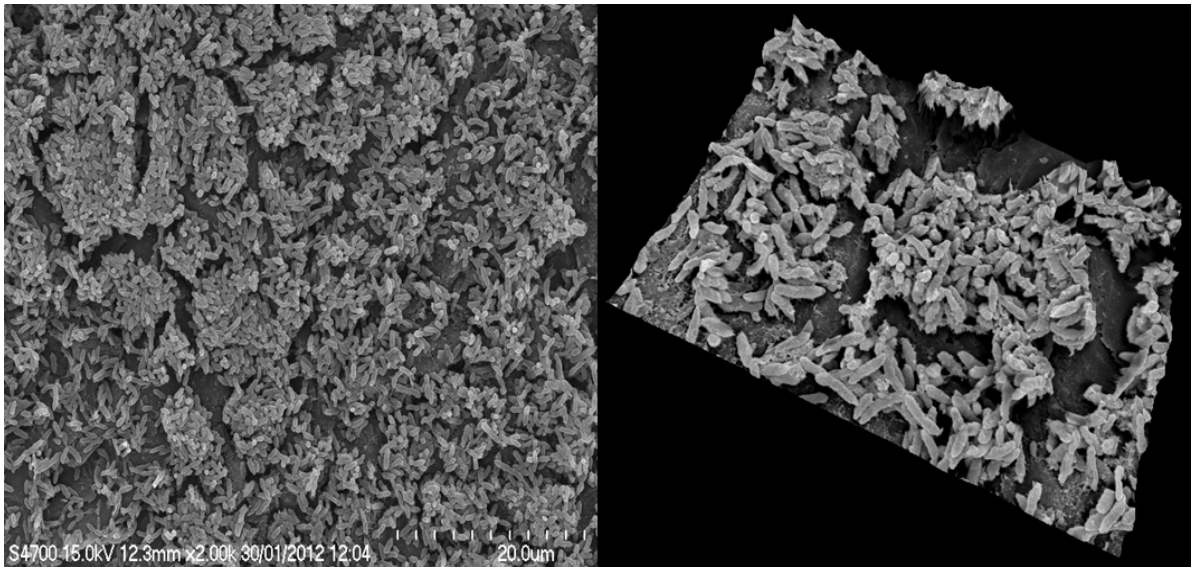

Figure 1.4 Example of biofilm grown on graphite rod observed under scanning electron microscopy (*Geobacter sulfurreducens* grown on graphite rod electrode in microbial fuel cell)

1.4 Applications of MFC

There are many applications proposed for microbial fuel cells that mainly fall into either power generation or wastewater treatment. Other potential applications, such as use as sensors, desalination and gas production are briefly presented, as these do not form a part of this thesis topic.

1.4.1 Biosensors

MFCs can be used as biosensors for online monitoring of organic matter concentration based on proportional correlation between electricity generation and organic load of the wastewater (Kim *et al*., 2003; Moon *et al*., 2004). Microbial fuel cells enriched with EAB have been used as biochemical oxygen demand (BOD) and toxicity detection biosensors. Besides BOD sensors, MFCs have also been applied for measurement of levels of several other toxic chemicals such as cadmium, lead, chromium(VI), mercury, cyanide, arsenic, organophosphorus and surfactants (Kim *et al*., 2006).

1.4.2 Desalination

Current desalination techniques to convert sea and brackish water to drinking water are dependent on high energy and capital investment. The main desalination technologies used are reverse osmosis, electro-dialysis, and distillation (Cao *et al*., 2009a). Microbial fuel cell technology could be used to remove dissolved salts from water without any external electrical energy input by adding a third chamber in between the two chambers of a standard MFC and filling it with sea water. The positive and negative electrodes of the cell attract the oppositely charged salt ions from water and consequently filter out the salt from the sea water (Cao *et al*., 2009a; Kim & Logan, 2013).

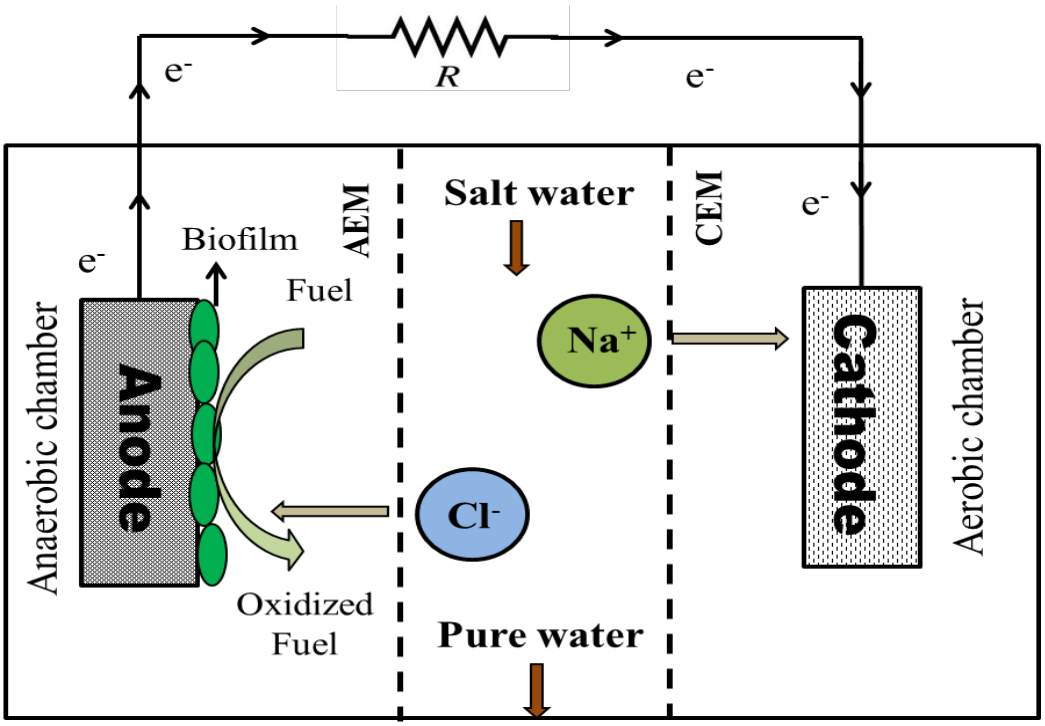

Figure 1.5 A desalination microbial fuel cell.

1.4.3 Hydrogen production

Hydrogen is the only renewable energy source which generates water as a combustion product without production of additional gases that contribute towards global warming. Microbial fuel cell technology can be used to generate hydrogen from organic substrates. Hydrogen gas can be produced through modification of the MFC by addition of a small voltage to that produced by the electrogenic bacteria which are present in the anode chamber and by omitting oxygen from the cathode. While the power supply drives the released electrons from the anode to the cathode, an equal number of protons are transferred through the membrane and at the cathode, protons and electrons combine to form hydrogen gas (Cheng & Logan, 2007; Liu *et al*., 2005; Rozendal *et al*., 2006).

Typical electrode reactions in a MFC compartments are as follows when acetate is used as organic substrate.

$CH_3COO^- + 4H_2O \rightarrow 2HCO_3^- + H^+ + 4H_2$.

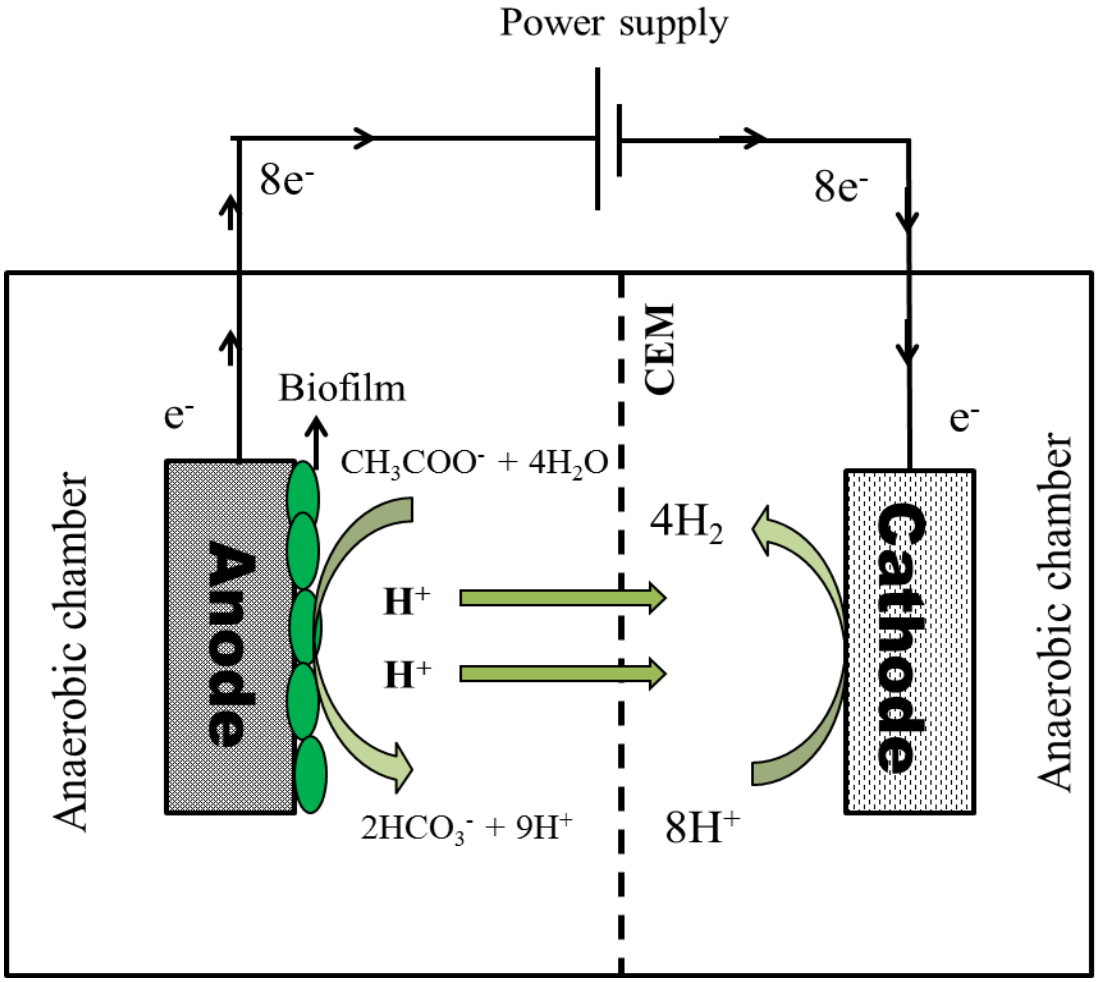

Figure 1.6 Schematic representation of hydrogen production through bio catalyzed electrolysis of acetate.

1.4.4 Remote power sensors:

MFCs can be used to operate low-power sensors that collect data from remote areas. Sediment MFCs, when the anode is submerged in mud sediment while the cathode is immersed in the water above the sediment, have been developed for this purpose. Power generated from sediment MFCs is stored in capacitors and the energy utilized to operate remote sensors through a power management system (Donovan *et al*., 2011; Shantaram *et al*., 2005). An ion exchange membrane is not necessary in sediment MFCs because of the decreasing oxygen gradient with depth. With the help of microbial fuel cells, various sensors can be powered, that monitor temperature, salinity, tidal patterns, the presence of algae and other life forms, migration patterns of fish and other marine wildlife, organic contamination from oil production and metallic compounds from other industrial processes (Scott *et al*., 2008).

1.5 Advantages of MFC

MFC technology has operational and functional benefits in comparison with other technologies used for wastewater treatment and energy generation from organic matter.

It is possible to generate electricity from various types of organic matter and renewable biomass

Direct conversions of organic substrate into electricity without any intermediate steps ensure high energy conversion efficiency.

The bacterial yield in the anaerobic process in MFC is about 1/5 that of an aerobic culture (Kim *et al*., 2007a) resulting in much lower sludge generation during wastewater treatment than in conventional activated sludge processes.

MFCs do not require any gas treatment because the off-gases are generally enriched with carbon dioxide (Rabaey & Verstraete, 2005).

MFCs do not need energy input for aeration provided the cathode is directly exposed to ambient air (Liu & Logan, 2004b; Liu *et al*., 2004).

1.6 Factors affecting the performance of MFC

The microbial degradation of organic substrates in the anode chamber is one of the key processes for MFC electricity generation. The power output is limited by high internal resistance of MFCs. There are various other internal and external factors associated with MFCs performance, such as reactor configuration, electrode and separator materials, anode and cathode catalysts, electron acceptor, substrate type, substrate concentration, feed pH, hydraulic retention time (HRT) and temperature that increase the internal resistance of the MFC. This section summarizes the various factors affecting MFC performance.

1.6.1 Potential losses in MFC

MFCs achieve a maximum voltage of 0.3 – 0.7 V. The voltage is a function of the external resistance (R_{ex}) or load on the circuit, and the current (I). Positive potential difference (E_{cell}) between the electrodes of the MFCs, and the flow of electrons (I) provide a power ($P = E_{cell} \times I$). The actual voltage obtained in the MFC (E_{cell}) is usually considerably lower than the cell electromotive force thermodynamically predicted (E_{thermo}) because of various potential losses, often referred to as over-potentials. The irreversible losses in MFCs are presented in the following equation (Rismani-Yazdi *et al*., 2008)

$$E_{cell} = E_{thermo} - [(\eta_{act} + \eta_{ohmic} + \eta_{conc})_{\text{cathode}} + (\eta_{act} + \eta_{ohmic} + \eta_{conc})_{\text{anode}}]$$

Where η_{act} is the activation loss due to slow reaction kinetics, η_{ohmic} is the ohmic loss from ionic and electronic resistances, and η_{conc} is the concentration loss due to mass transport limitations. Activation and concentration losses occur at anode and cathode chamber, while ohmic losses occur throughout the cell. Each of these losses has different, yet cumulative, effects on the operating cell voltage of the fuel cell.

1.6.1.1 Activation losses

Activation losses occur due to the energy losses for initiating the oxidation or reduction reaction. Activation losses are dominant at lower current density as an energy barrier at the electrodes should be overcome before current can flow (Du *et al*., 2007). In MFCs the activation losses are basically representative of a loss of overall voltage due to the bacterial metabolism of organic matter. Activation overpotential can be reduced by increasing the electrode surface area, increasing electrode catalysis (Park & Zeikus, 2003), adding mediators to facilitate efficient electron transfer from bacteria cell to anode surface (Ieropoulos *et al*., 2005b; Park & Zeikus, 2000) enriching electrogenic biofilms on the anode and operational conditions inside anode and cathode compartments (Du *et al*., 2007; Logan *et al*., 2006b; Rismani-Yazdi *et al*., 2008).

1.6.1.2 Ohmic losses

Ohmic losses are universal in any type of electrochemical cell. In MFCs, ohmic losses occur due to the resistance of electrode materials which hampers electron flow, interconnections and resistance to flow of protons through PEM and anolyte and catholyte (Larminie & Dicks, 2013). To reduce ohmic losses, it is necessary to use highly conductive electrodes and minimize the electrode spacing, thus giving the protons a shorter distance to travel before they combine with oxygen and electrons (Cheng *et al*., 2006; Rismani-Yazdi *et al*., 2008; Zhao *et al*., 2006). Increasing the membrane surface area relative to the total MFC volume has also been

shown to enhance proton flux which reduces ohmic losses (He *et al.*, 2005; Rabaey & Verstraete, 2005).

1.6.1.3 Concentration losses

The continuous supply of electron donor to the anode biofilm is very important to maintain continuous steady state current generation. At very high current densities, mass transport limitation of electron donation to the electrode can cause a decline in the output voltage, this is referred to as concentration losses (Logan *et al.*, 2006b).

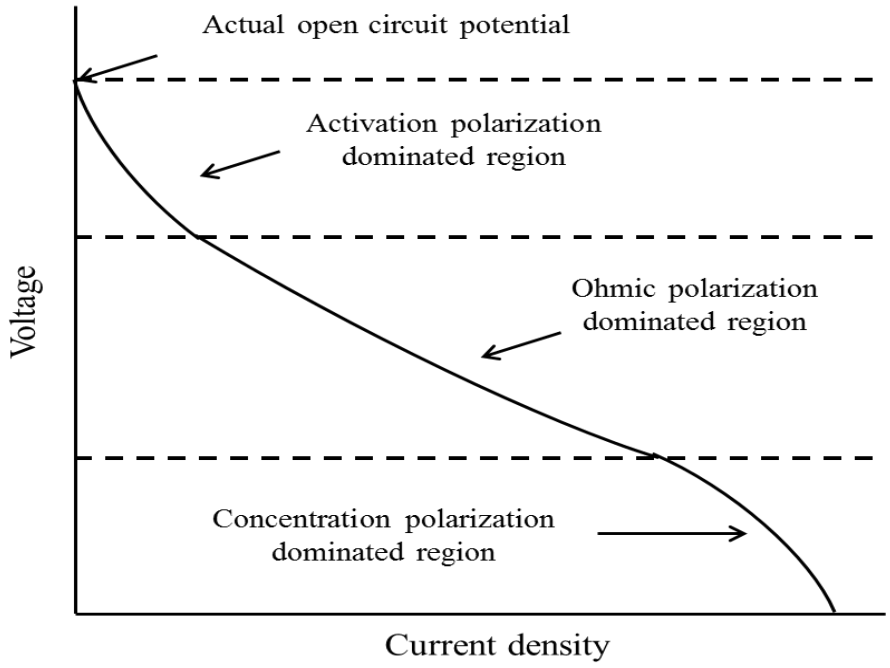

Figure 1.7 General polarization curve for a microbial fuel cell showing regions dominated by various types of losses.

1.7 Reactor configuration of MFCs

Microbial fuel cells are an emerging technology for simultaneous wastewater treatment and electricity generation. Different reactor configurations of the MFC

affect the performance by significantly altering the internal resistance. MFCs have been operated either as dual chambered MFC, single chambered MFC or stacked MFC. Single-chamber, air cathode MFCs are the most promising design for practical applications because they use passive oxygen transfer to the cathode, the electron acceptor, and also the single chamber design avoids the need for a membrane (Ahn *et al*., 2014).

1.7.1 Dual chambered microbial fuel cell

Conventionally a MFC consists of two compartments, containing an anode and cathode separated by an ion exchange membrane, which permit the proton flow from anode chamber to cathode chamber while acting as an obstruction to the diffusion of oxygen from the cathode chamber to the anode chamber. The widely used dual chamber is of an H-type MFC, consisting of two bottles connected by a tube containing a separator (Katuri *et al*., 2012; Min *et al*., 2005; Oh & Logan, 2006; Picot *et al*., 2011). The power generation in an H-type reactor is limited by its high internal resistance (Logan *et al*., 2006b). H-type MFC reactors have several problems related to the PEM that affects the power production, including proton transfer efficiency, bio-fouling and oxygen leakage (Kim *et al*., 2007b). This type of MFC is suitable for optimizing basic parameters such as new electrode or separator materials, microbial communities, degradation of specific compounds, and applied potential.

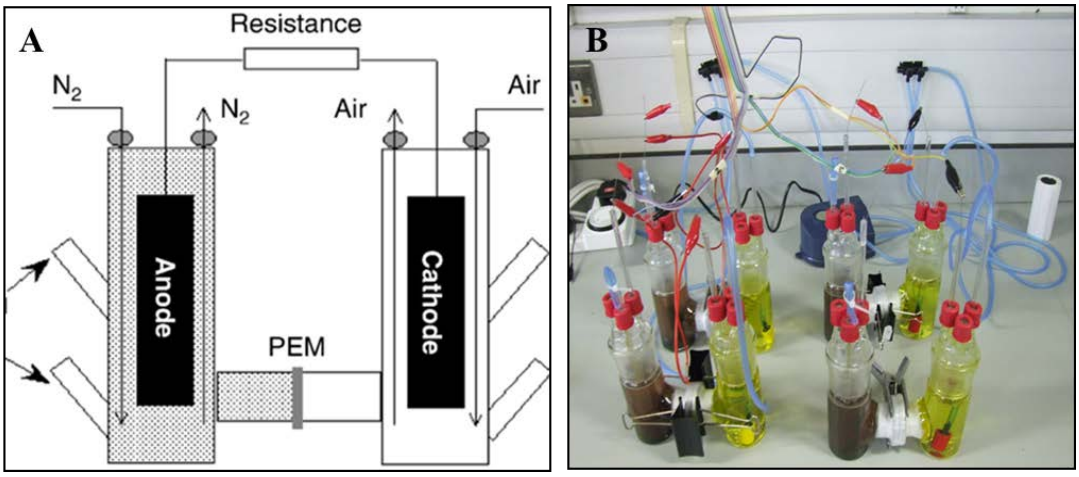

Figure 1.8 some conventional dual chambered MFC (A) Min *et al*., 2005 (B) (Katuri *et al*., 2012)

1.7.2 Single chamber microbial fuel cell

Recently many researchers have chosen to use single chamber air cathode MFCs due to their simple economic design and practical implementation characteristics. Single chamber MFCs can be constructed by removing the cathode chamber and keeping the cathode in direct contact with air. The single chamber air-cathode MFC provides advantages over the two chamber system for simple scale up (Abourached *et al*., 2014; Liu & Li, 2014; Liu & Logan, 2004a; Mahdi Mardanpour *et al*., 2012; Park & Zeikus, 2003; Sciarria *et al*., 2013; Sukkasem *et al*., 2008; Zhang *et al*., 2011). However, the major challenge for a membrane-less MFCs coulombic efficiency (CE) is much lower than that of MFC containing a membrane when a mixed culture is used due to the consumption of substrate with electron transfer to oxygen diffused through the cathode (Liu & Logan, 2004b). Development of new separators, which can reduce the oxygen diffusion without increasing the internal resistance of cell and affecting the power density, could resolve these problems.

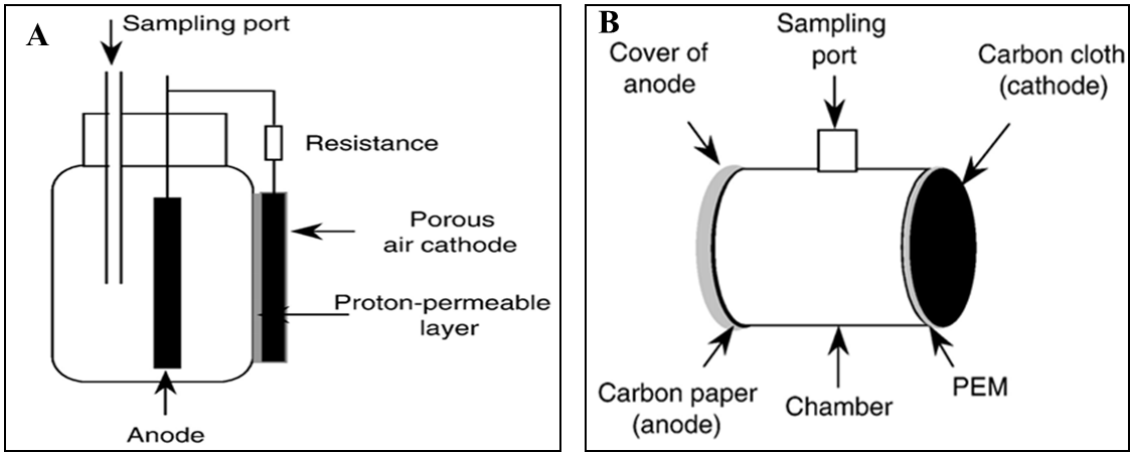

Figure 1.9 some single chambered MFCs as reported on in Liu and Logan

1.7.3 Stacked MFCs

In another type of configuration, cells are stacked to increase voltage or current output of MFCs. They can be either stacked in series or parallel Connecting several fuel cells in series adds the voltages, and one common current flows through all fuel cells (Larminie & Dicks, 2013). Both have their own importance and are high in power efficiency, thus can be practically utilized as power source (Ieropoulos *et al*., 2005a). Individual MFCs or MFCs connected in parallel are appropriate for rapid substrate degradation and high current densities. The MFCs connected in series and parallel worked, respectively, at an average current and voltage determined by the performance of the individual MFCs. (Oh and Logan, 2007) have reported charge reversal in one of the two air-cathode MFC stacks, which resulted in reverse polarity in one cell, thereby decreasing the power generation.

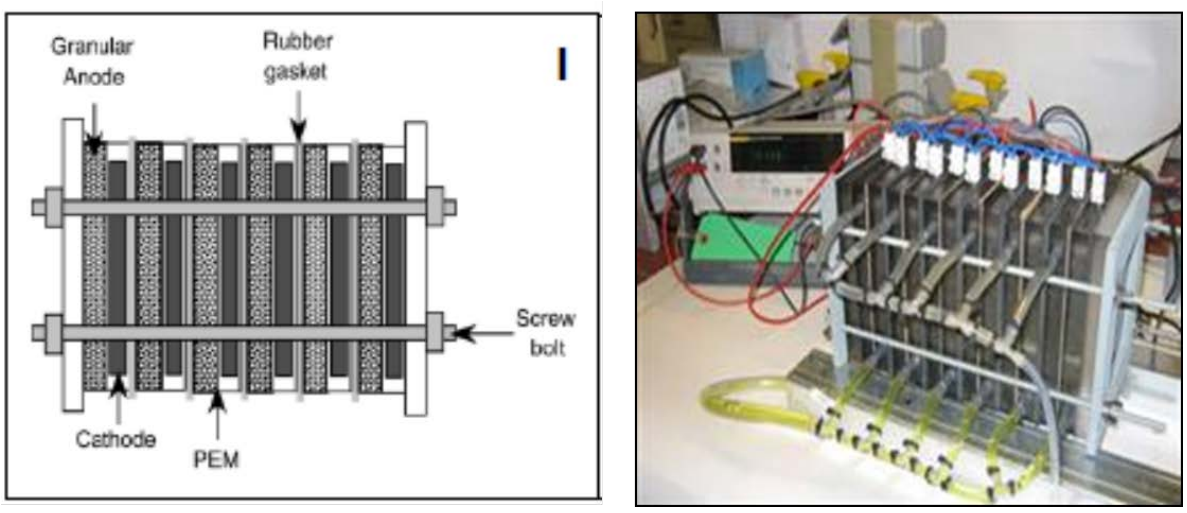

Figure 1.10 Stacked MFCs (Aelterman *et al*., 2006)

1.7.4 Operating conditions in the anode chamber

Operating conditions also affect the performance of MFCs. Anaerobic wastewater treatment may involve several groups of bacteria, having their own optimum working conditions. MFCs running under optimized anodic and cathodic operating conditions facilitate proper growth of electrogenic biofilm during start up and enhance the subsequent performance during long term operation. For an existing MFC it is also possible to enhance MFC performance by optimization of the operating conditions including pH, alkalinity, substrate type, substrate concentration, organic loading rate (OLR) which affects the activity of these anaerobic microorganisms. The anodic conditions affecting the performance of MFC are described below.

1.8 Inoculum

The most important biological factors affecting the performance of MFCs are the type and source of inoculums. Microorganisms as biocatalysts are a vital factor that affects the power output by contributing to electron transfer rates, biofilm thickness, conductance, substrate uptake rate and overall internal resistance of the cell (Borole *et al*., 2011). Pure culture bacteria are suitable for foundation studies because of high electrochemically activity. Cultures of EAB such as *Geobacter* sp. (Bond & Lovley, 2003; Cao *et al*., 2009b; Dumas *et al*., 2008; Zhou *et al*., 2005) *Shewanella* sp. (Biffinger *et al*., 2007; Kim *et al*., 1999; Ringeisen *et al*., 2006), *Rhodoferax* sp. (Liu *et al*., 2007) have been studied in MFC configurations. Mixed cultures are more suitable for practical application due to their different substrate affinity. Mixed culture inocula have been used from a variety of sources such as domestic wastewater (Min & Logan, 2004), soil (Niessen *et al*., 2006), fresh as well as marine sediments (Zhang *et al*., 2006), activated sludge (Ki *et al*., 2008; Patil *et al*., 2009), and anaerobic digester sludge (Chae *et al*., 2010; Kim *et al*., 2004). Gram negative bacteria normally produce higher power than Gram-positive bacteria because of the different cell structures of these two types (Borole *et al*., 2011).

Bacteria in pure culture systems grow slowly, having a high risk of contamination and generally high substrate selectivity compared to mixed-culture systems (Rabaey *et al*., 2003). Besides EAB, there are several other types of bacteria such as methanogens, denitrifying bacteria, hydrogen scavenging bacteria which can consume electrons and decrease MFC performance. For large scale application of MFCs, mixed cultures such as anaerobic digester sludge are generally preferred over pure cultures as inoculum source because they are readily available in bulk quantities and are more tolerant to environmental instabilities.

1.8 Substrate

Substrate type is an important factor affecting the performance of MFC. Different types of substrate influences the bacterial biofilm growth and the MFC performance including the power density and coulombic efficiency. Several chemicals, and chemical mixtures, have been studied in MFCs such as glucose (Rabaey *et al*., 2003) acetate, butyrate (Liu *et al*., 2005) cysteine (Logan *et al*., 2005), proteins (Heilmann & Logan, 2006), lignocellulose (Rismani-Yazdi *et al*., 2007), xylose and humic acid (Huang *et al*., 2008), and complex waste streams such as domestic wastewater (Min & Logan, 2004; You *et al*., 2006b), food processing wastewater (Oh & Logan, 2005), saline sea food wastewater (You *et al*., 2010), dairy wastewater (Venkata Mohan *et al*., 2010), molasses wastewater (Zhong *et al*., 2011), paper wastewater, bakery wastewater (Velasquez-Orta *et al*., 2011), dye wastewater (Kalathil *et al*., 2011), slaughterhouse wastewater (Katuri *et al*., 2012), uric salt (You *et al*., 2014) and brewery wastewater (Feng *et al*., 2008). If MFCs are to be used in the real world they must be tested for use in real wastewaters.

1.9 Effect of pH

Electrolyte pH is one of the most important environmental factors in bacterial cell growth and physiology. The electrolyte pH plays an important role in MFC power output. Effect of anodic pH microenvironment on performance of MFC has

been reported in many studies. Generally bacteria require a pH close to neutral for their optimal growth. Continuous operation of an MFC causes pH to become acidic in nature at the anode as a result of increase of protons produced through the microbial oxidation of organic compounds, whilst due to slow and incomplete proton diffusion through the membrane an alkalinisation is observed on the cathode side (Oliveira *et al*., 2013). Anodic pH microenvironment can influence substrate metabolic activity which affects the electron and proton generation mechanism. The acidified anode can decrease bacterial activity and can affect the biofilm performance and stability (Behera & Ghangrekar, 2009; Patil *et al*., 2011; Zhuang *et al*., 2010). The optimal pH range for chosen MFC configuration is reported to be between 7 and 8 (Gil *et al*., 2003) or 8 to10 (He *et al*., 2008). Only a narrow pH window ranging from 6 to 9 was suitable for growth and operation of biofilms (Oliveira *et al*., 2013). However (Raghavulu *et al*., 2009) found that MFCs operated at low anodic pH may have higher proton transfer rates increasing the availability of protons at the cathode. The pH of the cathode solution can also vary, affecting the overall cathode potential. Generally dual chambered MFCs are operated at different anodic and cathodic pH, and the difference in performance may also stem from the difference in anodic and cathodic pH.

1.10 Organic loading rate (OLR)

Organic loading rate (OLR) significantly affects the start-up performance of a microbial fuel cell. Since the electricity generation, substrate degradation, coulombic efficiency and energy efficiency of the MFCs depend on OLR plays an important role in MFCs performance. The production of current in MFC is directly linked to the ability of the bacteria to oxidize a substrate and transfer electrons as a result of oxidation to the anode electrode. OLR could be maintained through hydraulic retention time and flow rate of media. MFC operation under continuous mode poses hydrodynamic challenges that can affect the microbial communities sustained and developed in the biofilm (Rochex *et al*., 2008). Running the anodic biofilm formation

under continuous flow mode might result in developing more robust biofilm. This would be positive in effective operation of the MFC treating large volumes of wastewater at high flow rates where planktonic microbes are quickly flushed from the system, contributing a small fraction to the power output (Ieropoulos *et al*., 2010). Higher substrate concentration yields greater power generation over a wide concentration range (Du *et al*., 2007). The improvements in power generation and substrate degradation indicate that more organic matter is utilized for power generation at higher OLR. It was also found that the internal resistance of the cell decreases with an increase of the OLR. This is due to improvement of the ionic strength of the anodic liquid, resulting from higher volatile fatty acid concentrations, an increased catalytic activity and density of the anodophilic microorganism (Martin *et al*., 2010; Velvizhi & Venkata Mohan, 2012). Nam *et al* have studied the effect of OLR on the performance of a single chamber MFC fed with fermented wastewater by varying the OLR from 1.92 to 4.80 g (L.d). They observed that power density increased to 2981 mW/m^3 at an OLR of 3.84 g/L d and then decreased to 2959 mW/ m^3 at OLR of 4.80 g/L/d (Nam *et al*., 2010). Martin *et al*. also observed similar effect of OLR on the performance of a glucose fed single chamber air cathode MFC by varying the OLR from 0.2 to 7.4 g/L d. They observed that power density increased to 8.2 W/m^3 at an OLR of 3.72 g/L d and then decreased to 6.6 W/ m^3 at OLR of 7.44 g/L d (Martin *et al*., 2010). Kim *et al*. have reported the effect of low strength OLR on the performance of a sucrose fed modular single chamber air cathode MFC by varying the OLR from 0.04 to 0.41 g/L d. They observed that maximum power output increased with organic loading rate. The maximum power outputs were between 2.8 to125 mW/m^2 (Kim *et al*., 2010). He *et al*. have operated up-flow MFCs fed with sucrose solution at OLR varied from 0.3 to 3.4 kg COD/(m^3.d) at a constant HRT of 1.0 day, i.e., varying the influent COD concentration from 300 mg/L to 3400 mg/L at 300 Ω external resistor. The study showed that the highest power density occurred at OLR of 2.0 kg COD/(m^3.d) (influent COD of 2000 mg/L) with no noticeable change by increasing OLR was observed, whereas COD removal efficiency increased with increase in OLR (He *et al*., 2005). Normally higher OLR generates higher power, but the coulombic efficiency increased with a decreased

OLR and substrate degradation may have been due to methanogens competing with EAB. The studies regarding the effect of OLR on MFCs show that with an optimized OLR, methane production can be avoided and that the electricity-to-methane production rate can be successfully shifted towards electricity production (Oliveira *et al*., 2013).

1.11 Cathode performance in a MFC

Current production in a MFC not only depends on the anode performance but on cathode performance also. In the cathode chamber oxygen is the main terminal electron acceptor and the reduction of oxygen is the dominant electrochemical reaction at the surface of cathode electrodes (Rismani-Yazdi *et al*., 2008). The cathode material, surface area, cathode catalyst, cathodic electron acceptor and cathodic operating conditions (such as cathode oxidant concentration, temperature and catholyte pH) are the various factors that affect the cathode performance.

1.11.1 Cathode catalyst

Due to the slow oxygen reduction rates on the surface of graphite electrodes, an additional catalyst or mediator can be added to improve the cathode performance. Platinum is the most widely used catalyst for oxygen reduction in MFCs (Liu & Logan, 2004a; Oh *et al*., 2004). The application of platinum-coated cathode for wastewater treatment is however not practical because of the excessive cost and possible sulfide poisoning in the wastewater (Freguia *et al*., 2007). Some transition metals show potential as catalysts on the cathode surface for oxygen reduction such as lead dioxide (PbO_2) (Morris *et al*., 2007), pyrolyzed-Fe(II) phthalocyanine (pyr-FePc) (Zhao *et al*., 2006) and cobalt tetra methyl phenylporphyrin (CoTMPP) (Zhao *et al*., 2005). These have been tested in MFCs, and give similar performances to Pt, providing an opportunity for future large-scale applications of MFCs.

1.11.2 Cathode material

Cathode material may significantly affect the MFC power output. Graphite was used in the cathode in most of the MFCs. However due to slow kinetics of the oxygen reduction at plain carbon, and the resulting large over-potential, the use of such cathodes may limit the use of this material (Logan *et al*., 2006b). Various electrode materials have been investigated in attempts to increase the available reaction sites in the cathode compartment while maximizing the surface area per unit volume (specific surface area). To overcome the problems of limited surface area of graphite plate and carbon paper cathodes, woven graphite felt (Gil *et al*., 2003; Park & Zeikus, 2003; Rabaey *et al*., 2005), granular graphite (Freguia *et al*., 2007) and reticulated vitreous carbon (He *et al*., 2005; Ringeisen *et al*., 2006) have been tested due to their specific surface area lower than for graphite plate of identical dimensions. Several design criteria should be considered before selecting cathode material including the thickness, porosity, composition, geometry, and high specific surface area of the electrode. Ideally these characteristics should improve hydrodynamic flow to facilitate mass transport and prevent accumulation of water at the cathode (Rismani-Yazdi *et al*., 2008).

1.11.3 Cathodic electron acceptor

Oxygen is widely used as electron acceptor in MFCs for the cathodic reaction. However the cathode activation over-potential for oxygen can be reduced by employing cathodic electron acceptors having lower activation overpotential such as ferricyanide (Liu & Li, 2007; Ringeisen *et al*., 2006), permanganate (You *et al*., 2006a), persulfate (Li *et al*., 2009), dichromate (Wang *et al*., 2008) and hydrogen peroxide (Tartakovsky & Guiot, 2006). The disadvantage of these chemical electron acceptors is that they cannot be regenerated, or only very slowly regenerated by oxidation with oxygen, which requires regular replenishment, and they may diffuse

through the membrane over long-term operation which eventually reduces the overall performance of the MFCs.

1.13 Challenges in MFC application

Microbial fuel cell technology is not only a novel wastewater treatment process with continuous energy generation potential but can be used in biosensors for oxygen and pollutants, in desalination and in hydrogen production. The performance of MFCs is dependent on several factors, such as various losses, poor oxygen reduction kinetics at the cathode, reactor configuration, rate of substrate degradation, membrane separator etc. The high cost of the Nafion membrane, the oxygen and substrate diffusion through this membrane along with associated problem of bio-fouling limits its option for scaling up MFCs. Hence, there is a demand for cost effective membrane material, which would have high proton conductivity and high strength to sustain the hydrodynamic pressure in the large scale MFC construction. In addition MFCs present many technological challenges that need to be overcome before any commercial application. These may be solved using engineering approaches but additionally studies aimed at understanding electron transfer mechanisms, charge transport, biofilm structure and dynamics are important to better transfer MFC technology from laboratory scale to practical field. This thesis aims to contribute to understanding of these key issues, whilst also attempting to study application of novel membranes and novel waste sources in MFC technologies.

1.14 Objectives

The aim of the present research is to study the fundamental aspects of electrogenic bacteria at MFC anodes. The research investigates also the performance of MFCs employing low-cost materials, and wastewater sources, which would have possible application in wastewater treatment plants and associated economic perspectives.

To achieve this aim, the following objectives were identified:

- Employing low-cost materials as a membrane in MFCs
- Probing charge transport in films of *Geobacter sulfurreducens* on graphite electrodes as a function of film thickness
- Probing *Geobacter sulfurreducens* biofilm growth on electrodes using combined mass, film dielectric and electrochemical measurements
- Probing differences in *Geobacter sulfurreducens* proteome when grown using soluble versus solid electron acceptors
- Comparing operation of an MFC to that of an anaerobic digestion system

1.15 Organization of the thesis

The thesis comprises of seven chapters which have been organized as

Chapter 1: Introduction

A brief overview of the requirement for sustainable wastewater treatment, effect of operating parameters on substrate degradation rate and power generation in MFC, requirement for cost effective alternative separator in MFC is presented in this chapter. The context and relevance of the present research and the defined specific objectives of the present study are mentioned.

Chapter 2: Comparison of performance of an earthen plate and Nafion as membrane separators in dual chamber microbial fuel cells

The characteristics of the selected membrane separator can significantly affect the performance of an MFC. Nafion is the most widely used membrane separator because it's the high proton conductivity. The present report focuses on an effort to better compare performances of MFCs operated using the earthen plate as membrane separator to that of Nafion separated MFCs by fabrication of polyacrylate MFCs with earthen plate separator of the same exposed geometrical surface area to

that of the Nafion separator. The comparison of MFC performance is evaluated by operation of both types of MFC under continuous mode feeding of acetate as synthetic waste, following initial batch incubation with acetate and anaerobic sludge, as inoculums, and using a ferricyanide solution as a model oxidant in the catholyte.

Chapter 3: Charge transport in films of *Geobacter sulfurreducens* on graphite electrodes as a function of film thickness

Microbial fuel cell devices which uses electroactive bacteria (EAB) to oxidize organic substrates, degrading wastes and generating electricity, have received a great deal of attention in recent years. Proposed mechanisms of electron transfer within films of EAB to produce current at solid anode surfaces include production and use of electron shuttling mediating molecules and redox active membrane-bound proteins (cytochromes), self-exchange within redox conducting films or even, controversially, via conductive nanowires (pili). The exact mechanism or combination of mechanisms that drives electron transfer within films of EAB to solid surfaces is not yet fully understood. Here we report comparison of biofilm thickness over time to voltammetric responses in the presence and absence of acetate as electron donor. In the absence of electron donor, redox site concentration, within the biofilms and charge transport across the biofilm vary as a function of film thickness, providing an insight into the factors that may affect current generation at microbial fuel cell anodes.

Chapter 4: Real-time monitoring of *Geobacter sulfurreducens* biofilm formation in EQCM-D system

Bacterial attachment is an important first step of any biofilm formation. Bacterial attachment is dependent on some physiological factors, like surface properties, hydrodynamic affects and the physiochemical properties of the cell. Recently researchers have used the quartz crystal microbalance (QCM) technique for better understanding of the interaction between cell and the surface on which they are attached. In the present study we report the combined effect of *Geobacter sulfurreducens* adhesion to the QCM gold sensor and electricity generation. We also

observed the mass changes and energy dissipation as a function of time using a continuous flow Quartz crystal microbalance.

Chapter 5: Proteome dependence on terminal electron acceptor in *Geobacter sulfurreducens.*

Proteomics is the large-scale study of proteins, particularly their structures and functions. The focus of proteomics is a biological group called the proteome. The proteome is dynamic, defined as the set of proteins expressed in a specific cell, under particular set of conditions. The proteome is the entire complement of proteins produced by an organism or system. This will vary with time. Proteomics is often considered the next step after genomics in the study of biological systems. In the present study we report the differential protein expression of *Geobacter sulfurreducens* grown on carbon cloth electrode and pure culture.

Chapter 6: Bioelectricity generation from dairy wastewaters in microbial fuel cells.

The experiment was carried out to design a MFC for wastewater treatment with simultaneous electricity production. Two identical MFCs were used with high concentration of synthetic substrate and real dairy wastewater with 4 g/L of COD. The MFCs were operated at sub-ambient temperatures (15 °C) and controlled temperature (30 °C) to evaluate the performance as a form of electricity generation and substrate degradation.

Chapter 7: Modified electrode for anode in microbial fuel cell

Here we report the preliminary findings of the controlled modification of graphite anodes with the electrochemical reduction of aryl diazonium salts, and its subsequent effect on the power output of microbial fuel cells.

Chapter 8: Conclusions and future scope of the study

References

Abourached, C., Catal, T., Liu, H. 2014. Efficacy of single-chamber microbial fuel cells for removal of cadmium and zinc with simultaneous electricity production. *Water Research*, **51**(0), 228-233.

Aelterman, P., Rabaey, K., The Pham, H., Boon, N., Verstraete, W. 2006. Continuous electricity generation at high voltages and currents using stacked microbial fuel cells. *Communications in agricultural and applied biological sciences*, **71**(1), 63-66.

Ahn, Y., Hatzell, M.C., Zhang, F., Logan, B.E. 2014. Different electrode configurations to optimize performance of multi-electrode microbial fuel cells for generating power or treating domestic wastewater. *Journal of Power Sources*, **249**(0), 440-445.

Allen, R.M., Bennetto, H.P. 1993. Microbial fuel-cells - Electricity production from carbohydrates. *Applied Biochemistry and Biotechnology*, **39-40**(1), 27-40.

Behera, M., Ghangrekar, M.M. 2009. Performance of microbial fuel cell in response to change in sludge loading rate at different anodic feed pH. *Bioresource Technology*, **100**(21), 5114-5121.

Behera, M., Jana, P.S., Ghangrekar, M.M. 2010a. Performance evaluation of low cost microbial fuel cell fabricated using earthen pot with biotic and abiotic cathode. *Bioresource Technology*, **101**(4), 1183-1189.

Behera, M., Jana, P.S., More, T.T., Ghangrekar, M.M. 2010b. Rice mill wastewater treatment in microbial fuel cells fabricated using proton exchange membrane and earthen pot at different pH. *Bioelectrochemistry*, **79**(2), 228-233.

Bennetto, H.P., Stirling, J.L., Tanaka, K., Vega, C.A. 1983. Anodic reactions in microbial fuel cells. *Biotechnology and Bioengineering*, **25**(2), 559-568.

Biffinger, J.C., Fitzgerald, L.A., Ray, R., Little, B.J., Lizewski, S.E., Petersen, E.R., Ringeisen, B.R., Sanders, W.C., Sheehan, P.E., Pietron, J.J., Baldwin, J.W., Nadeau, L.J., Johnson, G.R., Ribbens, M., Finkel, S.E., Nealson, K.H. 2011. The utility of Shewanella japonica for microbial fuel cells. *Bioresource Technology*, **102**(1), 290-297.

Biffinger, J.C., Pietron, J., Ray, R., Little, B., Ringeisen, B.R. 2007. A biofilm enhanced miniature microbial fuel cell using Shewanella oneidensis DSP10 and oxygen reduction cathodes. *Biosensors and Bioelectronics*, **22**(8), 1672-1679.

Bond, D.R., Holmes, D.E., Tender, L.M., Lovley, D.R. 2002. Electrode-reducing microorganisms that harvest energy from marine sediments. *Science*, **295**(5554), 483-485.

Bond, D.R., Lovley, D.R. 2003. Electricity production by Geobacter sulfurreducens attached to electrodes. *Applied and Environmental Microbiology*, **69**(3), 1548-1555.

Bond, D.R., Strycharz-Glaven, S.M., Tender, L.M., Torres, C.I. 2012. On Electron Transport through Geobacter Biofilms. *ChemSusChem*, **5**(6), 1099-1105.

Borole, A.P., Reguera, G., Ringeisen, B., Wang, Z.W., Feng, Y., Kim, B.H. 2011. Electroactive biofilms: Current status and future research needs. *Energy and Environmental Science*, **4**(12), 4813-4834.

Cao, X., Huang, X., Liang, P., Xiao, K., Zhou, Y., Zhang, X., Logan, B.E. 2009a. A new method for water desalination using microbial desalination cells. *Environmental Science and Technology*, **43**(18), 7148-7152.

Cao, X.X., Fan, M.Z., Liang, P., Huang, X. 2009b. Effects of anode potential on the electricity generation performance of geobacter sulfurreducens. *Gaodeng Xuexiao Huaxue Xuebao/Chemical Journal of Chinese Universities*, **30**(5), 983-987.

Chae, K.J., Choi, M.J., Kim, K.Y., Ajayi, F.F., Park, W., Kim, C.W., Kim, I.S. 2010. Methanogenesis control by employing various environmental stress conditions in two-chambered microbial fuel cells. *Bioresource Technology*, **101**(14), 5350-5357.

Cheng, S., Liu, H., Logan, B.E. 2006. Increased power generation in a continuous flow MFC with advective flow through the porous anode and reduced electrode spacing. *Environmental Science and Technology*, **40**(7), 2426-2432.

Cheng, S., Logan, B.E. 2007. Sustainable and efficient biohydrogen production via electrohydrogenesis. *Proceedings of the National Academy of Sciences of the United States of America*, **104**(47), 18871-18873.

Donovan, C., Dewan, A., Peng, H., Heo, D., Beyenal, H. 2011. Power management system for a 2.5 W remote sensor powered by a sediment microbial fuel cell. *Journal of Power Sources*, **196**(3), 1171-1177.

Du, Z., Li, H., Gu, T. 2007. A state of the art review on microbial fuel cells: A promising technology for wastewater treatment and bioenergy. *Biotechnology Advances*, **25**(5), 464-482.

Dumas, C., Basseguy, R., Bergel, A. 2008. Electrochemical activity of Geobacter sulfurreducens biofilms on stainless steel anodes. *Electrochimica Acta*, **53**(16), 5235-5241.

Fan, Y., Han, S.-K., Liu, H. 2012. Improved performance of CEA microbial fuel cells with increased reactor size. *Energy and Environmental Science*, **5**(8), 8273-8280.

Fan, Y., Hu, H., Liu, H. 2007. Enhanced coulombic efficiency and power density of air-cathode microbial fuel cells with an improved cell configuration. *Journal of Power Sources*, **171**(2), 348-354.

Feng, Y., Wang, X., Logan, B.E., Lee, H. 2008. Brewery wastewater treatment using air-cathode microbial fuel cells. *Applied Microbiology and Biotechnology*, **78**(5), 873-880.

Foley, J.M., Rozendal, R.A., Hertle, C.K., Lant, P.A., Rabaey, K. 2010. Life cycle assessment of high-rate anaerobic treatment, microbial fuel cells, and microbial electrolysis cells. *Environmental Science and Technology*, **44**(9), 3629-3637.

Freguia, S., Rabaey, K., Yuan, Z., Keller, J. 2007. Non-catalyzed cathodic oxygen reduction at graphite granules in microbial fuel cells. *Electrochimica Acta*, **53**(2), 598-603.

Gil, G.C., Chang, I.S., Kim, B.H., Kim, M., Jang, J.K., Park, H.S., Kim, H.J. 2003. Operational parameters affecting the performance of a mediator-less microbial fuel cell. *Biosensors and Bioelectronics*, **18**(4), 327-334.

Harnisch, F., Schröder, U., Scholz, F. 2008. The suitability of monopolar and bipolar ion exchange membranes as separators for biological fuel cells. *Environmental science & technology*, **42**(5), 1740-1746.

Hasan, K., Patil, S.A., Górecki, K., Leech, D., Hägerhäll, C., Gorton, L. 2013. Electrochemical communication between heterotrophically grown Rhodobacter capsulatus with electrodes mediated by an osmium redox polymer. *Bioelectrochemistry*, **93**(0), 30-36.

He, Z., Huang, Y., Manohar, A.K., Mansfeld, F. 2008. Effect of electrolyte pH on the rate of the anodic and cathodic reactions in an air-cathode microbial fuel cell. *Bioelectrochemistry*, **74**(1), 78-82.

He, Z., Minteer, S.D., Angenent, L.T. 2005. Electricity generation from artificial wastewater using an upflow microbial fuel cell. *Environmental Science and Technology*, **39**(14), 5262-5267.

Heilmann, J., Logan, B.E. 2006. Production of electricity from proteins using a microbial fuel cell. *Water Environment Research*, **78**(5), 531-537.

Huang, L., Zeng, R.J., Angelidaki, I. 2008. Electricity production from xylose using a mediator-less microbial fuel cell. *Bioresource Technology*, **99**(10), 4178-4184.

Ieropoulos, I., Greenman, J., Melhuish, C., Hart, J. 2005a. Energy accumulation and improved performance in microbial fuel cells. *Journal of Power Sources*, **145**(2), 253-256.

Ieropoulos, I., Winfield, J., Greenman, J. 2010. Effects of flow-rate, inoculum and time on the internal resistance of microbial fuel cells. *Bioresource Technology*, **101**(10), 3520-3525.

Ieropoulos, I.A., Greenman, J., Melhuish, C., Hart, J. 2005b. Comparative study of three types of microbial fuel cell. *Enzyme and Microbial Technology*, **37**(2), 238-245.

Jana, P.S., Behera, M., Ghangrekar, M.M. 2010. Performance comparison of up-flow microbial fuel cells fabricated using proton exchange membrane and earthen cylinder. *International Journal of Hydrogen Energy*, **35**(11), 5681-5686.

Kalathil, S., Lee, J., Cho, M.H. 2011. Granular activated carbon based microbial fuel cell for simultaneous decolorization of real dye wastewater and electricity generation. *New Biotechnology*, **29**(1), 32-37.

Katuri, K.P., Enright, A.M., O'Flaherty, V., Leech, D. 2012. Microbial analysis of anodic biofilm in a microbial fuel cell using slaughterhouse wastewater. *Bioelectrochemistry*, **87**, 164-171.

Ki, D., Park, J., Lee, J., Yoo, K. 2008. Microbial diversity and population dynamics of activated sludge microbial communities participating in electricity generation in microbial fuel cells, *Water Science and Technology*, 58, 2195-2201.

Kim, B.H., Chang, I.S., Gadd, G.M. 2007a. Challenges in microbial fuel cell development and operation. *Applied Microbiology and Biotechnology*, **76**(3), 485-494.

Kim, B.H., Chang, I.S., Gil, G.C., Park, H.S., Kim, H.J. 2003. Novel BOD (biological oxygen demand) sensor using mediator-less microbial fuel cell. *Biotechnology Letters*, **25**(7), 541-545.

Kim, B.H., Ikeda, T., Park, H.S., Kim, H.J., Hyun, M.S., Kano, K., Takagi, K., Tatsumi, H. 1999. Electrochemical activity of an Fe(III)-reducing bacterium, Shewanella putrefaciens IR-1, in the presence of alternative electron acceptors. *Biotechnology Techniques*, **13**(7), 475-478.

Kim, B.H., Park, H.S., Kim, H.J., Kim, G.T., Chang, I.S., Lee, J., Phung, N.T. 2004. Enrichment of microbial community generating electricity using a fuel-cell-type electrochemical cell. *Applied Microbiology and Biotechnology*, **63**(6), 672-681.

Kim, J.R., Cheng, S., Oh, S.-E., Logan, B.E. 2007b. Power generation using different cation, anion, and ultrafiltration membranes in microbial fuel cells. *Environmental Science and Ttechnology*, **41**(3), 1004-1009.

Kim, J.R., Min, B., Logan, B.E. 2005. Evaluation of procedures to acclimate a microbial fuel cell for electricity production. *Applied Microbiology and Biotechnology*, **68**(1), 23-30.

Kim, J.R., Premier, G.C., Hawkes, F.R., Rodríguez, J., Dinsdale, R.M., Guwy, A.J. 2010. Modular tubular microbial fuel cells for energy recovery during sucrose wastewater treatment at low organic loading rate. *Bioresource Technology*, **101**(4), 1190-1198.

Kim, M., Park, H.S., Jin, G.J., Cho, W.H., Lee, D.K., Hyun, M.S., Choi, C.H., Kim, H.J. 2006. A novel combined biomonitoring system for BOD measurement and toxicity detection using microbial fuel cells. *5th IEEE Conference*, 1247-1248.

Kim, Y., Logan, B.E. 2013. Microbial desalination cells for energy production and desalination. *Desalination*, **308**(0), 122-130.

Kreth, J., Hagerman, E., Tam, K., Merritt, J., Wong, D., Wu, B., Myung, N., Shi, W., Qi, F. 2004. Quantitative analyses of Streptococcus mutans biofilms with quartz

crystal microbalance, microjet impingement and confocal microscopy. *Biofilms*, **1**(4), 277-284.

Larminie, J., Dicks, A. 2013. Proton Exchange Membrane Fuel Cells. in: *Fuel Cell Systems Explained*, John Wiley & Sons, Ltd,. pp. 67-119.

Lefebvre, O., Shen, Y., Tan, Z., Uzabiaga, A., Chang, I.S., Ng, H.Y. 2011. A comparison of membranes and enrichment strategies for microbial fuel cells. *Bioresource Technology*, **102**(10), 6291-6294.

Li, J., Fu, Q., Liao, Q., Zhu, X., Ye, D.d., Tian, X. 2009. Persulfate: A self-activated cathodic electron acceptor for microbial fuel cells. *Journal of Power Sources*, **194**(1), 269-274.

Listowski, A., Ngo, H., Guo, W., Vigneswaran, S., Shin, H., Moon, H. 2011. Greenhouse gas (GHG) emissions from urban wastewater system: future assessment framework and methodology. *Journal of Water Sustainability*, **1**(1), 113-125.

Liu, B., Li, B. 2014. Single chamber microbial fuel cells (SCMFCs) treating wastewater containing methanol. *International Journal of Hydrogen Energy*, **39**(5), 2340-2344.

Liu, H., Grot, S., Logan, B.E. 2005. Electrochemically assisted microbial production of hydrogen from acetate. *Environmental Science and Technology*, **39**(11), 4317-4320.

Liu, H., Logan, B. 2004a. Electricity generation using an air-cathode single chamber microbial fuel cell (MFC) in the absence of a proton exchange membrane. *Environmental science & technology*, 38(14), 4040-4046.

Liu, H., Logan, B.E. 2004b. Electricity generation using an air-cathode single chamber microbial fuel cell in the presence and absence of a proton exchange membrane. *Environmental Science and Technology*, **38**(14), 4040-4046.

Liu, H., Ramnarayanan, R., Logan, B.E. 2004. Production of electricity during wastewater treatment using a single chamber microbial fuel cell. *Environmental Science and Technology*, **38**(7), 2281-2285.

Liu, J., Qiao, Y., Guo, C.X., Lim, S., Song, H., Li, C.M. 2012. Graphene/carbon cloth anode for high-performance mediatorless microbial fuel cells. *Bioresource Technology*, **114**(0), 275-280.

Liu, Z.D., Du, Z.W., Lian, J., Zhu, X.Y., Li, S.H., Li, H.R. 2007. Improving energy accumulation of microbial fuel cells by metabolism regulation using Rhodoferax ferrireducens as biocatalyst. *Letters in Applied Microbiology*, **44**(4), 393-398.

Liu, Z.D., Li, H.R. 2007. Effects of bio- and abio-factors on electricity production in a mediatorless microbial fuel cell. *Biochemical Engineering Journal*, **36**(3), 209-214.

Logan, B.E. 2005. Simultaneous wastewater treatment and biological electricity generation. *Water Science Technology*, 52, 31-37.

Logan, B.E., Hamelers, B., Rozendal, R., Schröder, U., Keller, J., Freguia, S., Aelterman, P., Verstraete, W., Rabaey, K. 2006b. Microbial fuel cells: Methodology and technology†. *Environmental Science and Technology*, **40**(17), 5181-5192.

Logan, B.E., Murano, C., Scott, K., Gray, N.D., Head, I.M. 2005. Electricity generation from cysteine in a microbial fuel cell. *Water Research*, **39**(5), 942-952.

Logan, B.E., Regan, J.M. 2006. Microbial fuel cells - Challenges and applications. *Environmental Science and Technology*, **40**(17), 5172-5180.

Lovley, D.R. 2006a. Bug juice: harvesting electricity with microorganisms. *Nature Reviews. Microbiology*, **4**(7), 497-508.

Lovley, D.R. 2006b. Microbial fuel cells: novel microbial physiologies and engineering approaches. *Current Opinion in Biotechnology*, **17**(3), 327-332.

Mahdi Mardanpour, M., Nasr Esfahany, M., Behzad, T., Sedaqatvand, R. 2012. Single chamber microbial fuel cell with spiral anode for dairy wastewater treatment. *Biosensors and Bioelectronics*, **38**(1), 264-269.

Marcus, I.M., Herzberg, M., Walker, S.L., Freger, V. 2012. Pseudomonas aeruginosa attachment on QCM-D sensors: the role of cell and surface hydrophobicities. *Langmuir*, **28**(15), 6396-6402.

Marsili, E., Baron, D.B., Shikhare, I.D., Coursolle, D., Gralnick, J.A., Bond, D.R. 2008. Shewanella secretes flavins that mediate extracellular electron transfer. *Proceedings of the National Academy of Sciences*, **105**(10), 3968-3973.

Martin, E., Savadogo, O., Guiot, S.R., Tartakovsky, B. 2010. The influence of operational conditions on the performance of a microbial fuel cell seeded with mesophilic anaerobic sludge. *Biochemical Engineering Journal*, **51**(3), 132-139.

Min, B., Cheng, S., Logan, B.E. 2005. Electricity generation using membrane and salt bridge microbial fuel cells. *Water Research*, **39**(9), 1675-1686.

Min, B., Logan, B.E. 2004. Continuous electricity generation from domestic wastewater and organic substrates in a flat plate microbial fuel cell. *Environmental Science and Technology*, **38**(21), 5809-5814.

Moon, H., Chang, I.S., Kang, K.H., Jang, J.K., Kim, B.H. 2004. Improving the dynamic response of a mediator-less microbial fuel cell as a biochemical oxygen demand (BOD) sensor. *Biotechnology Letters*, **26**(22), 1717-1721.

Morris, J.M., Jin, S., Wang, J., Zhu, C., Urynowicz, M.A. 2007. Lead dioxide as an alternative catalyst to platinum in microbial fuel cells. *Electrochemistry Communications*, **9**(7), 1730-1734.

Nam, J.-Y., Kim, H.-W., Lim, K.-H., Shin, H.-S. 2010. Effects of organic loading rates on the continuous electricity generation from fermented wastewater using a single-chamber microbial fuel cell. *Bioresource Technology*, **101**(1, Supplement), S33-S37.

Newman, M.E.H.a.D.K. 2001. Extracellular electron transfer. *Cellular and Molecular Life Sciences*, **58**, 1562-1571.

Niessen, J., Harnisch, F., Rosenbaum, M., Schröder, U., Scholz, F. 2006. Heat treated soil as convenient and versatile source of bacterial communities for microbial electricity generation. *Electrochemistry Communications*, **8**(5), 869-873.

Oh, S., Logan, B.E. 2005. Hydrogen and electricity production from a food processing wastewater using fermentation and microbial fuel cell technologies. *Water Research*, **39**(19), 4673-4682.

Oh, S., Min, B., Logan, B.E. 2004. Cathode performance as a factor in electricity generation in microbial fuel cells. *Environmental Science and Technology*, **38**(18), 4900-4904.

Oh, S.E., Logan, B.E. 2006. Proton exchange membrane and electrode surface areas as factors that affect power generation in microbial fuel cells. *Applied Microbiology and Biotechnology*, **70**(2), 162-169.

Oh, S.E., Logan, B.E. 2007. Voltage reversal during microbial fuel cell stack operation. *Journal of Power Sources*, **167**(1), 11-17.

Oliveira, V.B., Simões, M., Melo, L.F., Pinto, A.M.F.R. 2013. Overview on the developments of microbial fuel cells. *Biochemical Engineering Journal*, **73**, 53-64.

Olsson, A.L., van der Mei, H.C., Busscher, H.J., Sharma, P.K. 2008. Influence of cell surface appendages on the bacterium− substratum interface measured real-time using QCM-D. *Langmuir*, **25**(3), 1627-1632.

Otto, K., Silhavy, T.J. 2002. Surface sensing and adhesion of Escherichia coli controlled by the Cpx-signaling pathway. *Proceedings of the National Academy of Sciences*, **99**(4), 2287-2292.

Pant, D., Van Bogaert, G., De Smet, M., Diels, L., Vanbroekhoven, K. 2010. Use of novel permeable membrane and air cathodes in acetate microbial fuel cells. *Electrochimica Acta*, **55**(26), 7710-7716.

Park, D.H., Zeikus, J.G. 2000. Electricity generation in microbial fuel cells using neutral red as an electronophore. *Applied and Environmental Microbiology*, **66**(4), 1292-1297.

Park, D.H., Zeikus, J.G. 2003. Improved fuel cell and electrode designs for producing electricity from microbial degradation. *Biotechnology and Bioengineering*, **81**(3), 348-355.

Pasco, N., Hay, J., Scott, A., Webber, J. 2005. Redox coupling to microbial respiration: an evaluation of secondary mediators as binary mixtures with ferricyanide. *Australian Journal of Chemistry*, **58**(4), 288-293.

Patil, S.A., Harnisch, F., Koch, C., Hübschmann, T., Fetzer, I., Carmona-Martínez, A.A., Müller, S., Schröder, U. 2011. Electroactive mixed culture derived biofilms in microbial bioelectrochemical systems: The role of pH on biofilm formation, performance and composition. *Bioresource Technology*, **102**(20), 9683-9690.

Patil, S.A., Surakasi, V.P., Koul, S., Ijmulwar, S., Vivek, A., Shouche, Y.S., Kapadnis, B.P. 2009. Electricity generation using chocolate industry wastewater and its treatment in activated sludge based microbial fuel cell and analysis of developed microbial community in the anode chamber. *Bioresource Technology*, **100**(21), 5132-5139.

Picot, M., Lapinsonnière, L., Rothballer, M., Barrière, F. 2011. Graphite anode surface modification with controlled reduction of specific aryl diazonium salts for

improved microbial fuel cells power output. *Biosensors and Bioelectronics*, **28**(1), 181-188.

Rabaey, K., Boon, N., Denef, V., Verhaege, M., Höfte, M., Verstraete, W. 2004a. Bacteria produce and use redox mediators for electron transfer in microbial fuel cells. Philadelphia, PA. pp. 1481-1484.

Rabaey, K., Boon, N., Siciliano, S.D., Verhaege, M., Verstraete, W. 2004b. Biofuel cells select for microbial consortia that self-mediate electron transfer. *Applied and Environmental Microbiology*, **70**(9), 5373-5382.

Rabaey, K., Clauwaert, P., Aelterman, P., Verstraete, W. 2005. Tubular microbial fuel cells for efficient electricity generation. *Environmental Science and Technology*, **39**(20), 8077-8082.

Rabaey, K., Girguis, P., Nielsen, L.K. 2011. Metabolic and practical considerations on microbial electrosynthesis. *Current Opinion in Biotechnology*, **22**(3), 371-377.

Rabaey, K., Lissens, G., Siciliano, S.D., Verstraete, W. 2003. A microbial fuel cell capable of converting glucose to electricity at high rate and efficiency. *Biotechnology Letters*, **25**(18), 1531-1535.

Rabaey, K., Verstraete, W. 2005. Microbial fuel cells: novel biotechnology for energy generation. *Trends in Biotechnology*, **23**(6), 291-298.

Raghavulu, S.V., Mohan, S.V., Goud, R.K., Sarma, P.N. 2009. Effect of anodic pH microenvironment on microbial fuel cell (MFC) performance in concurrence with aerated and ferricyanide catholytes. *Electrochemistry Communications*, **11**(2), 371-375.

Reguera, G., Nevin, K.P., Nicoll, J.S., Covalla, S.F., Woodard, T.L., Lovley, D.R. 2006. Biofilm and nanowire production leads to increased current in Geobacter sulfurreducens fuel cells. *Applied and Environmental Microbiology*, **72**(11), 7345-7348.

Ringeisen, B.R., Henderson, E., Wu, P.K., Pietron, J., Ray, R., Little, B., Biffinger, J.C., Jones-Meehan, J.M. 2006. High power density from a miniature microbial fuel cell using Shewanella oneidensis DSP10. *Environmental Science and Technology*, **40**(8), 2629-2634.

Rismani-Yazdi, H., Carver, S.M., Christy, A.D., Tuovinen, O.H. 2008. Cathodic limitations in microbial fuel cells: A overview. *Journal of Power Sources*, **180**(2), 683-694.

Rismani-Yazdi, H., Christy, A.D., Dehority, B.A., Morrison, M., Yu, Z., Tuovinen, O.H. 2007. Electricity generation from cellulose by rumen microorganisms in microbial fuel cells. *Biotechnology and Bioengineering*, **97**(6), 1398-1407.

Rochex, A., Godon, J.-J., Bernet, N., Escudié, R. 2008. Role of shear stress on composition, diversity and dynamics of biofilm bacterial communities. *Water Research*, **42**(20), 4915-4922.

Rozendal, R.A., Hamelers, H.V.M., Euverink, G.J.W., Metz, S.J., Buisman, C.J.N. 2006. Principle and perspectives of hydrogen production through biocatalyzed electrolysis. *International Journal of Hydrogen Energy*, **31**(12), 1632-1640.

Schaetzle, O., Barrière, F., Baronian, K. 2008. Bacteria and yeasts as catalysts in microbial fuel cells: Electron transfer from micro-organisms to electrodes for green electricity. *Energy and Environmental Science*, **1**(6), 607-620.

Sciarria, T.P., Tenca, A., D'Epifanio, A., Mecheri, B., Merlino, G., Barbato, M., Borin, S., Licoccia, S., Garavaglia, V., Adani, F. 2013. Using olive mill wastewater to improve performance in producing electricity from domestic wastewater by using single-chamber microbial fuel cell. *Bioresource Technology*, **147**(0), 246-253.

Scott, K., Cotlarciuc, I., Hall, D., Lakeman, J.B., Browning, D. 2008. Power from marine sediment fuel cells: The influence of anode material. *Journal of Applied Electrochemistry*, **38**(9), 1313-1319.

Scott, K., Murano, C. 2007. Microbial fuel cells utilising carbohydrates. *Journal of Chemical Technology and Biotechnology*, **82**(1), 92-100.

Shantaram, A., Beyenal, H., Veluchamy, R.R.A., Lewandowski, Z. 2005. Wireless sensors powered by microbial fuel cells. *Environmental Science and Technology*, **39**(13), 5037-5042.

Strycharz-Glaven, S.M., Snider, R.M., Guiseppi-Elie, A., Tender, L.M. 2011. On the electrical conductivity of microbial nanowires and biofilms. *Energy and Environmental Science*, **4**(11), 4366-4379.

Sukkasem, C., Xu, S., Park, S., Boonsawang, P., Liu, H. 2008. Effect of nitrate on the performance of single chamber air cathode microbial fuel cells. *Water Research*, **42**(19), 4743-4750.

Sun, J., Hu, Y., Bi, Z., Cao, Y. 2009. Improved performance of air-cathode single-chamber microbial fuel cell for wastewater treatment using microfiltration membranes and multiple sludge inoculation. *Journal of Power Sources*, **187**(2), 471-479.

Sydow, A., Krieg, T., Mayer, F., Schrader, J., Holtmann, D. 2014. Electroactive bacteria—molecular mechanisms and genetic tools. *Applied Microbiology and Biotechnology*, 1-15.

Tartakovsky, B., Guiot, S.R. 2006. A comparison of air and hydrogen peroxide oxygenated microbial fuel cell reactors. *Biotechnology Progress*, **22**(1), 241-246.

Ter Heijne, A., Hamelers, H.V.M., De Wilde, V., Rozendal, R.A., Buisman, C.J.N. 2006. A bipolar membrane combined with ferric iron reduction as an efficient cathode system in microbial fuel cells. *Environmental Science and Technology*, **40**(17), 5200-5205.

Vega, C.A., Fernández, I. 1987. Mediating effect of ferric chelate compounds in microbial fuel cells with Lactobacillus plantarum, Streptococcus lactis, and Erwinia dissolvens. *Bioelectrochemistry and Bioenergetics*, **17**(2), 217-222.

Velvizhi, G., Venkata Mohan, S. 2012. Electrogenic activity and electron losses under increasing organic load of recalcitrant pharmaceutical wastewater. *International Journal of Hydrogen Energy*, **37**(7), 5969-5978.

Venkata Mohan, S., Mohanakrishna, G., Velvizhi, G., Babu, V.L., Sarma, P.N. 2010. Bio-catalyzed electrochemical treatment of real field dairy wastewater with simultaneous power generation. *Biochemical Engineering Journal*, **51**(1-2), 32-39.

Von Canstein, H., Ogawa, J., Shimizu, S., Lloyd, J.R. 2008. Secretion of flavins by Shewanella species and their role in extracellular electron transfer. *Applied and Environmental Microbiology*, **74**(3), 615-623.

Wang, G., Huang, L., Zhang, Y. 2008. Cathodic reduction of hexavalent chromium [Cr(VI)] coupled with electricity generation in microbial fuel cells. *Biotechnology Letters*, **30**(11), 1959-1966.

White, S. 2008. Sustainable water: Chemical Science Priorities, RSC Report.

You, J., Greenman, J., Melhuish, C., Ieropoulos, I. 2014. Small-scale microbial fuel cells utilising uric salts. *Sustainable Energy Technologies and Assessments*, **6**(0), 60-63.

You, S., Zhao, Q., Zhang, J., Jiang, J., Zhao, S. 2006a. A microbial fuel cell using permanganate as the cathodic electron acceptor. *Journal of Power Sources*, **162**(2 SPEC. ISS.), 1409-1415.

You, S.J., Zhang, J.N., Yuan, Y.X., Ren, N.Q., Wang, X.H. 2010. Development of microbial fuel cell with anoxic/oxic design for treatment of saline seafood wastewater and biological electricity generation. *Journal of Chemical Technology and Biotechnology*, **85**(8), 1077-1083.

You, S.J., Zhao, Q.L., Jiang, J.Q., Zhang, J.N. 2006b. Treatment of domestic wastewater with simultaneous electricity generation in microbial fuel cell under continuous operation. *Chemical and Biochemical Engineering Quarterly*, **20**(4), 407-412.

Zhang, E., Xu, W., Diao, G., Shuang, C. 2006. Electricity generation from acetate and glucose by sedimentary bacterium attached to electrode in microbial-anode fuel cells. *Journal of Power Sources*, **161**(2), 820-825.

Zhang, F., Pant, D., Logan, B.E. 2011. Long-term performance of activated carbon air cathodes with different diffusion layer porosities in microbial fuel cells. *Biosensors and Bioelectronics*, **30**(1), 49-55.

Zhang, X., Cheng, S., Wang, X., Huang, X., Logan, B.E. 2009. Separator characteristics for increasing performance of microbial fuel cells. *Environmental Science and Technology*, **43**(21), 8456-8461.

Zhao, F., Harnisch, F., Schröder, U., Scholz, F., Bogdanoff, P., Herrmann, I. 2005. Application of pyrolysed iron(II) phthalocyanine and CoTMPP based oxygen reduction catalysts as cathode materials in microbial fuel cells. *Electrochemistry Communications*, **7**(12), 1405-1410.

Zhao, F., Harnisch, F., Schröder, U., Scholz, F., Bogdanoff, P., Herrmann, I. 2006. Challenges and constraints of using oxygen cathodes in microbial fuel cells. *Environmental Science and Technology*, **40**(17), 5193-5199.

Zhong, C., Zhang, B., Kong, L., Xue, A., Ni, J. 2011. Electricity generation from molasses wastewater by an anaerobic baffled stacking microbial fuel cell. *Journal of Chemical Technology and Biotechnology*, **86**(3), 406-413.

Zhou, L., Liu, Z., Lian, J., Li, F., Du, Z., Li, H. 2005. Microbial fuel cell used in study on dissimilatory ferric oxides reduction by Geobacter metallireducens. *Huagong Xuebao/Journal of Chemical Industry and Engineering (China)*, **56**(12), 2398-2403.

Zhuang, L., Zhou, S., Li, Y., Yuan, Y. 2010. Enhanced performance of air-cathode two-chamber microbial fuel cells with high-pH anode and low-pH cathode. *Bioresource Technology*, **101**(10), 3514-3519.

Chapter 2

Comparison of performance of an earthen plate and Nafion as membrane separators in dual chamber microbial fuel cells

2.1 Introduction

Microbial fuel cells (MFC) are an emerging technology which has been paid much attention in recent years (Logan *et al.,* 2006; Logan & Regan 2006; Harnisch *et al.,* 2008; Zuo *et al.,* 2008; Zhang *et al.,* 2009) for application to wastewater treatment with simultaneous electricity generation. A MFC is a bio-electrochemical system (BES) where bacteria catalyze the degradation of organic matter under anaerobic conditions to convert energy stored in chemical bonds of organic compounds to electrical energy. The MFC performance is affected by many factors, such as reactor configuration, type of electrode material and membrane separator, solution pH, temperature, substrate type and concentration, hydraulic retention time (HRT), inoculum selection or enrichment, cathodic electron acceptor selection, etc (Pant *et al,.* 2010; Pant *et al.,* 2012). In the past decade many advances have been made in MFC research aimed at enhancing MFC (Park & Zeikus 2003; Rabaey *et al.,* 2004; Min *et al.,* 2005; Logan *et al.,* 2006). However, MFC construction, operation and maintenance cost, still need to be minimized to make this technology sustainable on economical ground (Logan & Regan 2006; Zuo *et al.,* 2008).

The characteristics of the membrane separator selected can significantly affect the performance of an MFC (Zhang *et al.,* 2009). Nafion is the most widely

used membrane separator because of the high proton conductivity (Logan *et al.,* 2006; Harnisch *et al.,* 2008) but is not necessarily the best separator under neutral pH conditions used in MFCs. The high cost of Nafion makes the potential production cost of MFC commercially unacceptable (Pant *et al.,* 2010). Many studies explore use of various other separators for MFC (Park & Zeikus 2003; Rabaey *et al.,* 2004; Min *et al.,* 2005; Logan & Regan 2006; Ter Heijne *et al.,* 2006; Fan *et al.,* 2007; Sun *et al.,* 2009; Behera *et al.,* 2010a; Martin *et al.,* 2010; Lefebvre *et al.,* 2011). For example, the use of a salt bridge (Min *et al.,* 2005), ultrex membrane (Rabaey *et al.,* 2004), a porcelain septum made from kaolin (Park & Zeikus 2003), anion exchange membranes (Martin *et al.* 2010), bipolar membranes (Ter Heijne *et al.,* 2006), microfiltration membranes (Sun *et al.,* 2009), J-Cloths (Fan *et al.,* 2007), a selemion HSF membrane (Logan *et al.,* 2006), ultrafiltration discs (Lefebvre *et al.,* 2011) as separators in MFCs has been reported. We recently (Behera *et al.,* 2010a; Behera *et al.,* 2010b) reported on the treatment of synthetic and rice mill wastewater in fed-batch MFCs fabricated using an earthen pot acting as both anode half-cell container, and a membrane separator, with the performance compared to MFCs fabricated using a Nafion membrane separator (Jana *et al.,* 2010). The earthen pot MFCs demonstrated better performance in terms of organic matter removal and electricity generation compared to the Nafion membrane, but the surface area available for ion transfer through the wall of earthenware was much larger than that in the Nafion-based MFC, making direct comparison difficult in that study. The thickness of the earthen pot membrane/anode container was also shown to affect both MFC internal resistances, and as a consequence MFC power generation (Behera & Ghangrekar 2011). The present report focuses on an effort to better compare performances of MFCs operated using the earthen plate as membrane separator to that of Nafion separated MFCs; by fabrication of polyacrylate MFCs with earthen plate separator of the same exposed geometrical surface area to that of the Nafion separator. The comparison of MFC performance is evaluated by operation of both types of MFC under continuous mode feeding of acetate as synthetic waste, following initial batch incubation with acetate and anaerobic sludge, as inoculums, and using a model ferricyanide solution as oxidant in the catholyte.

2.2 Material and methods

2.2.1. Experimental set-up

The study was carried out in two identical up-flow dual chambered polyacrylic MFCs separated by the same exposed area of either a Nafion117 proton-exchange membrane (PEM, Sigma Aldrich) or an earthen plate membrane (EP, 3.7 mm thick). The earthen plates were prepared from soil (elemental composition: Al-32%, Si-47.80%, K-4.90%, Ca-1.20%, Ti-0.90%, Fe-13%) sourced from Midnapore, India and baked at 550-650°C for 6.0 hours, as described previously (Behera *et al.* 2010a). The cylindrical MFCs consisted of a cylindrical outer catholyte chamber separated from a rectangular polyacrylic inner anolyte chamber, with membranes inserted in two, opposite, faces of the inner chamber (Fig.1). Each membrane was of 20 cm^2 surface area, making the total exposed membrane surface area of 40 cm^2. The working volume of the anolyte chamber of both MFCs was 350 mL, whilst that of the catholyte chamber was 1200 mL.

Two graphite plates of 70 cm^2 each were used as electrodes and placed in the anolyte and catholyte, giving a total surface area of 140 cm^2 each for anode and cathode in all MFCs. The electrodes were connected externally with titanium wire through an external resistance of 100 Ω. The cell culture medium anolyte was supplied to the MFCs from the bottom of the anode chamber using a peristaltic pump (Gilson, France) with effluent exiting at the top of the reactor. The catholyte consisted of 50 mM ferricyanide in 100 mM phosphate buffer (pH 7.0).

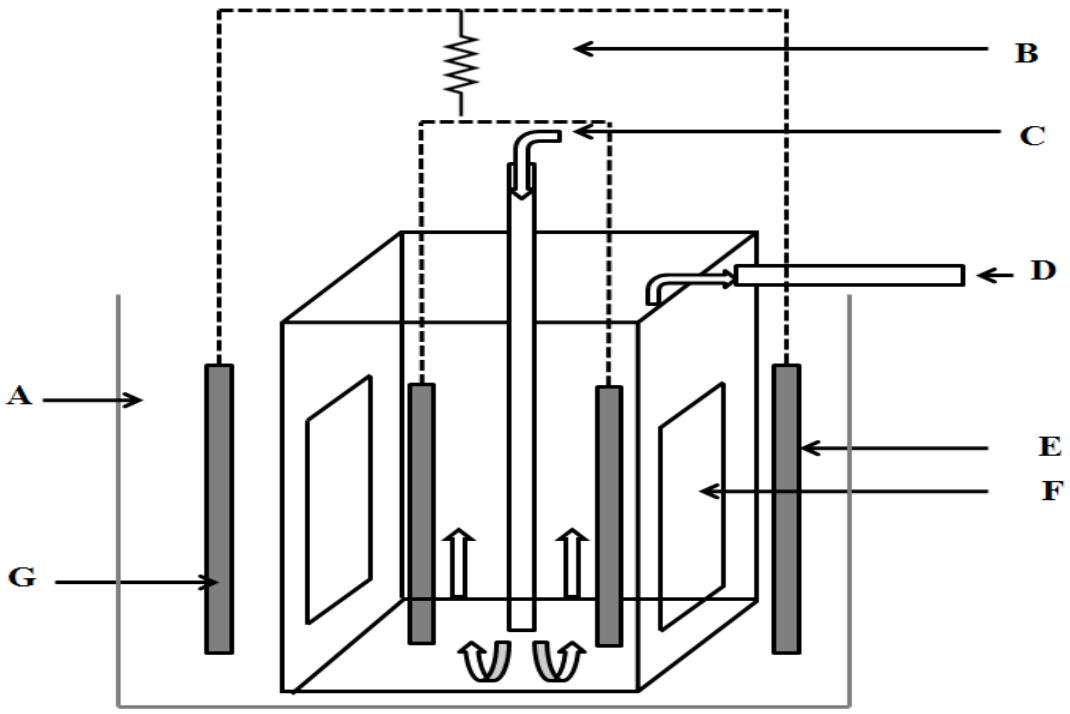

Figure 2.1 Schematic diagram of the MFCs used in the study: (A) $K_3Fe(CN)_6$ catholyte (B) external resistance load (C) cell culture medium anolyte influent (D) anolyte effluent (E) cathode (F) membrane (G) anode.

2.2.2 MFC operation

The MFCs were inoculated with anaerobic sludge collected from an anaerobic digester (Mutton Island wastewater treatment center, Galway). The granular sludge was crushed in a grinder for 10 seconds and 60 mL of the resultant sludge was added to the anode chamber to establish a sludge loading at 0.75 kg COD kg VSS^{-1} (Behera & Ghangrekar 2009). Synthetic media containing acetate as a source of electron donor having COD of 1250 mg L^{-1} was used as feed. The acetate medium also contained (per L): 0.1 g KCl, 0.15 g NH_4Cl, 0.6 g Na_2HPO_4, 2.5 g $NaHCO_3$, 10 mL trace element solution and 10 mL vitamin solution (Katuri *et al.* 2012b) prepared according to http://www.dsmz.de (medium No. 826). The feed pH was in the range of 7.2-7.5 throughout the experiments and the MFCs were operated at temperatures that varied from 28 to 32 ^{o}C. Initially both the MFCs were operated

under batch mode condition to encourage the attachment of electrogenic bacteria to the graphite plate anodes. The first batch consisted of the inoculum supplemented with 290 mL of acetate medium, with the two subsequent batches prepared by replacement of half of the anolyte volume by acetate medium (no additional inoculums). After these three feed cycles, the MFCs were operated in continuous mode at organic loading rate (OLR) of 2.5 kg COD m^{-3} d^{-1}, by maintaining a hydraulic retention time (HRT) of 12 h using the peristaltic pump. After reaching a steady state voltage output across the 100 Ω resistors, the performance of PEM-MFC and EP-MFC was evaluated by polarization experiments using a CH instruments 650 potentiostat (USA).

2.2.3. Analyses and calculations

The cell voltages were recorded continuously using a digital multimeter with data acquisition unit (Pico data logger, UK) throughout the batch and continuous feed experiments by connecting anode and cathode across a 100 Ω external resistor. Current (*I)* was calculated using Ohm's law ($I = V/R$) with MFC power estimated by $P = IV$, where I is cell current and V is the cell voltage. Polarization studies were carried out for the MFCs by linear sweep voltammetry at a scan rate of 1 mVs^{-1} using a potentiostat (CH instruments, USA) with a two electrode assembly system. Power density was normalized to the anode surface area. Internal resistance of the MFCs was estimated from the slope of linear portion of the plot of voltage versus current (Picioreanu *et al.* 2007).

The SS, VSS, and COD levels were monitored according to APHA standard methods (APHA 1998). Chemical compositions of earthen plates were estimated from Scanning Electron Microscopy (SEM, Hitachi SU-70) images with Energy Dispersive X-ray Microanalysis (EDX, Oxford Instruments). Nitrogen absorption isotherms measured with an ASAP2010 adsorption analyser were used to estimate earthen plate membrane specific surface area, using the Brunauer–Emmett–Teller (BET) method. Pore sizes distribution curves were calculated by the BJH method from the desorption branch (Ye *et al.*, 2011).

Oxygen mass transfer coefficient (*ko*, cm/s) for the earthen plate was calculated as described previously (Chae *et al.*, 2008). Briefly, both reactor chambers were filled with 50 mM phosphate buffer solution and the dissolved oxygen (DO) content of the anode chamber solution removed by purging with N_2 gas, whilst that of the cathode chamber solution was saturated by continuous supply of air. The change in DO of the anode chamber solution was monitored using a DO meter (Cyber Scan, CD 650, Eutech Instruments, Singapore) and *ko* etimated using equation 1

$$k_0 = -\frac{v}{At} ln\left(\frac{C_0 - C}{C_0}\right) \qquad (1)$$

where *v* is the liquid volume of anode chamber, *A* is the earthen plate cross-sectional area, c_0 is the saturated DO concentration, and *c* is the DO concentration at time t. The oxygen diffusion coefficient (*Do*, cm^2/s) through the membrane was calculated as *Do* = *koL*, where *L* = thickness of earthen plate membrane.

The coulombic efficiency (*CE*) was estimated using the ratio of charge produced (by integrating the measured current over time) to theoretical charge on the basis of consumed COD, with the theoretical charge production estimated as (*F* x *n* x *w*)/*M*, where *F* is Faraday's constant, *n* is the number of moles of electrons produced per mole of substrate (= 4 for wastewater COD), *w* is the daily COD load consumed in gram and *M* is molar mass of acetate (Logan *et al.*, 2006).

2.3. Results and Discussion

2.3.1. MFC operation

After inoculation, a gradual increase in the voltage produced across the 100 Ω external resistance load was observed in both the MFCs over the first 48 hrs, with a slight delay in response of the PEM-MFC compared to that for the EP-MFC, leading to generation of a maximum voltage of ~0.3 V over the first batch feed cycle, Figure 2. In this set-up, it is presumed that the cathode does not limit the current, as the ferricyanide catholyte was supplemented periodically over the time course of the

experiments resulting in a constant electron acceptor concentration close to 50 mM, as reported on previously (Katuri *et al.*, ; Kong *et al.*, 2010; Katuri *et al.*, 2012a). After two further batch fed cycles, represented by the arrows in Figure 2, the feed was switched to continuous mode on the 7th day of operation, providing a flow of 20 mM acetate to the chamber (HRT 12 hrs). The measured cell voltage for both MFCs stabilized after this, with average sustainable current generation across 100 Ω external resistances over the 7 to 26 day continuous feed time period (Figure 2) of 5.14 mA and 4.34 mA for the PEM-MFC and EP-MFC, respectively. The cells thus provide average power densities of 190 mW m^2 and 138 mW m^{-2}, respectively, under these steady-state conditions. Under these conditions both cells establish the same OCV of 0.68 V. This OCV is close to the 0.76 V observed by Kong *et al.*, 2010 for a PEM-MFC fed with acetate and using potassium ferricyanide solution as catholyte.

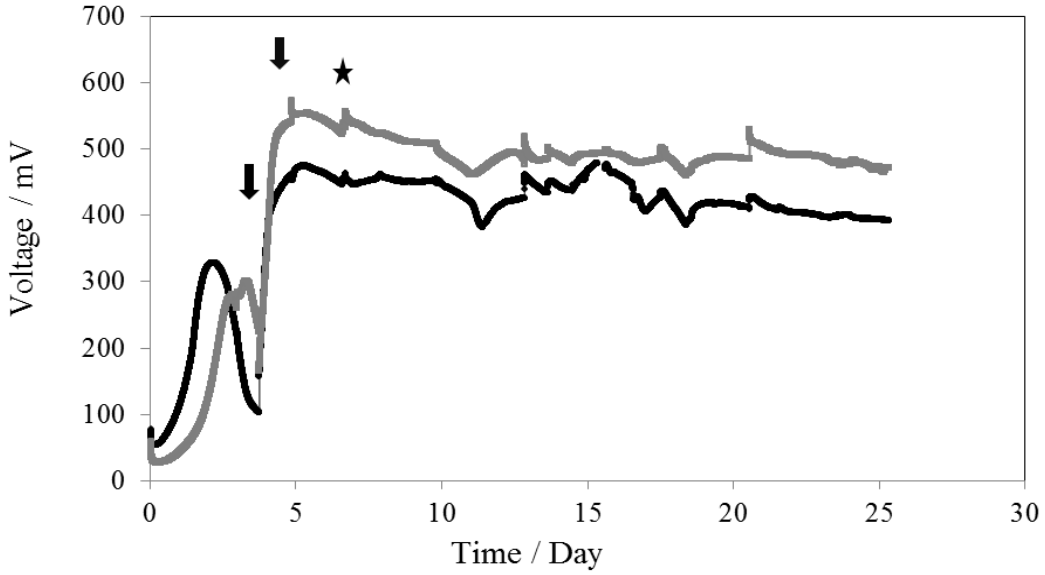

Figure.2.2 Voltage generations as a function of time for the PEM-MFC (grey) and the EP-MFC (black). Arrows indicate replacement with fresh feed and star indicates the time when the reactors were switched from batch to continuous mode operation.

To examine the catalytic activity of the anodic biofilm slow scan cyclic voltammograms were recorded in situ in the cell culture medium. Sigmoidal shaped voltammograms shown in figure 3, permit estimation from the first derivative of the

CVs (not shown) of acetate oxidation centred at −0.44 vs. Ag/AgCl. The sigmoidal shaped CV is indicative of catalytic oxidation of the substrate by the biofilm and heterogeneous electron transfer to the electrode, with similar responses reported on for acetate oxidation by anodic biofilms of *Geobacter sulfurreducens* (Katuri *et al.,* 2010; Marsili *et al.,* 2010; Katuri *et al.,* 2012b) and by mixed culture biofilms (Liu *et al.,* 2008). From the difference in the ferricyanide reduction potential in buffer of ~+0.24 V vs. Ag/AgCl and that of the redox couple centred at −0.44 vs. Ag/AgCl an estimate of the cell voltage of ~0.68 V is obtained, agreeing well with the OCV measured for both cells.

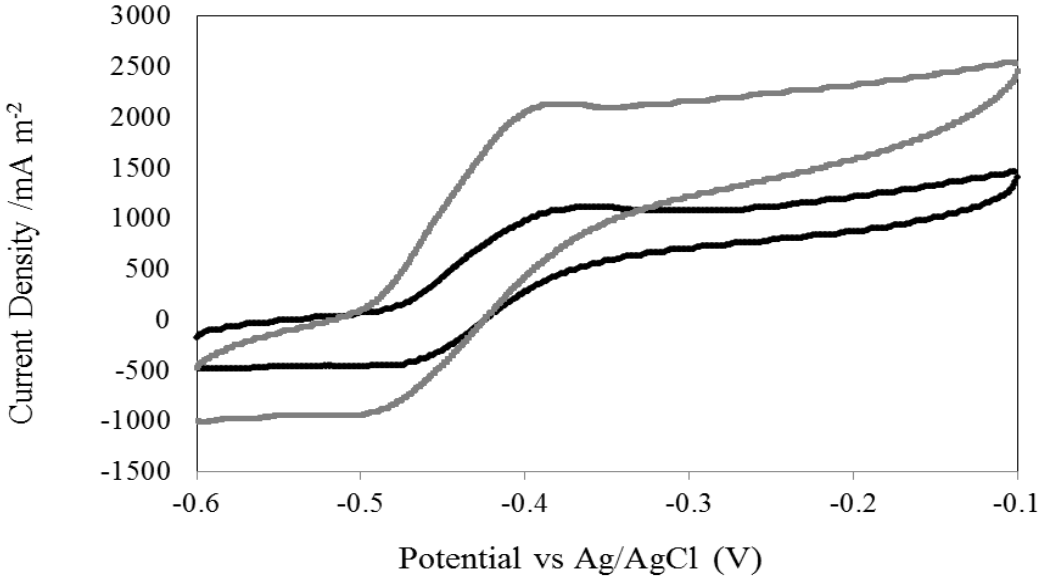

Figure 2.3 Cyclic voltammograms (1 mV/s) of anodic biofilm, recorded *in-situ* on the 19th day of operation of the cells under 100 Ω external resistors, for the PEM-MFC (grey) and EP-MFC (black) systems.

Efficient proton and ion transfer between anolyte and catholyte is important in MFC systems, to maintain electro-neutrality during current flow. The ability of the earthen plate separation membrane to permit ion-exchange was therefore evaluated

and compared to that of the Nafion PEM. For this experiment, 1 M H_2SO_4 was added to the anolyte chamber of both MFCs and the pH change in the catholyte, initially containing distilled, deionized, water was measured as a function of time. The catholyte pH decreased with time as protons migrated from anolyte to catholyte with the extent of proton exchange through the earthen plate membrane similar to that observed for proton exchange through the Nafion separator (Fig 4). The specific surface area of the earthen plate membrane, as determined by nitrogen absorption, is relatively high at 39.8 $m^2\ g^{-1}$, whilst providing a pore volume of 0.068 $cm^3\ g^{-1}$ and an average pore diameter of 19.2 Å, indicating mesoporous structure of the ceramic membrane (Colomer 2006). For comparison, narrow hydrophilic pores of 10–60 Å diameter are reportedly available for mass transport in Nafion 117 (Fang *et al.,* 2004).

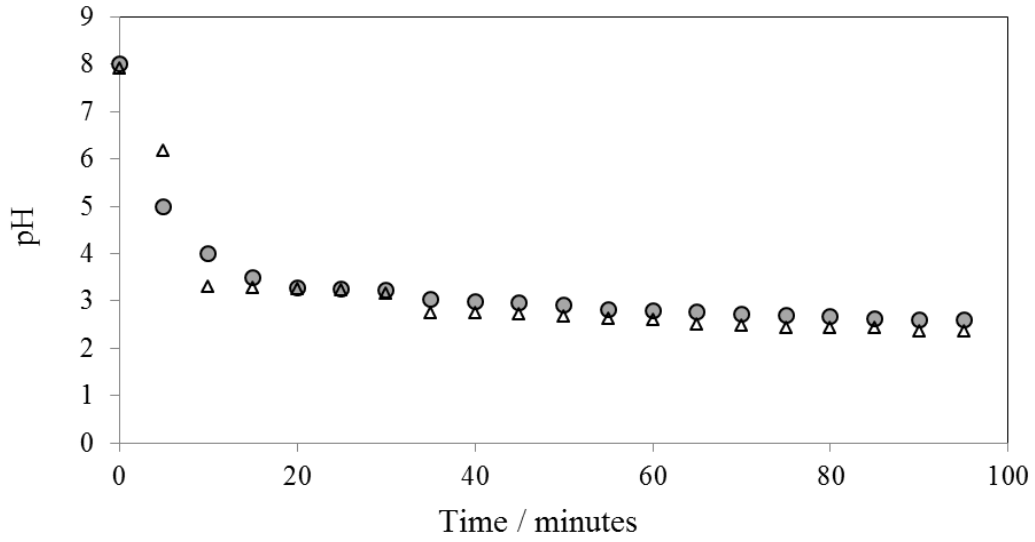

Fiureg.2.4 A comparison of the change in pH of the catholyte chamber, initially containing distilled deionized water, as a function of time upon introduction of 1 M sulphuric acid into the anolyte chamber for PEM (grey) and earthen plate (black) MFCs.

2.3.2. Organic matter removal

Initially both MFCs were operated in batch mode to avoid the washout of the sludge inoculum and thus encourage attachment of bacteria to the anode surface. After ~7 days of operation in batch mode, MFC operation was switched to continuous mode at an OLR of 2.5 kg COD m^{-3} d^{-1}. Steady state conditions for stable substrate degradation, represented by COD removal, and electricity generation were already established at this stage (Figure 5).

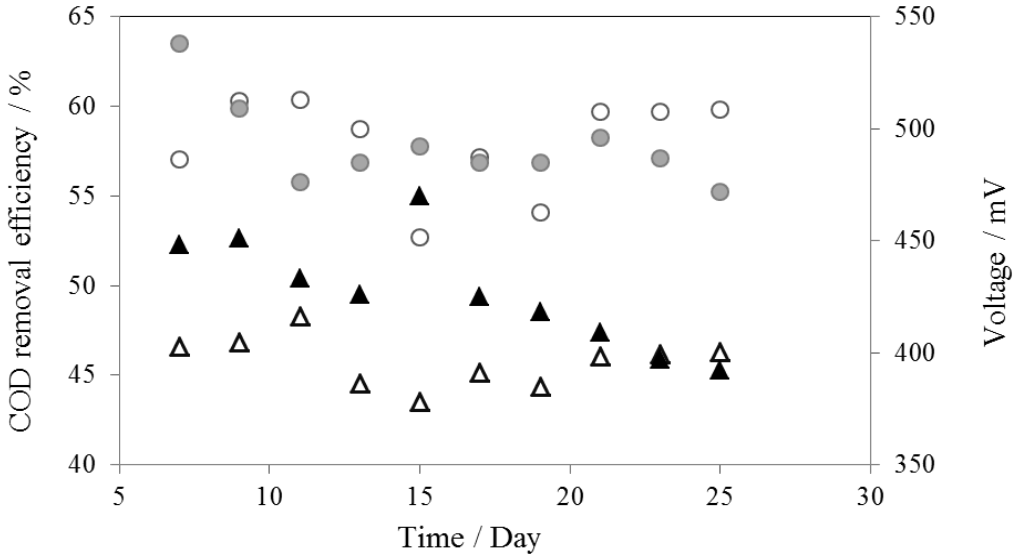

Figure 2.5 COD removal efficiency (open) and voltage generation across the 100 Ω resistance (closed) of PEM-MFC (grey circles) and EP-MFC (black triangles) as a function of time during continuous feed of MFCs (commenced at day 7).

During the subsequent steady state operation in continuous feed mode over an 18 day period, the PEM-MFC demonstrated an average COD removal efficiency of 60%, compared to an average COD removal efficiency of 48% for the EP-MFC. The earthen plate material may be permeable to oxygen (Behera & Ghangrekar 2011),

which could be one reason for the relatively lower COD removal efficiency for the EP-MFC compared to the PEM-MFC. An oxygen mass transfer coefficient, k_0, and oxygen diffusion coefficient, D_0, of 6.11×10^{-6} cm/s and 2.44×10^{-6} cm^2/s were determined, respectively, for the 3.7 mm thick earthen plate membrane, as described in the experimental section. Comparison of these values to those previously reported for oxygen diffusion through Nafion 117 of 0.175 mm thickness of 2.80×10^{-4} cm/s and 5.35×10^{-6} cm^2/s, respectively (Chae *et al.*, 2008) implies that the earthen plate is not as permeable to oxygen as the Nafion membrane, and that this is not the major factor contributing to differences in COD removal efficiency between the two MFCs.

3.3.3. Polarization studies

At the end of the continuous feed period (day 25) polarization studies were carried out for the MFCs by slow scan linear sweep voltammetry yielding the polarization curves (Figure 6) with a maximum power density of 250 mW m^{-2} at 35 Ω resistance for the PEM-MFC and 145 mW m^{-2} at 67 Ω resistance for the EP-MFC. Maximum volumetric power density of 10.0W m^{-3} and 5.8W m^{-3} were estimated based on anolyte volume from the polarization curves for the PEM-MFC and EP-MFC, respectively.

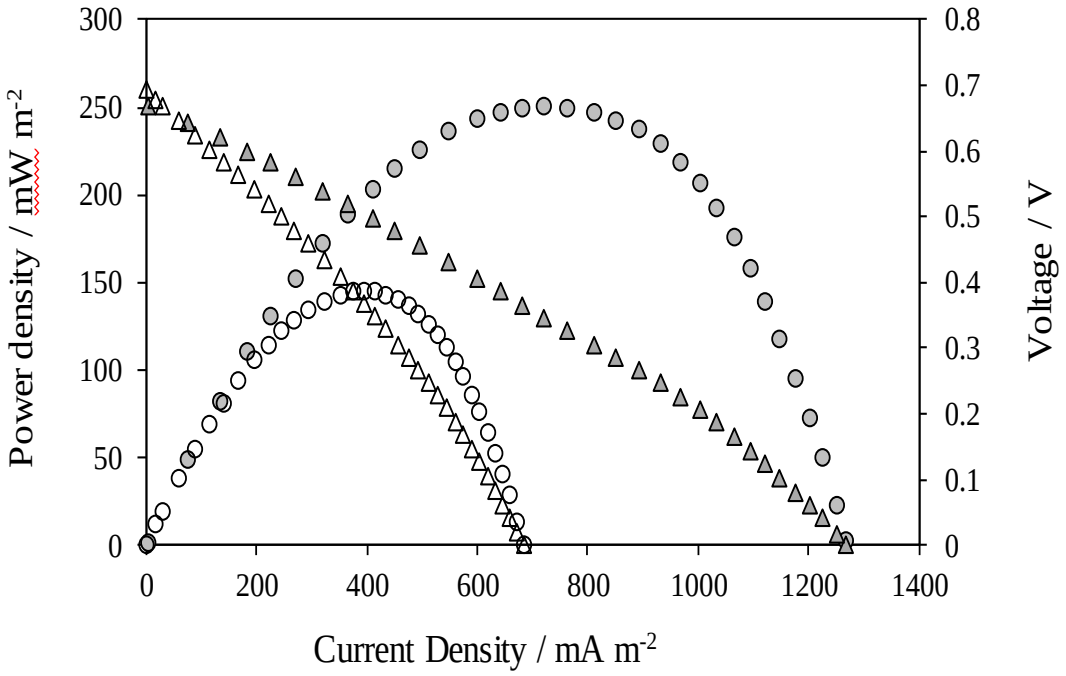

Figure 2.6 *In-situ* polarization curves, recorded on day 25, cell voltage and power density versus current density for PEM (grey closed) and earthen plate (black open) MFCs.

Internal resistances of 36 Ω and 70 Ω were estimated from the slope of the linear portion of the plot of cell voltage versus current (figure 6), for the PEM-MFC and EP-MFC, respectively. The earthen plate membrane is substantially thicker (~3.7 mm) than the Nafion 117 (~0.17 mm), which might contribute towards the higher internal resistance for these cells. The higher internal resistance, and thus lower current density during MFC operation is thus proposed to be the main factor contributing to the lower power density, and COD removal efficiency for the EP-MFC reactor, compared to the PEMFC. For example, Jung *et al.* (Jung *et al.,* 2007) report internal resistances of dual chamber MFCs using a range of membrane separators to be from 1239 to1344 Ω, depending on factors such as electrode spacing (Chae *et al.,* 2008) and membrane, with higher internal resistance resulting in MFC

with lower power densities in this configuration. Lower internal resistances of 84-98 Ω, and higher power densities, were obtained for MFCs in a single chamber, air-breathing cathode configuration with much closer electrode spacing (Ye *et al.,* 2011). Using a dual chamber Nafion-separated MFC system similar to the configuration in this report (Katuri *et al.,* 2012a) report a maximum power density of 6.4 W m^{-3} based on anolyte volume for the MFC operating on slaughterhouse waste-waters, whilst others (Kong *et al.,* 2010) observe maximum power density of 4.35 W m^{-3} using acetate as feed. Improvement in power density may be achieved, as reported on recently (Zhang *et al.,* 2011) by use of high surface area anodes, glass fiber as a separator, in a single chamber, air-breathing-cathode MFC configuration, providing a power density of 75 W m^{-3}.

MFCs	Voltage with 100 Ω load (V)	Power density with 100 Ω load (mW m^{-2})	Maximum Power density (optimum resistance) (mW m^{-2})	Volumetric power density with 100 Ω load (W m^{-3})	Maximum volumetric power density (optimum resistance) (W m^{-3})	Internal Resistance (Ω)
PEM-MFC	0.52	190	250 (35 Ω)	7.6	10.0 (35 Ω)	36
EP-MFC	0.44	138	145 (67 Ω)	5.5	5.8 (67 Ω)	70

Table 1 Comparison of performance of PEM-MFC and EP-MFC

Table 1 shows the comparison of the performance of the EP-MFC and PEM-MFC. From the polarization curve and the data in Table 1 the EP-MFC generates ~40% less maximum power density, with an internal cell resistance 48% higher than the PEM-MFC. Over the 18 day period of steady state operation in continuous feed mode the same, although low (<10 %), coulombic efficiencies are estimated for both the PEM-MFC and the EP-MFC under the 100 Ω resistance load. Many different

membrane separator configurations have been studied in MFCs, such as the use of single chamber porous air cathode (Park & Zeikus 2003), tubular air cathode system with an outer cathode and an inner anode (Rabaey *et al.,* 2005) and more recently (Zhang *et al.,* 2010) nylon and glass fiber filter separators in air-cathode single-chamber microbial fuel cells. A potential disadvantage to all these configurations is the susceptibility of the membrane separators to degradation (Zhang *et al.,* 2009) or mechanical deformation (Zhang *et al.,* 2011) over long periods. The use of an earthen plate separator as an alternative membrane provides a low cost, durable option, with a small fractional of loss in performance compared to the same exposed area of a Nafion PEM as a benchmark.

2.4. Conclusion

This study demonstrated by comparison to Nafion, that an earthen plate membrane may provide a low-cost, more durable, alternative to Nafion in continuous flow MFCs. The MFC using Nafion membrane as separator showed slightly better performance in terms of organic matter removal and electricity generation than the MFC based on earthen plate membrane separators, butt both show comparable coulombic efficiency. The performance of earthen the plate MFC may be enhanced by increasing the membrane surface area or decreasing the membrane thickness. The 40 cm^2 Nafion 117 membranes used in the present experiment costs approximately €30.0 whilst the same area of the earthen plate costs approximately €0.025, making it 99% cheaper. Utilization of low cost separators may contribute to further developing of economical MFC technology.

References

APHA 1998, Standard methods for the examination of water and wastewater. 20th edn, American public Health association/American water works association/water environment federation, washington DC,USA.

Behera M.,Ghangrekar M. M. 2009. Performance of microbial fuel cell in response to change in sludge loading rate at different anodic feed pH. *Bioresource Technology*, **100**, 5114-21.

Behera M.,Ghangrekar M. M. 2011. Electricity generation in low cost microbial fuel cell made up of earthenware of different thickness. *Water Science and Technology*, **64**, 2468-73.

Behera M., Jana P. S.,Ghangrekar M. M. 2010a. Performance evaluation of low cost microbial fuel cell fabricated using earthen pot with biotic and abiotic cathode. *Bioresource Technology*, **101**, 1183-9.

Behera M., Jana P. S., More T. T.,Ghangrekar M. M. 2010b. Rice mill wastewater treatment in microbial fuel cells fabricated using proton exchange membrane and earthen pot at different pH. *Bioelectrochemistry*, **79**, 228-33.

Chae K. J., Choi M., Ajayi F. F., Park W., Chang I. S.,Kim I. S. 2008. Mass transport through a proton exchange membrane (Nafion) in microbial fuel cells. *Energy and Fuels*, **22**, 169-76.

Colomer M. T. 2006. Nanoporous anatase ceramic membranes as fast-proton-conducting materials. *Journal of the European Ceramic Society*, **26**, 1231-6.

Fan Y., Hu H.,Liu H. 2007. Enhanced coulombic efficiency and power density of air-cathode microbial fuel cells with an improved cell configuration. *Journal of Power Sources*, **171**, 348-54.

Fang C., Wu B.,Zhou X. 2004. Nafion membrane electrophoresis with direct and simplified end-column pulse electrochemical detection of amino acids. *Electrophoresis*, **25**, 375-80.

Harnisch F., Schröder U.,Scholz F. 2008. The suitability of monopolar and bipolar ion exchange membranes as separators for biological fuel cells. *Environmental Science and technology*, **42**, 1740-6.

Jana P. S., Behera M.,Ghangrekar M. M. 2010. Performance comparison of up-flow microbial fuel cells fabricated using proton exchange membrane and earthen cylinder. *International Journal of Hydrogen Energy*, **35**, 5681-6.

Jung R. K., Cheng S., Oh S. E.,Logan B. E. 2007. Power generation using different cation, anion, and ultrafiltration membranes in microbial fuel cells. *Environmental*

Science and Technology, **41**, 1004-9.

Katuri K. P., Enright A.-M., O'Flaherty V.,Leech D. 2012a. Microbial analysis of anodic biofilm in a microbial fuel cell using slaughterhouse wastewater. *Bioelectrochemistry*, **87**, 164-71,87, 164-171.

Katuri K. P., Kavanagh P., Rengaraj S.,Leech D. 2010. Geobacter sulfurreducens biofilms developed under different growth conditions on glassy carbon electrodes: insights using cyclic voltammetry. *Chemical Communications*, **46**, 4758-60.

Katuri K. P., Rengaraj S., Kavanagh P., O'Flaherty V.,Leech D. 2012b. Charge transport through Geobacter sulfurreducens biofilms grown on graphite rods. *Langmuir*, **28**, 7904-13.

Kong X., Sun Y., Yuan Z., Li D., Li L.,Li Y. 2010. Effect of cathode electron-receiver on the performance of microbial fuel cells. *International Journal of Hydrogen Energy*, **35**, 7224-7.

Lefebvre O., Shen Y., Tan Z., Uzabiaga A., Chang I. S.,Ng H. Y. 2011. A comparison of membranes and enrichment strategies for microbial fuel cells. *Bioresource Technology*, **102**, 6291-4.

Liu Y., Harnisch F., Fricke K., Sietmann R.,Schröder U. 2008. Improvement of the anodic bioelectrocatalytic activity of mixed culture biofilms by a simple consecutive electrochemical selection procedure, *Biosensors and Bioelectronics*, **24**, 1006-11.

Logan B. E., Hamelers B., Rozendal R., Schröder U., Keller J., Freguia S., Aelterman P., Verstraete W.,Rabaey K. 2006. Microbial fuel cells: Methodology and technology. *Environmental Science and Technology*, **40**, 5181-92.

Logan B. E.,Regan J. M. 2006. Microbial fuel cells - Challenges and applications. *Environmental Science and Technology*, **40**, 5172-80.

Marsili E., Sun J.,Bond D. R. 2010. Voltammetry and growth physiology of Geobacter sulfurreducens biofilms as a function of growth stage and imposed electrode potential. *Electroanalysis*, **22**, 865-74.

Martin E., Savadogo O., Guiot S. R.,Tartakovsky B. 2010. The influence of operational conditions on the performance of a microbial fuel cell seeded with mesophilic anaerobic sludge. *Biochemical Engineering Journal*, **51**, 132-9.

Min B., Cheng S.,Logan B. E. 2005. Electricity generation using membrane and salt

bridge microbial fuel cells. *Water Research*, **39**, 1675-86.

Pant D., Singh A., Van Bogaert G., Irving Olsen S., Singh Nigam P., Diels L.,Vanbroekhoven K. 2012. Bioelectrochemical systems (BES) for sustainable energy production and product recovery from organic wastes and industrial wastewaters. *RSC Advances*, **2**, 1248-63.

Pant D., Van Bogaert G., De Smet M., Diels L.,Vanbroekhoven K. 2010. Use of novel permeable membrane and air cathodes in acetate microbial fuel cells. *Electrochimica Acta*, **55**, 7710-6.

Park D. H.,Zeikus J. G. 2003. Improved fuel cell and electrode designs for producing electricity from microbial degradation. *Biotechnology and Bioengineering*, **81**, 348-55.

Picioreanu C., Head I. M., Katuri K. P., van Loosdrecht M. C. M.,Scott K. 2007. A computational model for biofilm-based microbial fuel cells. *Water Research*, **41**, 2921-40.

Rabaey K., Boon N., Siciliano S. D., Verhaege M.,Verstraete W. 2004. Biofuel cells select for microbial consortia that self-mediate electron transfer. *Applied and Environmental Microbiology*, **70**, 5373-82.

Rabaey K., Clauwaert P., Aelterman P.,Verstraete W. 2005. Tubular microbial fuel cells for efficient electricity generation, *Environmental Science and Technology*. **39**, 8077-82.

Sun J., Hu Y., Bi Z.,Cao Y. 2009. Improved performance of air-cathode single-chamber microbial fuel cell for wastewater treatment using microfiltration membranes and multiple sludge inoculation. *Journal of Power Sources*, **187**, 471-9.

Ter Heijne A., Hamelers H. V. M., De Wilde V., Rozendal R. A.,Buisman C. J. N. 2006. A bipolar membrane combined with ferric iron reduction as an efficient cathode system in microbial fuel cells. *Environmental Science and Technology*, **40**, 5200-5.

Ye Y.-S., Liang G.-W., Chen B.-H., Shen W.-C., Tseng C.-Y., Cheng M.-Y., Rick J., Huang Y.-J., Chang F.-C.,Hwang B.-J. 2011. Effect of morphology of mesoporous silica on characterization of protic ionic liquid-based composite membranes. *Journal of Power Sources*, **196**, 5408-15.

Zhang X., Cheng S., Huang X.,Logan B. E. 2010. The use of nylon and glass fiber filter separators with different pore sizes in air-cathode single-chamber microbial fuel cells. *Energy and Environmental Science*, **3**, 659-64.

Zhang X., Cheng S., Liang P., Huang X.,Logan B. E. 2011. Scalable air cathode microbial fuel cells using glass fiber separators, plastic mesh supporters, and graphite fiber brush anodes. *Bioresource Technology*, **102**, 372-5.

Zhang X., Cheng S., Wang X., Huang X.,Logan B. E. 2009. Separator characteristics for increasing performance of microbial fuel cells. *Environmental Science and Technology*, **43**, 8456-61.

Zuo Y., Cheng S.,Logan B. E. 2008. Ion exchange membrane cathodes for scalable microbial fuel cells. *Environmental Science and Technology*, **42**, 6967-72.

Chapter-3

Charge transport in films *of Geobacter sulfurreducens* on graphite electrodes as a function of film thickness

3.1 Introduction

Microbial fuel cell (MFC) devices that use EAB to oxidize organic substrates, degrading wastes and generating electricity, have received a great deal of attention in recent years (Logan *et al*., 2006; Lovley, 2006; Rabaey & Verstraete, 2005; Schaetzle *et al*., 2008). Proposed mechanisms of electron transfer within films of EAB to produce current at solid anode surfaces include, production and use of electron shuttling mediating molecules (Baron *et al*., 2009) and redox active membrane-bound proteins (cytochromes) (Liu *et al*., 2011; Nevin *et al*., 2009) self-exchange within redox conducting films (Liu *et al*., 2011; Strycharz-Glaven *et al*., 2011) or even, controversially, *via* conductive nanowires (pili) (Malvankar *et al*., 2011). The exact mechanism or combination of mechanisms that drive electron transfer within films of EAB to solid surfaces is not yet, however, fully understood. Studies on biofilms of *Geobacter sulfurreducens* (GS) on electrodes for acetate oxidation, as a model EAB, have provided information on electrical communication between EAB and anodes (Bond *et al*., 2002; Katuri *et al*., 2012; Malvankar *et al*., 2012; Richter *et al*., 2009; Zhu *et al*., 2012). In recent years use of electroanalytical, (Fricke *et al*., 2008; Katuri *et al*., 2012; Marsili *et al*., 2008; Snider *et al*., 2012) and spectroelectrochemical (Liu *et al*., 2011; Millo *et al*., 2011; Virdis *et al*., 2012) techniques, often in combination with genetic engineering (Nevin *et al*., 2009) immunohistochemical staining (Leang *et al*., 2010) or NMR (Renslow *et al*., 2013) has helped elucidate the role of electron transferring species (cytochromes, pili) in

current production by GS biofilms on anodes. For example, genomic analysis of GS has identified coding sequences for periplasmic cytochromes, membrane cytochromes and other outer membrane proteins that can contribute to extracellular electron transport (Holmes *et al*., 2006; Inoue *et al*., 2010; Kim *et al*., 2008; Marsili *et al*., 2010; Strycharz-Glaven *et al*., 2011; Strycharz *et al*., 2011b; Zhu *et al*., 2012).

Recently, three electrode electrochemical cell configurations were used to induce biofilm growth on anodes, under a controlled applied potential versus a reference electrode, to achieve better control of the anode potential during biofilm growth, over use of a fixed resistance load imposed between anode and cathode (Inoue *et al*., 2010; Strycharz *et al*., 2011b). However, how cells and cellular components coordinate in the transport of electrons through a thick biofilm and across the biofilm anode interface and what limits the rate and distance that electrons can be transported through an EAB biofilm remains unresolved (Bond *et al*., 2012).

Little has yet been reported on how film thickness can affect how, and how rapid, charge is transported through GS biofilms on solid electrodes, and how this contributes to catalytic acetate oxidation current generation. Marsili *et al* (Marsili *et al*., 2010) reported on the correlation between the mass of protein from GS developed on electrodes as a function of time, and they observe an increment in acetate oxidation, from 2 mA mg^{-1} protein initially to 8 mA mg^{-1} protein within 6 hours of bacterial growth. Most recently Bond *et al* proposed that biofilms will grow in thickness until either the pH value near the anode surface becomes sufficiently low to inhibit cytochrome function of the innermost cells, thereby limiting the ability of all cells in the biofilm to transfer electrons to the anode, or until the local concentration of oxidized cytochromes experienced by the outermost cells becomes too low to support additional growth (Bond *et al*., 2012).

Here we report on GS biofilm production on graphite rod electrodes under continuous mode operation, using a multi-channel potentiostat to control the potential applied to multiple electrodes, permitting temporal sampling of biofilms under controlled conditions. This allows for a comparison of biofilm thickness over

time to voltammetric responses in the presence and absence of acetate as electron donor. In the absence of electron donor, redox site concentration, within the biofilms, and charge transport across the biofilm vary as a function of film thickness, providing an insight into the factors that may affect current generation on microbial fuel cell anodes.

3.2 Materials and methods

3.2.1 Experimental set-up

The study was carried out in a single-chambered electrochemical cell of 800 mL volume with multiple working electrodes assembled concentrically placed around a single counter and reference electrode (Figure.3.1). Eight graphite rods (3 mm diameter, Graphite Store product NC001300) with exposed area of 1.77 cm^2 each were used as working electrodes. Platinum mesh (2.5 cm × 2.5 cm dimension, Sigma-Aldrich, Dublin) was used as counter electrode and custom built Ag/AgCl (3 M KCl) with a porous vycor frit (Advanced Glass and Ceramics) acting as salt bridge were used as reference electrode. In this configuration influent was supplied to the cell from the bottom of the chamber using a peristaltic pump (Gilson, France) with effluent exiting the chamber at the top of the reactor, as shown in Figure 1.

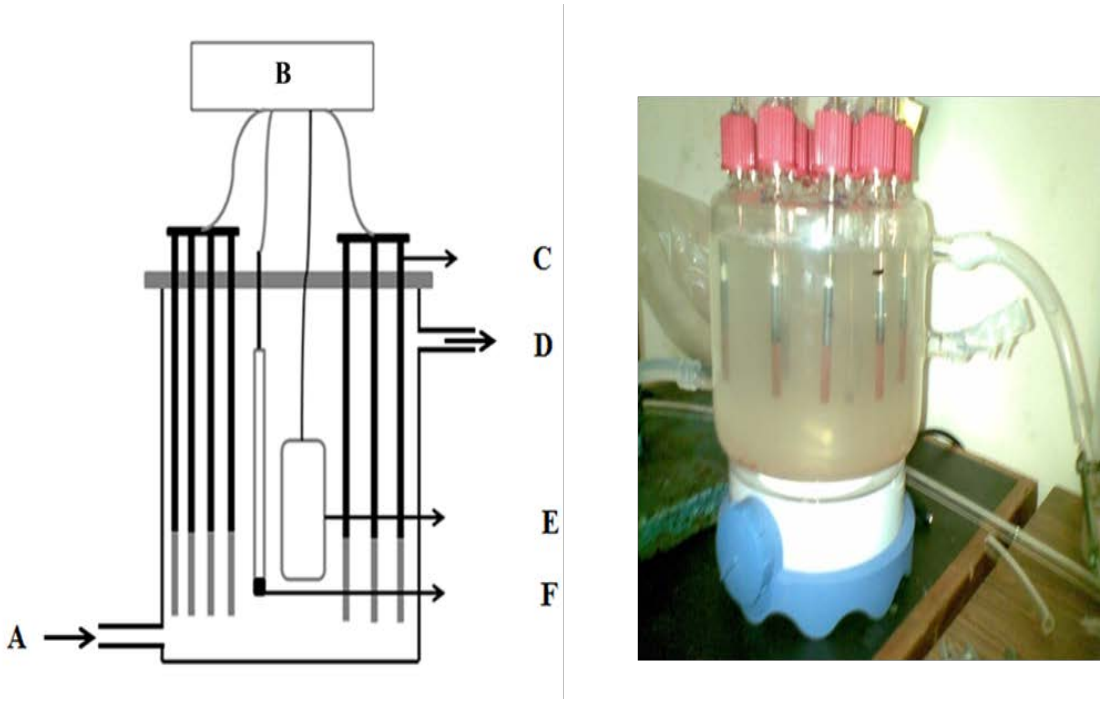

Figure.3.1 Schematic diagram left, and photograph, right, of the anaerobic electrochemical cell, where (A) is feed inlet (B) potentiostat (C) working electrodes with dark grey colour in diagram representing the available surface area, and the pink/red colour in the photograph indicative of GS biofilm formation, (D) is outlet (E) counter electrode and (F) reference electrode

3.2.2 Biofilm growth on electrode surface

Geobacter sulfurreducens (ATCC 51573) was used as a source of electroactive bacteria. The strain was sub-cultured in 100 mL airtight, rubber septa-sealed, anaerobic syringe bottles containing 90 mL of growth medium, prepared according to the protocol supplied by the culture centre (http://www.dsmz.de, medium no. 826). The bacteria were cultured in fumarate-containing *Geobacter* growth medium for 2 weeks (three sub-cultures) prior to inoculation in the electrochemical cell. Following inoculation biofilms were induced to grow on graphite-rod electrodes, with eight electrodes in the same electrochemical cell, under a constant applied potential (0 V vs Ag/AgCl) using a multichannel potentiostat (CHI-1030a, CH Instruments, Austin, TX). Growth media containing acetate as a source of electron donor (10 mM) was used as feed. The feed pH was in the range of

7.2-7.5 throughout the experiment and the cell was operated at temperatures that varied from 28 to 32 °C. Initially the reactor was operated over a single batch feed, by inoculation with GS directly from the culture bottles in an anaerobic glove-box, and operation under 0 V applied potential for 65 hours to encourage the attachment of bacteria to the graphite rod working electrodes. Thereafter the electrochemical cell was operated using continuous delivery of anaerobic, nitrogen-sparged, acetate-containing medium only (no further inoculum) with a peristaltic pump using a flow rate of 8.3 mL h^{-1}, with additional mixing within reactor provided by magnetic stirring at a rate of 50 rpm.

3.2.3 Cyclic Voltammetry

Stirring, and flow of media, was halted for 30 minutes prior to recording of *in-situ* cyclic voltammetry (CV) in the reactor. Non-turnover CV was recorded after removal of acetate from the electrode-attached biofilms, by washing electrodes, sampled under anaerobic conditions from the reactor, in acetate-free culture medium. The electrodes were then transferred into a separate vessel containing 100 mL of acetate-free culture medium and incubated for 30 min under anaerobic conditions to ensure dilution of the acetate concentration in the biofilm matrix. The electrodes were subsequently transferred into a separate electrochemical cell containing 100 mL of acetate-free culture medium to perform non-turnover CV.

3.2.4 Confocal laser scanning, and electron, microscopy

Electrodes removed from the reactor were sectioned into two pieces for subsequent scanning electron microscopy (SEM) and confocal laser scanning microscopy (CLSM) imaging. Prior to SEM imaging, fixation was undertaken, using a series of primary and secondary fixatives (Bond & Lovley, 2003; Kuo, 2007) by placing the electrode in the following solutions: (a) 1% glutaraldehyde, 2% paraformaldehyde, 0.2% picric acid, 10 mM 2-[4- (2-hydroxyethyl)-1-piperazinyl]ethanesulfonic acid (HEPES, pH 7.4) for 1 h, (b) 50 mM NaN_3 for 1 h,

(c) 2% tannic acid for 1 h, (d) 1% osmium tetroxide for 2 h, (e) 1% thiocarbohydrazide for 30 min, and (f) 1% osmium tetroxide overnight, with washing using 10 mM HEPES buffer (pH 7.4) between steps (all Sigma-Aldrich). The samples were then dehydrated in a graded series of aqueous ethanol solutions (10-100%) and oven-dried (2 h at 40 °C) to remove residual moisture. The dried samples were mounted over SEM stubs with double-sided conductivity tape and a thin layer of gold metal applied using an automated sputter coater (Emitech, K550) for 2 min and imaged using a model 4700 SEM instrument (Hitachi, Japan). For CLSM imaging, electrode sections were transferred into sterile vessels containing 50 mL of anaerobic acetate-free growth medium. The graphite rod was cross-sectioned into pieces (~3 mm in height) using a scalpel and stained, by incubation for 15 min in 10 mL of 10 mM potassium phosphate buffer, pH 7.0, containing 1 μL of propidium iodide and 1μL of syto 9 from a Molecular Probes bacLight LIVE/ DEAD L7012 stain kit (Invitrogen Corp., Carlsbad, CA) in the dark. The samples were then gently washed in phosphate buffer (10 mM, pH 7.0) to remove unbound residual dye from the biofilm matrix. The sectioned face of the rod was placed on a multi-well microscope slide to examine horizontal growth of biofilm through a Zeiss LSM 510 axiovert inverted confocal microscope with a 40× achroplan oil immersion lens. A minimum of 10 fields of biofilm views were imaged, and Z-series images were processed and analysed with Zeiss LSM510 operating software for biofilm thickness measurements. Images were obtained using an excitation wavelength of 488 nm and a BP500−550 emission filter for green fluorescence. The excitation wavelength was 543 nm, and emission filter LP605 was used to obtain images for red fluorescence.

3.3 Results and discussion

The three electrode electrochemical cell configuration using acetate as an electron donor, not deliberately adding electron acceptor, and a potential of 0 V vs. Ag/AgCl applied to the working electrodes initiates GS respiration on the polarised working electrodes, and subsequent biofilm growth. Eight graphite electrodes were used as working electrodes in the same electrochemical cell, allowing each electrode

to experience similar conditions (temperature, feed, ionic strength, pH etc) and permitting removal of pairs of electrodes at intervals during the biofilm growth period.

A disadvantage of using a single chamber electrochemical cell is that the counter electrode reaction products are free to diffuse to the working electrode and this could potentially generate uncontrolled experimental parameters (Kumar *et al*., 2013; Seeliger *et al*., 1998). For example, in a single chamber three electrode cell, diffusion of hydrogen produced at the counter electrode to the working electrode can be utilized by EAB to produce a current higher than that expected with the supplied electron donor (Holmes *et al*., 2006; Lee *et al*., 2009). In use of non-separated anode and cathode, in three electrode electrochemical cells can result in different trends in the anode potential required for maximum steady-state current density from biofilms induced to grow on electrodes using mixed-culture innocula (Kumar *et al*., 2012; Kumar *et al*., 2013). Continuous flow reactors operation is thus used to remove electrolysis products whilst ensuring that substrate (fuel) is available for current production, simplifying analysis of results. The applied potential of 0 V vs Ag/AgCl was chosen based on CV analysis (Katuri *et al*., 2010; Katuri *et al*., 2012) to provide sufficient driving force to drive electron transfer from biofilm to solid electrode surface (Babauta *et al*., 2012; Richter *et al*., 2009; Strycharz *et al*., 2011a; Strycharz *et al*., 2011b).

After inoculation, an increase in the oxidation current production was observed over time, Figure 2. Although the amperometric trace is the sum of the current through all interconnected graphite working electrodes, it was confirmed that each individual electrode responds in a similar, reproducible, manner, by connecting each as a working electrode in a slow-scan CV experiment at defined intervals along the growth curve, Figure 3A. For example, the CV response sampled for each electrode produces steady-state acetate oxidation current densities (*vide infra*) of 4.0 ± 0.4 A m^{-2} after 65 h, 5.8 ± 0.4 A m^{-2} after 79 h and 7.0 ± 0.3 A m^{-2} after 129 h operation in the reactor.

The pattern of biofilm growth and current generation can vary depending on a range of factors, such as feed concentration, inoculum concentration and stage, electrode material, and potential (Katuri *et al*., 2012; Logan *et al*., 2006; Lovley, 2006). In this study we observe a 45 h lag phase prior to commencement of a rapid increase in current production, associated with the exponential growth phase for the bacterial biofilm. Others have reported a similar trend to current production by electrode-attached GS biofilms on graphite in electrochemical reactors. For example, Fricke *et al* (Fricke *et al*., 2008) and Torres *et al* (Torres *et al*., 2008) report current generation within 100 hours of reactor start-up for biofilms of GS on carbon electrodes using acetate as model substrate. Slight differences in the lag phase duration may be due to differences in the selected anode potential or electrochemical cell configuration to induce biofilm current generation.

After 65 h of operation in 10 mM acetate as electron donor in *Geobactor* medium, without any added electron acceptor, the electrochemical cell was switched to continuous mode at a flow rate of 200 ml/day to prevent electron donor depletion and to wash out suspended bacteria. The rapid growth in current at this stage indicates that GS electroactive bacteria are capable of transferring electrons to the anode as a result of acetate oxidation, with SEM, CLSM and cell count results (*vide infra*) demonstrating formation of layers of GS cells on the electrode surface.

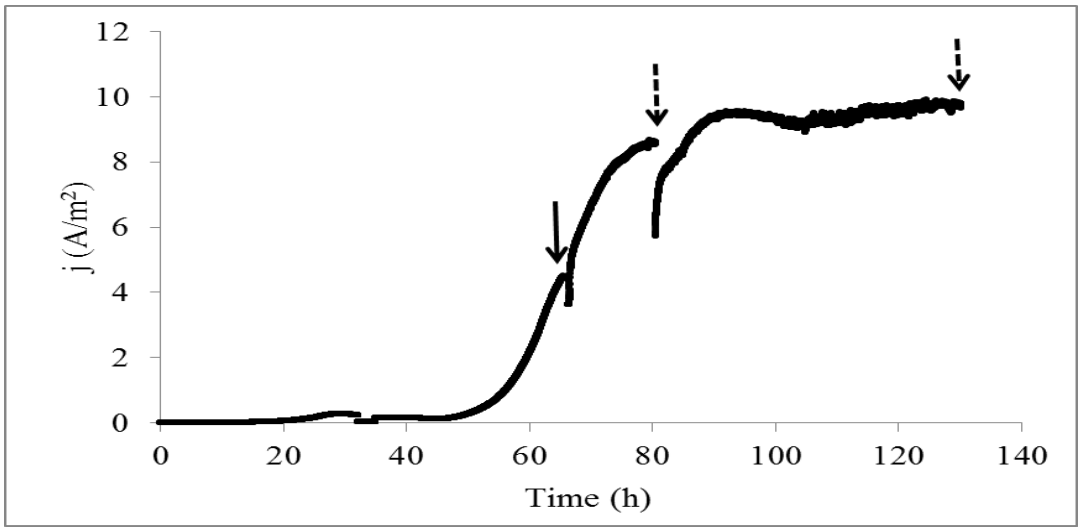

Figure.3.2 Amperometric response of graphite rod working electrodes, as a function of time, during GS biofilm growth operation (10 mM acetate) under 0 V vs. Ag/AgCl applied potential. Solid arrow indicates the region where the reactor was switched from batch to continuous mode operation. Arrows represent biofilm sampling points for analysis by *in-situ* CV, *ex-situ* CV, and for biofilm thickness.

Current generation increases from 45 to 85 h until a steady state current of ~9 A m^{-2} is reached, providing current densities similar to those reported on previously. For example, Marsilli *et al* (Marsili *et al*., 2010) reported a steady-state current density, in 20 mM acetate, of 4-7 A m^{-2} achieved after 72 hours under an applied potential of 0.04 V vs. Ag/AgCl by GS biofilms at graphite or roughened glassy carbon electrodes. More recently, Katuri *et al* (Katuri *et al*., 2012) reported a steady-state amperometric current density for actetate oxidation by GS biofilm on carbon electrodes of 9.2 A m^{-2} after 142 h of repeated batch mode experiments. A series of experiments was conducted at defined times during the operation of the reactor to examine the correlation between current generation, content of redox active material, and biofilm thickness. This was possible as all 8 electrodes showed similar current generation capabilities (Figure 3.3A) permitting sampling of electrodes from the reactor at defined times, as follows. The *in situ* voltammetric behaviour of biofilms was recorded at the time intervals of 65, 79 and 129 h after reactor initiation, using slow-scan cyclic voltammetry. Redox-active content of biofilms was probed using *ex-situ* voltammetry of one sampled electrode, at each of these times, recorded in

growth medium with no added substrate (acetate), whilst *ex-situ* microscopy (SEM/CLSM) and fluorescence microscopy of biofilms on a second sampled electrode at each of these times was used to provide information on film thickness.

Sigmoidal cyclic voltammograms recorded at the time intervals of 65, 79 and 129 h after reactor initiation, using slow-scan cyclic voltammetry, permit estimation, from the first derivative of the voltammogram, of acetate oxidation centered at −0.41 V vs. Ag/AgCl in good agreement with that reported on by others (Fricke *et al*., 2008; Katuri *et al*., 2010; Liu *et al*., 2011; Srikanth *et al*., 2008; Torres *et al*., 2008; Zhu *et al*., 2012). The sigmoidal voltammogram, with examples shown in Figure 3.3, is indicative of catalytic oxidation of the acetate substrate by the biofilm with heterogeneous electron transfer to the electrode, with similar responses reported on for acetate oxidation by biofilms of GS (Katuri *et al*., 2010).

The change in magnitude of the steady-state catalytic oxidation current observed in the slow scan cyclic voltammograms as a function of time and growth conditions correlate with the changes observed in amperometric current over the same period. It is to be noted however that amperometric currents are higher than the steady-state catalytic currents observed in the slow-scan cyclic voltammograms. Convective substrate mass transport may provide an additional contribution to current in the reactor during amperometry compared to that during *in-situ* voltammetry, as the flow of media was stopped 30 minutes prior to recording for all voltammetric analysis. For example, amperometric current densities of 8.6 A m^{-2} are obtained after 79 h of reactor operation compared to catalytic current densities from CV of only 5.8 A m^{-2}. Recently Katuri *et al* (Katuri *et al*., 2012) and Snider *et al* (Snider *et al*., 2012) reported on a simple model (equation 1) of the catalytic CV response at slow scan rates, assuming that the current at each potential in a scan reflects a Nernstian equilibrium distribution of the oxidized and reduced dominant redox species responsible for transferring electrons between the biofilm and the electrode,

$$j = \frac{j_{\lim}}{1 + \exp\left\{\frac{nF(E^{0'} - E)}{RT}\right\}}$$

where j_{lim} is the limiting current density and $E^{0'}$ categorizes the formal redox potential of the dominant redox species. This approach, as previously demonstrated (Richter *et al*., 2009) permits fitting of the anodic linear sweep voltammogram from CV (Figure 3.3B), at each biofilm thickness, to the model for n = 1 (Figure 3C dashed line), once a correction for the iR drop between the working and reference electrodes is applied (Figure 3C grey line). In this case CVs recorded for all biofilms provide an estimate of an average 80 Ω iR drop in the electrochemical reactor. This iR drop may be due to electrolyte conductivity, based on the distance between reference and working electrode(s) and the conductance of the electrolyte medium (Katuri *et al*., 2012; Snider *et al*., 2012; Torres *et al*., 2010; Yi *et al*., 2009). For example, an estimate of 78 Ω uncompensated resistance is obtained using a conductivity of 1.44 S/m for the electrolyte culture medium (Torres *et al*., 2008) an electrode area of 1.77×10^{-4} m^2 and an approximate distance between working and reference electrodes of 0.020 m.

To attempt to correlate current generation with biofilm thickness, CLSM imaging of sampled working electrodes was used to estimate biofilm thickness as a function of time, as reported on by others (Marsili *et al*., 2008; Nevin *et al*., 2008). Each sampled graphite rod electrode was cross-sectioned into pieces (2-3 mm) for imaging, Figure 3.4A, providing average biofilm thicknesses of 5 ± 2 μm, 17 ± 3 μm and 50 ± 9 μm for the biofilms on the electrodes sampled at 65, 79, and 129 h respectively. For comparison, Marsili *et al* (Marsili *et al*., 2008) use CLSM to estimate GS biofilm thickness of ~15 μm after 72 h of growth with 20 mM acetate as the electron donor whilst Liu *et al* (Liu *et al*., 2011) estimate formation of 30 μm thick GS biofilms after 96 h of growth with 30 mM acetate as the electron donor, using CLSM of electroactive biofilms. In addition, Laspidou *et al* (Laspidou & Rittmann, 2004) report that the outermost layers of heterogeneous biofilms are fluffy,

while the surface-associated layers are 5–10 times more dense than the layers near the top of the biofilm.

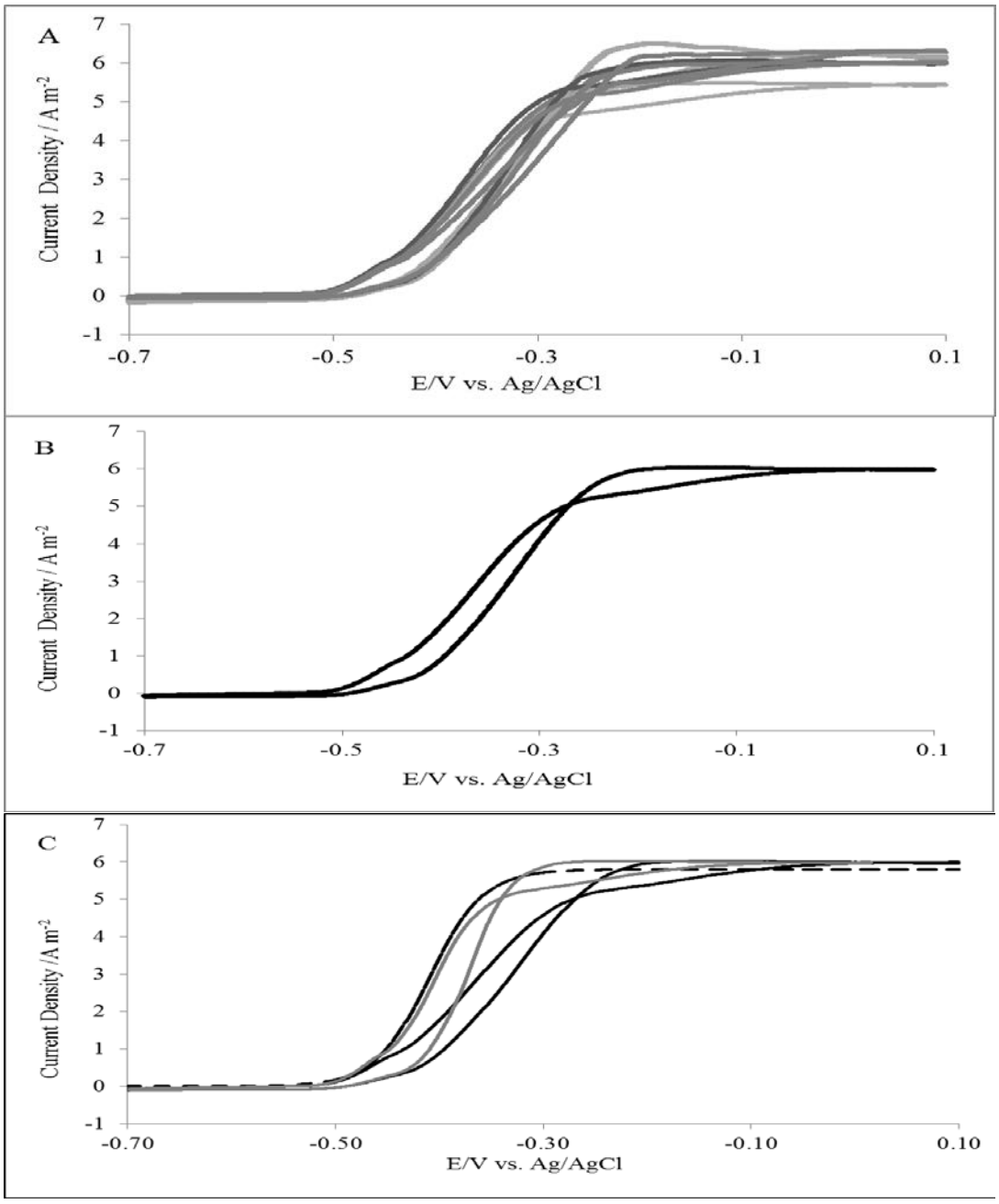

igure.3.3 Cyclic voltammetry (1 mV s^{-1}) at graphite-rod electrodes after 79 h reactor operation recorded for; A) each of 6 working electrodes individually, B) all 6 working electrodes simultaneously. C) shows the recorded CV response from B

(black) corrected for 80 Ω iR drop (grey), compared to the model of equation 1 with n = 1 (dashed line), with $E^{0\prime} = -0.41$ V vs. Ag/AgCl and j_{lim} of 5.8 A m^{-2}.

Electron microscopy is used to examine morphological structure, cell attachment, topography and bacterial cell distribution in GS biofilms on the surfaces. The images show formation of a thin layer of bacterial cells on the electrode surface sampled after 65 h Figure 4B, with much thicker biofilms with multiple layers of GS cells apparent for growth over longer time periods, Figure. 3.4C and 3.4D, as observed by others (Liu *et al*., 2011; Reguera *et al*., 2006; Richter *et al*., 2008). The presence of characteristic 2 µm long rod-shaped bacteria in all the SEM images is comparable to the dimensions reported for GS cells, and the images are similar to those observed by others for biofilms grown on graphite electrodes (Bond & Lovley, 2003; Strycharz-Glaven *et al*., 2011; Torres *et al*., 2008). It should be noted that the biofilms, as evident from Figure 3.4, present more complex geometric features (channels, gaps and protrusions) as a function of film thickness, as recently confirmed by Virdis *et al* (Virdis *et al*., 2012) using non-invasive confocal Raman microscopy to image ~20 µm thick biofilms grown from wastewater inoculum on graphite rods.

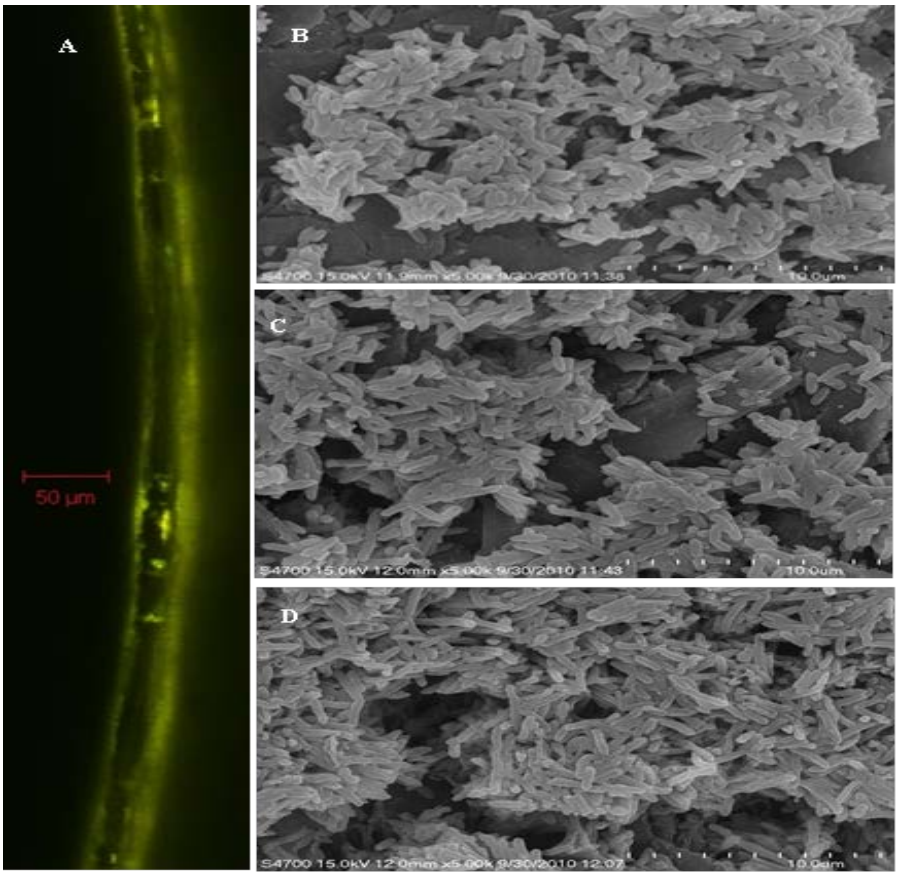

Figure.3.4 CLSM (A) and SEM (B-D) images of electrodes sampled from the reactor at 79 h (A, C), 65 h (B), and 129 h (D).

In our reactor a 3.4-fold increment in biofilm thickness (from 5 µm to 17 µm) is observed from 65 h to 79 h of reactor operation, whilst the acetate oxidation current density, based on the amperometric and voltammetric data, results in only an approximately 2-fold increment over the same time period. A further ~3 fold increment in biofilm thickness (from 17 µm to 50 µm) observed from 79 h to 129 h of reactor operation results in only a ~1.2 fold increment in current density over the same time period. This lack of direct correlation between film thickness and catalytic current implies that either mass or charge transport limits the overall catalytic current or that the biofilm formed over time displays differences in bacterial cell densities, viability and/or redox response. In addition Bond *et al* (Bond *et al.*, 2012) report that generation of protons by cells within a GS biofilm anode oxidizing acetate, and their diffusion out of the biofilm is predicted to result in the formation of a proton

concentration gradient across the biofilm. In this gradient, a drop in the pH value is expected to occur close to the biofilm/anode interface. This drop becomes more pronounced as the biofilm grows thicker. The lower pH that this gradient generates at this interface may affect the metabolic activity of the cells in those layers, perhaps contributing to the lack of correlation between acetate oxidation current density and biofilm thickness.

The CV response for biofilms under non-turnover conditions can provide detail on the surface concentration of redox species (Katuri *et al*., 2012). Typical non-turnover voltammograms of GS biofilms are shown in Fig. 5 each displaying peaks associated with more than one redox. For example, the non-turnover response for the biofilm sampled after 65 h (5 μm thickness, Figure. 3.5A) clearly shows redox transitions, additional to the main transition centred at −0.41 V, centered at −0.6 V and a shoulder on the main redox transition at around −0.48 V for oxidation and −0.37 V for reduction. The peak at −0.6 V is electrocatalytically inactive as no current generation is observed in a medium with substrate at this potential, as reported on recently (Fricke *et al*., 2008; Zhu *et al*., 2012). The non-turnover response for biofilms sampled at later times from the reactor (129 h, 50 μm thickness, Figure.3.5B) is also complex, displaying a broad oxidation peak at −0.37 V with a pre-peak shoulder obvious at −0.48 V and numerous un-resolved reduction peaks. *Geobacter sulfurreducens* produces multiple membrane associated cytochromes (Methé *et al*., 2003; Strycharz-Glaven *et al*., 2011) that can be differentially expressed in the organism during metabolism (Bond & Lovley, 2003; Holmes *et al*., 2006; Reguera *et al*., 2006; Richter *et al*., 2009). The redox potentials of some of these cytochromes have been characterized as −0.370 V vs. AgCl (Seeliger *et al*., 1998), (Lloyd *et al*., 2003), −0.300 and −0.390 V vs. AgCl. (Magnuson *et al*., 2000), −0.48 and −0.37 V vs. AgCl, (Zhu *et al*., 2012) and −0.46 V vs. AgCl (Snider *et al*., 2012).

Under non-turnover conditions, integration of the charge (Q) under a slow scan voltammogram can provide an estimation of the surface coverage of redox species ($\Gamma = Q/nFA$ in mol cm^{-2}) for the biofilms. The diffusion layer thickness in a

voltammetric experiment depends on the time scale of the experiment, with diffusion layer thicknesses estimated, at the 5 mV s^{-1} scan rate used, as 15, 26 and 79 μm, (*vide infra*) for films of 5, 17 and 50 μm thickness, respectively, indicating that the time-scale at this scan rate is sufficient to permit full electrolysis of redox species within the films. Whilst surface coverage increases as a function of growth time, and biofilm thickness, the increase does not scale linearly with thickness, as expected. A 3.4-fold increment in biofilm thickness (from 5 μm to 17 μm) results in an approximately 7-fold increment in surface coverage whilst a further ~3-fold increment in biofilm thickness (from 17 μm to 50 μm) results in only a ~2-fold increment in surface coverage. This again implies that the biofilm formed over time displays differences in bacterial cell densities, viability and/or redox site concentration and/or connectivity.

At more rapid scan rates, under non-turnover conditions, and assuming that the rate of heterogeneous electron transfer to the biofilm is not limiting and that diffusion is planar, the CV peak current density response can be modelled, as reported on previously, by the Randles−Sevçik equation 2:

$$j = 0.4463nFC_{redox}\left(\frac{nF}{RT}\right)^{1/2} D^{1/2}\nu^{1/2}$$

Where C_{redox} represents the concentration of redox species (mol cm^{-3}) within the film; ν is the scan rate (V s^{-1}); and D is an apparent diffusion coefficient (cm^2 s^{-1}). Thus, a charge transport related parameter ($D^{½}C_{redox}$) can be extracted from the linear portion of a plot of peak current density as a function of the square root of the scan rate for each biofilm, under these semi-infinite diffusion-limited conditions.

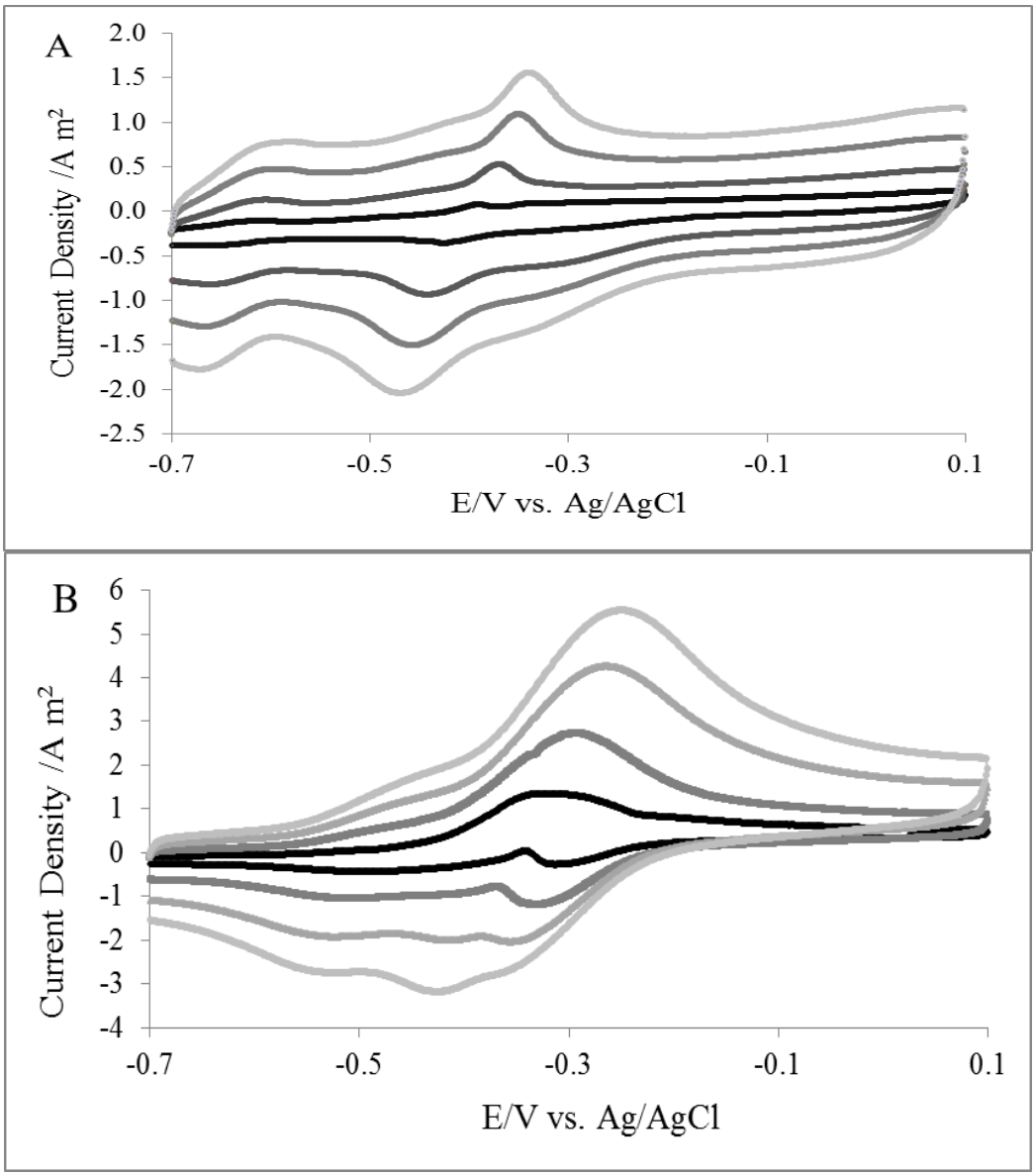

Figure.3.5 Cyclic voltammetry recorded at scan rates of 5, 20, 40, 60 mV s-1 (from lowest to highest signals) under non-turnover conditions for electrodes sampled from the reactor after A) 65 h and B) 129 h operation

In the case of redox polymer films on electrodes it has been shown that the diffusion coefficient for electron transport is directly related to the apparent rate of electron exchange (Dahms, 1968; Ruff, 1965; Ruff *et al*., 1971). In films on electrodes, such as those of redox polymers, where physical diffusion of redox species is restricted, charge transport is postulated to arise from electron hopping between adjacent electroactive moieties. The rate of charge, or the charge transport diffusion co-efficient, may thus be limited by an electron-hopping ion transport process accompanying the electron-hopping to maintain electro-neutrality, or the associated diffusional physical motions of the polymers to bring electron transfer sites into close enough proximity to transfer electrons (Blauch & Saveant, 1993; Kavanagh & Leech, 2013; Mao *et al*., 2003).

A charge transport related parameter ($D^{½}C_{redox}$) of 1.3 ± 0.3 × 10^{-9} mol cm^2 $s^{-1/2}$, 4.8 ± 0.9 × 10^{-9} mol cm^2 $s^{-1/2}$ and 7.5 ± 0.5 × 10^{-9} mol cm^2 $s^{-1/2}$ is obtained for biofilm thicknesses of 5 ± 2, 17 ± 3 and 50 ± 9 µm, respectively. Interestingly, reported $D^{1/2}C_{redox}$ values of 7.2 × 10^{-9} mol cm^2 $s^{-1/2}$ for films of a ferrocene redox polymer (Bunte *et al*., 2009) and 1.2 × 10^{-8} mol cm^2 $s^{-1/2}$ for films of osmium-based redox polymers (Macaodha *et al*., 2012) on electrodes are comparable to the values obtained for $D^{1/2}C_{redox}$ of GS biofilms in this study, perhaps indicative of a similar mechanism operating for electron transfer through the electroactive biofilms. The surface coverage divided by the average biofilm thickness gives an estimate of the concentration of redox species in the biofilm, C_{redox} of 2.8 ± 1.1, 5.9 ± 1.2 and 4.0 ± 1.1 mM for biofilms of thickness of 5 ± 2, 17 ± 3 and 50 ± 9 µm, respectively, permitting extraction of a value for D from the $D^{½}C_{redox}$ charge transport related parameter. The redox site concentrations estimated are similar to a value of 7.3 mM reported on previously for GS biofilms of 34 µm in thickness induced to grow through successive batch-feed cycles on graphite electrodes.

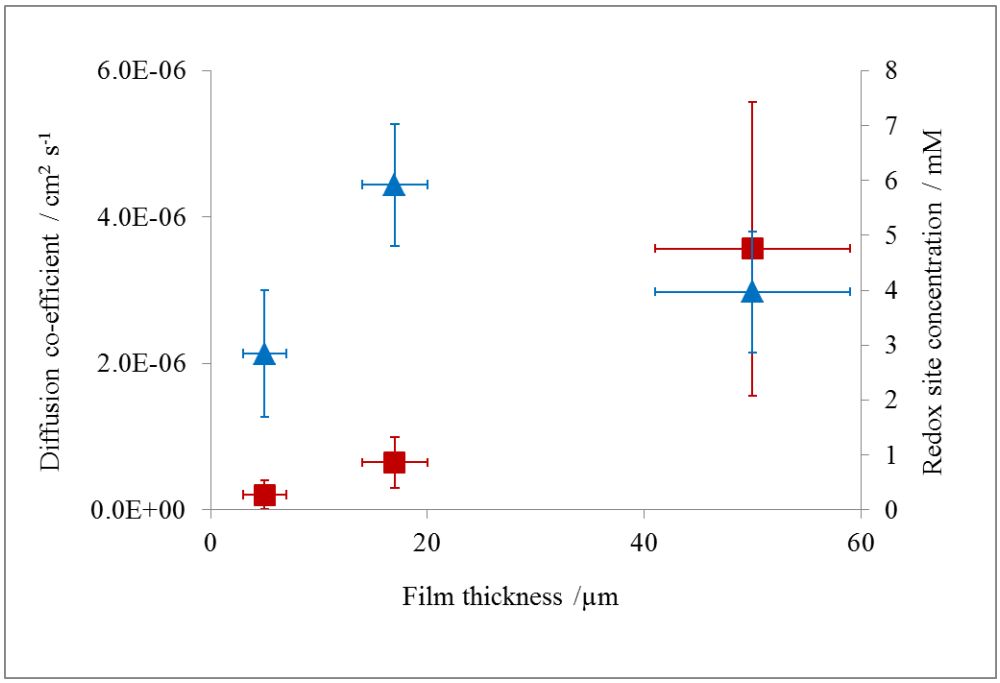

Figure.3.6 Plot of *D* (squares) and of C_{redox} (triangles) versus biofilm thickness.

Diffusion coefficients of 2.1 ± 1.4 × 10^{-7} cm^2 s^{-1}, 6.5 ± 2.5 × 10^{-7} cm^2 s^{-1} and 3.6 ± 1.4 × 10^{-6} cm^2 s^{-1} are thus obtained for biofilm thicknesses of 5 ± 2, 17 ± 3 and 50 ± 9 µm, respectively. These values are, again, similar to a value of 3.6 × 10^{-6} cm^2 s^{-1} reported on previously for GS biofilms of 34 µm in thickness induced to grow through successive batch-feed cycles on graphite electrodes. Diffusion coefficient and redox species concentration are both higher in biofilms of 17 µm thickness over their values in biofilms of 5 µm thickness (Figure.3.6). This increase in C_{redox} may be due to a decrease in film porosity, averaged over the entire biofilm, as a function of time, supported by the observation that the surface coverage increases 7-fold whilst film thickness only increases 3.4 fold, when comparing the 17 µm thick biofilm to the 5 µm thick biofilm. The more compact 17 µm thick biofilm has therefore a higher redox site concentration, and more rapid charge transport rate, possibly as a result of closer proximity of redox sites to each other facilitating electron hopping. The redox site concentration in the 50 µm thick biofilm is lower than that estimated in the 17 µm thick biofilm, again possibly because of increased porosity of the

outermost layers of the 50 μm thick biofilm, and thus an overall decrease in biofilm GS cell and redox site density. Interestingly a marked increase in *D* is obtained for charge transport through the 50 μm thick biofilm over that obtained in the thinner films. This can be a result of increased porosity of the thicker films contributing to ease of ion transport through the film, where ion transport may be the limiting factor for charge transport under this condition. Recently Renslow *et al* (Renslow *et al*., 2013) reported a bulk liquid water diffusion coefficient value of 2.8×10^{-5} cm^2 s^{-1} within GS biofilms with an observation that the diffusion coefficient value for water is lower in the layers close to electrode compared to that in the outermost layers of the biofilms. This solvent transport diffusion coefficient, during acetate oxidation by GS biofilms, is an order of magnitude higher than the highest charge transport diffusion coefficient estimated, again indicative that charge transport may be limited by ion transport, and/or bacterial motions, to affect electron transfer through the films at the latter stage of biofilm growth, and not solvent or electron transfer.

3.4 Conclusions

Current generation, as a result of acetate oxidation, reaches a steady-state of 9 A m^{-2} for biofilms of GS induced to grow on graphite electrode under continuous flow conditions in a single-compartment three electrode cell, with 0 V vs Ag/AgCl applied anode potential. The increase in current over time does not scale linearly with film thickness or redox site coverage presumably because either mass or charge transport limits the current or that the biofilm formed over time displays differences in bacterial cell densities, viability and/or redox response. A combination of electrochemical and microscopic studies reveal that the biofilm developed to 50 ± 9 μm thickness after 129 h, when the catalytic current is at steady-state, displays more rapid charge transport diffusion, even though the overall redox site concentration is lower than in thinner films. Whilst the microbial biofilms may not display homogeneous distribution of cells, or indeed diffusion coefficient[21] across the entire film thickness an increase in the overall biofilm porosity for the 50 μm thick film

may contribute to improved charge transport, as ion transport required to maintain electroneutrality within the bulk film upon oxidation may be the limiting factor for charge transport under the non-turnover condition of the experiment. Whether this is also the case when the biofilm oxidising acetate substrate is not clear as yet.

References

Babauta, J., Renslow, R., Lewandowski, Z., Beyenal, H. 2012. Electrochemically active biofilms: facts and fiction. A review. *Biofouling*, **28**(8), 789-812.

Baron, D., LaBelle, E., Coursolle, D., Gralnick, J.A., Bond, D.R. 2009. Electrochemical measurement of electron transfer kinetics by shewanella oneidensis MR-1. *Journal of Biological Chemistry*, **284**(42), 28865-28873.

Blauch, D.N., Saveant, J.M. 1993. Effects of long-range electron transfer on charge transport in static assemblies of redox centers. *The Journal of Physical Chemistry*, **97**(24), 6444-6448.

Bond, D.R., Holmes, D.E., Tender, L.M., Lovley, D.R. 2002. Electrode-reducing microorganisms that harvest energy from marine sediments. *Science*, **295**(5554), 483-485.

Bond, D.R., Lovley, D.R. 2003. Electricity production by Geobacter sulfurreducens attached to electrodes. *Applied and Environmental Microbiology*, **69**(3), 1548-1555.

Bond, D.R., Strycharz-Glaven, S.M., Tender, L.M., Torres, C.I. 2012. On electron transport through Geobacter biofilms. *ChemSusChem*, **5**(6), 1099-1105.

Bunte, C., Prucker, O., König, T., Rühe, J.r. 2009. Enzyme containing redox polymer networks for biosensors or biofuel cells: A photochemical approach. *Langmuir*, **26**(8), 6019-6027.

Dahms, H. 1968. Electronic conduction in aqueous solution. *The Journal of Physical Chemistry*, **72**(1), 362-364.

Fricke, K., Harnisch, F., Schröder, U. 2008. On the use of cyclic voltammetry for the study of anodic electron transfer in microbial fuel cells. *Energy and Environmental Science*, **1**(1), 144-147.

Holmes, D.E., Chaudhuri, S.K., Nevin, K.P., Mehta, T., Methé, B.A., Liu, A., Ward, J.E., Woodard, T.L., Webster, J., Lovley, D.R. 2006. Microarray and genetic analysis of electron transfer to electrodes in Geobacter sulfurreducens. *Environmental Microbiology*, **8**(10), 1805-1815.

Inoue, K., Qian, X., Morgado, L., Kim, B.C., Mester, T., Izallalen, M., Salgueiro, C.A., Lovley, D.R. 2010. Purification and characterization of OmcZ, an outer-surface, octaheme c-type cytochrome essential for optimal current production by geobacter sulfurreducens. *Applied and Environmental Microbiology*, **76**(12), 3999-4007.

Katuri, K.P., Kavanagh, P., Rengaraj, S., Leech, D. 2010. Geobacter sulfurreducens biofilms developed under different growth conditions on glassy carbon electrodes: insights using cyclic voltammetry. *Chemical Communications*, **46**(26), 4758-4760.

Katuri, K.P., Rengaraj, S., Kavanagh, P., O'Flaherty, V., Leech, D. 2012. Charge transport through Geobacter sulfurreducens biofilms grown on graphite rods. *Langmuir*, **28**(20), 7904-7913.

Kavanagh, P., Leech, D. 2013. Mediated electron transfer in glucose oxidising enzyme electrodes for application to biofuel cells: recent progress and perspectives. *Physical Chemistry Chemical Physics*, **15**(14), 4859-4869.

Kim, B.C., Postier, B.L., DiDonato, R.J., Chaudhuri, S.K., Nevin, K.P., Lovley, D.R. 2008. Insights into genes involved in electricity generation in Geobacter sulfurreducens via whole genome microarray analysis of the OmcF-deficient mutant. *Bioelectrochemistry*, **73**(1), 70-75.

Kumar, A., Katuri, K., Lens, P., Leech, D. 2012. Does bioelectrochemical cell configuration and anode potential affect biofilm response? *Biochemical Society Transactions*, **40**(6), 1308-1314.

Kumar, A., Siggins, A., Katuri, K., Mahony, T., O'Flaherty, V., Lens, P., Leech, D. 2013. Catalytic response of microbial biofilms grown under fixed anode potentials depends on electrochemical cell configuration. *Chemical Engineering Journal*, **230**, 532-536.

Laspidou, C.S., Rittmann, B.E. 2004. Evaluating trends in biofilm density using the UMCCA model. *Water Research*, **38**(14–15), 3362-3372.

Leang, C., Qian, X., Mester, T., Lovley, D.R. 2010. Alignment of the c-type cytochrome OmcS along pili of Geobacter sulfurreducens. *Applied and Environmental Microbiology*, **76**(12), 4080-4084.

Lee, H.-S., Torres, C.s.I., Parameswaran, P., Rittmann, B.E. 2009. Fate of H2 in an upflow single-chamber microbial electrolysis cell using a metal-catalyst-free cathode. *Environmental Science and Ttechnology*, **43**(20), 7971-7976.

Liu, Y., Kim, H., Franklin, R.R., Bond, D.R. 2011. Linking spectral and electrochemical analysis to monitor c-type cytochrome redox status in living Geobacter sulfurreducens biofilms. *Physical Chemistry Chemical Physics*, **12**(12), 2235-2241.

Lloyd, J.R., Myerson, A.L.H., Leang, C., Coppi, M.V., Cuifo, S., Methè, B.A., Lovley, D., Sandler, S.J. 2003. Biochemical and genetic characterization of PpcA, a periplasmic c-type cytochrome in Geobacter sulfurreducens. *Biochemical Journal*, **369**, 153-161.

Logan, B.E., Hamelers, B., Rozendal, R., Schröder, U., Keller, J., Freguia, S., Aelterman, P., Verstraete, W., Rabaey, K. 2006. Microbial fuel cells: Methodology and technology. *Environmental Science and Technology*, **40**(17), 5181-5192.

Lovley, D.R. 2006. Bug juice: harvesting electricity with microorganisms. *Nature Reviews. Microbiology*, **4**(7), 497-508.

Macaodha, D., Ferrer, M.L., Conghaile, P.O., Kavanagh, P., Leech, D. 2012. Crosslinked redox polymer enzyme electrodes containing carbon nanotubes for high and stable glucose oxidation current. *physical chemistry, chemical physics*, **14**(42), 14667-14672.

Magnuson, T.S., Hodges-Myerson, A.L., Lovley, D.R. 2000. Characterization of a membrane-bound NADH-dependent Fe3+ reductase from the dissimilatory Fe3+-reducing bacterium Geobacter sulfurreducens. *FEMS Microbiology Letters*, **185**(2), 205-211.

Malvankar, N.S., Tuominen, M.T., Lovley, D.R. 2012. Biofilm conductivity is a decisive variable for high-current-density Geobacter sulfurreducens microbial fuel cells. *Energy and Environmental Science*, **5**(2), 5790-5797.

Malvankar, N.S., Vargas, M., Nevin, K.P., Franks, A.E., Leang, C., Kim, B.-C., Inoue, K., Mester, T., Covalla, S.F., Johnson, J.P., Rotello, V.M., Tuominen, M.T., Lovley, D.R. 2011. Tunable metallic-like conductivity in microbial nanowire networks. *Nature Nanotechnology*, **6**(9), 573-579.

Mao, F., Mano, N., Heller, A. 2003. Long tethers binding redox centers to polymer backbones enhance electron transport in enzyme "wiring" hydrogels. *Journal of the American Chemical Society*, **125**(16), 4951-4957.

Marsili, E., Rollefson, J.B., Baron, D.B., Hozalski, R.M., Bond, D.R. 2008. Microbial biofilm voltammetry: Direct electrochemical characterization of catalytic electrode-attached biofilms. *Applied and Environmental Microbiology*, **74**(23), 7329-7337.

Marsili, E., Sun, J., Bond, D.R. 2010. Voltammetry and growth physiology of Geobacter sulfurreducens biofilms as a function of growth stage and imposed electrode potential. *Electroanalysis*, **22**(7-8), 865-874.

Methé, B.A., Nelson, K.E., Eisen, J.A., Paulsen, I.T., Nelson, W., Heidelberg, J.F., Wu, D., Wu, M., Ward, N., Beanan, M.J., Dodson, R.J., Madupu, R., Brinkac, L.M., Daugherty, S.C., DeBoy, R.T., Durkin, A.S., Gwinn, M., Kolonay, J.F., Sullivan, S.A., Haft, D.H., Selengut, J., Davidsen, T.M., Zafar, N., White, O., Tran, B., Romero, C., Forberger, H.A., Weidman, J., Khouri, H., Feldblyum, T.V., Utterback, T.R., Van Aken, S.E., Lovley, D.R., Fraser, C.M. 2003. Genome of Geobacter sulfurreducens: Metal reduction in subsurface environments. *Science*, **302**(5652), 1967-1969.

Millo, D., Harnisch, F., Patil, S.A., Ly, H.K., Schröder, U., Hildebrandt, P. 2011. In situ spectroelectrochemical investigation of electrocatalytic microbial biofilms by surface-enhanced resonance raman spectroscopy. *Angewandte Chemie International Edition*, **50**(11), 2625-2627.

Nevin, K.P., Kim, B.C., Glaven, R.H., Johnson, J.P., Woodward, T.L., Methé, B.A., Didonato Jr, R.J., Covalla, S.F., Franks, A.E., Liu, A., Lovley, D.R. 2009. Anode biofilm transcriptomics reveals outer surface components essential for high density current production in Geobacter sulfurreducens fuel cells. *PLoS ONE*, **4**(5).

Nevin, K.P., Richter, H., Covalla, S.F., Johnson, J.P., Woodard, T.L., Orloff, A.L., Jia, H., Zhang, M., Lovley, D.R. 2008. Power output and columbic efficiencies from biofilms of Geobacter sulfurreducens comparable to mixed community microbial fuel cells. *Environmental Microbiology*, **10**(10), 2505-2514.

Rabaey, K., Verstraete, W. 2005. Microbial fuel cells: novel biotechnology for energy generation. *Trends in Biotechnology*, **23**(6), 291-298.

Reguera, G., Nevin, K.P., Nicoll, J.S., Covalla, S.F., Woodard, T.L., Lovley, D.R. 2006. Biofilm and nanowire production leads to increased current in Geobacter sulfurreducens fuel cells. *Applied and Environmental Microbiology*, **72**(11), 7345-7348.

Renslow, R.S., Babauta, J.T., Majors, P.D., Beyenal, H. 2013. Diffusion in biofilms respiring on electrodes. *Energy and Environmental Science*, **6**(2), 595-607.

Richter, H., McCarthy, K., Nevin, K.P., Johnson, J.P., Rotello, V.M., Lovley, D.R. 2008. Electricity generation by Geobacter sulfurreducens attached to gold electrodes. *Langmuir*, **24**(8), 4376-4379.

Richter, H., Nevin, K.P., Jia, H., Lowy, D.A., Lovley, D.R., Tender, L.M. 2009. Cyclic voltammetry of biofilms of wild type and mutant Geobacter sulfurreducens on fuel cell anodes indicates possible roles of OmcB, OmcZ, type IV pili, and protons in extracellular electron transfer. *Energy and Environmental Science*, **2**(5), 506-516.

Ruff, I. 1965. On the Role of Water in Electron-Transfer Reactions. I. *The Journal of Physical Chemistry*, **69**(9), 3183-3186.

Ruff, I., Friedrich, V.J., Demeter, K., Csillag, K. 1971. Transfer diffusion. II. Kinetics of electron exchange reaction between ferrocene and ferricinium ion in alcohols, J*ournal of Physical Chemistry*, 75, 3303–3309.

Schaetzle, O., Barrière, F., Baronian, K. 2008. Bacteria and yeasts as catalysts in microbial fuel cells: Electron transfer from micro-organisms to electrodes for green electricity. *Energy and Environmental Science*, **1**(6), 607-620.

Seeliger, S., Cord-Ruwisch, R., Schink, B. 1998. A periplasmic and extracellular c-type cytochrome of Geobacter sulfurreducens acts as a ferric iron reductase and as an electron carrier to other acceptors or to partner bacteria. *Journal of Bacteriology*, **180**(14), 3686-3691.

Snider, R.M., Strycharz-Glaven, S.M., Tsoi, S.D., Erickson, J.S., Tender, L.M. 2012. Long-range electron transport in Geobacter sulfurreducens biofilms is redox gradient-driven. *Proceedings of the National Academy of Sciences*, **109**(38), 15467-15472.

Srikanth, S., Marsili, E., Flickinger, M.C., Bond, D.R. 2008. Electrochemical characterization of Geobacter sulfurreducens cells immobilized on graphite paper electrodes. *Biotechnology and Bioengineering*, **99**(5), 1065-1073.

Strycharz-Glaven, S.M., Snider, R.M., Guiseppi-Elie, A., Tender, L.M. 2011. On the electrical conductivity of microbial nanowires and biofilms. *Energy and Environmental Science*, **4**(11), 4366-4379.

Strycharz, S.M., Glaven, R.H., Coppi, M.V., Gannon, S.M., Perpetua, L.A., Liu, A., Nevin, K.P., Lovley, D.R. 2011a. Gene expression and deletion analysis of mechanisms for electron transfer from electrodes to Geobacter sulfurreducens. *Bioelectrochemistry*, **80**(2), 142-150.

Strycharz, S.M., Malanoski, A.P., Snider, R.M., Yi, H., Lovley, D.R., Tender, L.M. 2011b. Application of cyclic voltammetry to investigate enhanced catalytic current generation by biofilm-modified anodes of Geobacter sulfurreducens strain DL1 vs. variant strain KN400. *Energy and Environmental Science*, **4**(3), 896-913.

Torres, C.I., Marcus, A.K., Lee, H.S., Parameswaran, P., Krajmalnik-Brown, R., Rittmann, B.E. 2010. A kinetic perspective on extracellular electron transfer by anode-respiring bacteria. *FEMS Microbiology Reviews*, **34**(1), 3-17.

Torres, C.I., Marcus, A.K., Parameswaran, P., Rittmann, B.E. 2008. Kinetic experiments for evaluating the nernst-monod model for anode-respiring bacteria (ARB) in a biofilm anode. *Environmental Science and Technology*, **42**(17), 6593-6597.

Virdis, B., Harnisch, F., Batstone, D.J., Rabaey, K., Donose, B.C. 2012. Non-invasive characterization of electrochemically active microbial biofilms using confocal Raman microscopy. *Energy and Environmental Science*, **5**(5), 7017-7024.

Yi, H., Nevin, K.P., Kim, B.C., Franks, A.E., Klimes, A., Tender, L.M., Lovley, D.R. 2009. Selection of a variant of Geobacter sulfurreducens with enhanced

capacity for current production in microbial fuel cells. *Biosensors and Bioelectronics*, **24**(12), 3498-3503.

Zhu, X., Yates, M.D., Logan, B.E. 2012. Set potential regulation reveals additional oxidation peaks of Geobacter sulfurreducens anodic biofilms. *Electrochemistry Communications*, **22**(0), 116-119.

Chapter 4

Monitoring *Geobacter sulfurreducens* biofilm formation and response using electrochemistry coupled to a quartz crystal microbalance

4.1 Introduction

Bacterial attachment is an important initial step for any biofilm formation (Kreth *et al*., 2004; Otto & Silhavy, 2002). Bacterial attachment depends on physiological factors, such as surface properties, hydrodynamic effects and the physiochemical properties of the cell (Marcus *et al*., 2012). Biofilm formation is an important process with implications in health and wellbeing, and in wastewater treatment processes and in soil and plant ecology (Olsson *et al*., 2008). In the case of microbial electrochemical cell technology, biofilm development is a key factor contributing to electricity generation. Bacterial biofilms transfer electrons to a solid electrode through at least one of the following mechanisms (i) electron shuttling mediating molecules, (ii) redox active membrane-bound proteins (cytochromes), (iii) via conductive nanowires (pili) (Liu *et al*., 2011; Malvankar *et al*., 2011; Nevin *et al*., 2009). Recent reports (Snider *et al*., 2012; Strycharz-Glaven *et al*., 2011) highlight that different extracellular electron transfer rates are observed during different stages of bacterial growth, but the exact electron transfer mechanism is still not fully understood. The use of a quartz crystal microbalance (QCM) can provide details on the interactions between biomass of the biofilms and the surface on which they get attached (Brown-Malker *et al*., 2010; Gutman *et al*., 2012; Lau *et al*., 2009; Marcus *et al*., 2012; Schofield *et al*., 2007; Xie *et al*., 2010).

The quartz crystal microbalance with dissipation monitoring (QCM-D) provides simultaneous measurement of changes in frequency (Δf) and energy dissipation factor (ΔD) of an oscillating AT-cut quartz crystal (Chen *et al*., 2012). The frequency changes provide an estimation of change in mass and mechanical property of the attached bacterial layer. The frequency and dissipation results may thus provide information on microbial growth kinetics and strength of attachment to surfaces, which can improve fundamental understanding of how EAB interact with solid electron acceptors (Brown-Malker *et al*., 2010). The QCM system can measure *in situ* mass variation without disturbing the sensor and it can be combined with electrochemical techniques such as cyclic voltammetry and chronoamperometry (Kwon & Evans, 2004). *Geobacter* species have many potential advantages and can completely oxidize organic compounds to carbon dioxide with recovery of over 90 % of the electrons available in the substrate as electricity (Richter *et al*., 2008). In the present study we report the combined effect of *Geobacter sulfurreducens* (GS) biomass changes on the QCM gold sensor with electricity generation. We observed the frequency change and energy dissipation as a function of time using a continuous flow QCM. This investigation has led to use of the EQCM-D measurement technique to monitor the in situ change of the biofilm properties and to correlate the response with the electrochemical performance in this work.

4.2 Experimental

The QCM-D measurements were performed with gold-coated AT-cut quartz crystals mounted in an E1 system (Q-sense AB, Gothenburg, Sweden), equipped with an electrochemical module to permit simultaneous electrochemistry and QCM-D (EQCM-D) monitoring to be achieved. One face of the gold-coated sensor is used, in this configuration, as a working electrode for *in situ* electrochemical analysis. The gold-coated sensor, Ag/AgCl reference and platinum-plate counter electrode were rinsed with 75 % ethanol solution followed by Milli-Q water and dried with N_2 gas, for surface sterilisation, prior to mounting inside the EQCM-D module. The changes

in frequency and energy dissipation were measured for six different overtones, n= 3, 5, 7, 9, 11 and 13, with the Q-soft-401 software (Q-sense, Gothenburg, Sweden). A potentiostat (CHI-650, CH Instruments, Austin, TX) was used to record simultaneous chronoamperometry at a constant applied potential of 0 V vs Ag/AgCl, or cyclic voltammetry responses, both simultaneous to the QCM-D signals. A diagram of the overall experimental set-up is shown in Figure 4.1.

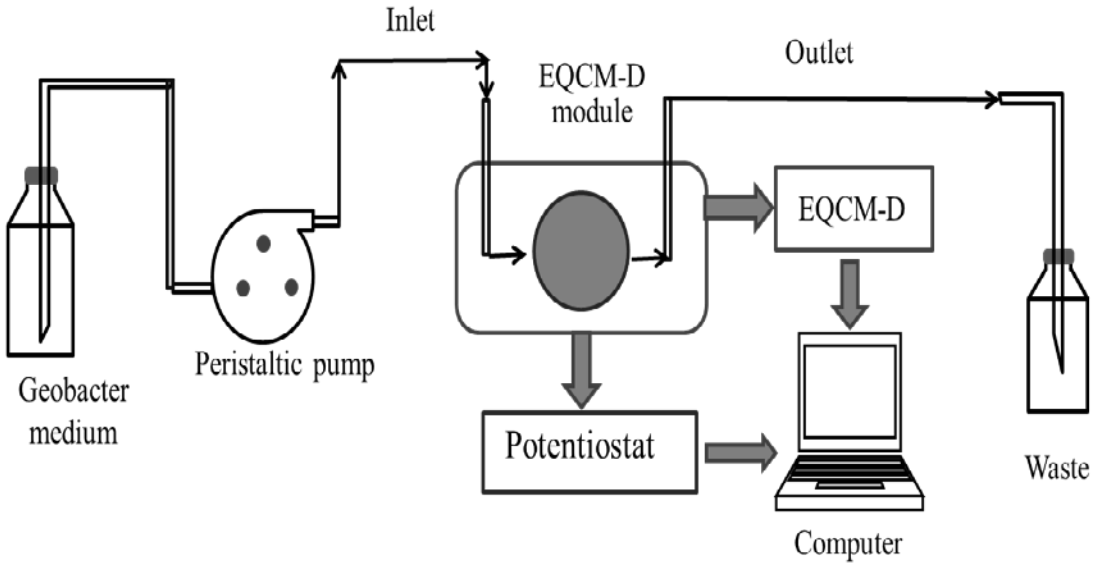

Figure 4.1 Schematic diagram of the experiment setup for real-time monitoring of *Geobacter* biofilm formation in EQCM-D system. temperature 30 ± 1 ºC.

The GS strain (ATCC 51573) used as a source of electroactive bacteria was sub-cultured in 90 ml acetate (10 mM) and fumarate-containing GB growth medium. The acetate medium also contained (per L): 0.1 g KCl, 0.15 g NH_4Cl, 0.6 g Na_2HPO_4, 2.5 g $NaHCO_3$, 10 mL trace element solution and 10 mL vitamin solution prepared according to the protocol supplied by the culture centre (http://www.dsmz.de, medium no. 826), as described in chapter 3. The GS cells were

harvested during exponential of growth period (log phase) by measuring the OD_{600} 0.74 that corresponds to a log phase of growth by centrifugation (12 min at 12,100g) and re-suspension in sterilised medium prepared without addition of fumarate as electron acceptor.

Before inoculation into the flow cell of the EQCM-D module, the gold sensor was equilibrated in GS medium until a stable baseline was observed and then suspended bacteria were diluted (OD_{600} 0.48) with acetate containing (10 mM) GS media for introduction to the EQCM-D flow system using a peristaltic pump (Ismatec, Switzerland) at a flow rate of 100 µl/min. The solution pH was in the range 7.0 - 7.2 and the EQCM-D cell was operated at 30 °C throughout the experiment. After inoculation, frequency shifts (Δf), dissipation shifts (ΔD) and current generation were measured continuously, apart from intermittent interruptions to record cyclic voltammograms.

After 23 hours flow of GS containing medium, the medium was exchanged to remove the GS inoculum from the media to encourage self-growth of surface-attached GS on the EQCM-D sensor.

4.3 Results and discussion

Bacterial adhesion was studied under flow using an EQCM-D system. Initially fumarate-free GS media was pumped through the cell for 45 minutes to equilibrate the module response. After this initial period, the influent solution was changed to introduce inoculum. Immediately (~30 sec) upon addition of GS to the media (OD_{600} 0.48), the frequency (Δf) and dissipation (ΔD) response shows an upward spike, figure 4.2A. Both spikes can be attributed, as discussed by Chen *et al* to a change in the composition of the media upon the addition of GS to the media (Chen *et al*., 2012). After the initial spike, a decrease in frequency and increase in dissipation is observed. The changes in frequency and dissipation are proposed to be due to an increment of cell adhesion and attachment to the electrode surface, as reported on by others (Gutman *et al*., 2012; Otto & Silhavy, 2002). For example,

Kreth *et al* report exponential decrease in frequency when *Streptococcus mutans* cells attach to the QCM sensor (Kreth *et al*., 2004). More recently Babauta *et al* report on a similar trend of frequency shift when *Geobacter sulfurreducens* cells attach to a gold QCM sensor (Babauta *et al*., 2014). Based on the Sauerbrey equation, a negative frequency shift is expected upon attachment of bacteria to the electrode surface (Marcus *et al*., 2012). Biofilm growth and current generation depend on several factors such as electrode materials, substrate concentration and inoculum type (Wang *et al*., 2009; Zhou *et al*., 2011). In present study we observe a 40 hours lag phase between addition of inoculum and an increase in current production, figure 4.2B. The increase in current after this lag phase indicates that GS electroactive bacteria are capable of transferring electrons to the gold electrode as a terminal electron acceptor, as a result of acetate oxidation. Richter *et al* observe a similar lag period, followed by a rapid increase in current associated with growth of GS cells on a gold electrode (Richter *et al*., 2008). In chapter 3 section 3.3, fig 3.2 we reported a similar trend in current generation by GS biofilms on graphite electrodes, observing a 45 hours lag phase prior to current production (Jana *et al*., 2014a).

A frequency shift of -100 Hz and catalytic current density of 35 µA/cm^2 is observed after 70 hours of experiment. The frequency changes can be used to estimate the mass attached to the surface of the gold sensor using the Sauerbrey equation (4.1)(Sauerbrey, 1959) , using the simplifying assumption that the biofilm is a rigid layer.

$$\Delta f_n = -\frac{n}{c}\,\Delta m \qquad (4.1)$$

Here C = 17.7 ng^{-1}cm^{2}Hz is the resolution for a 5 MHz crystal and (*n)* is overtone number, (Δ*m*) mass of the adhering cell, with the resulting plot of mass and current density as a function of time shown in figure 4.3.

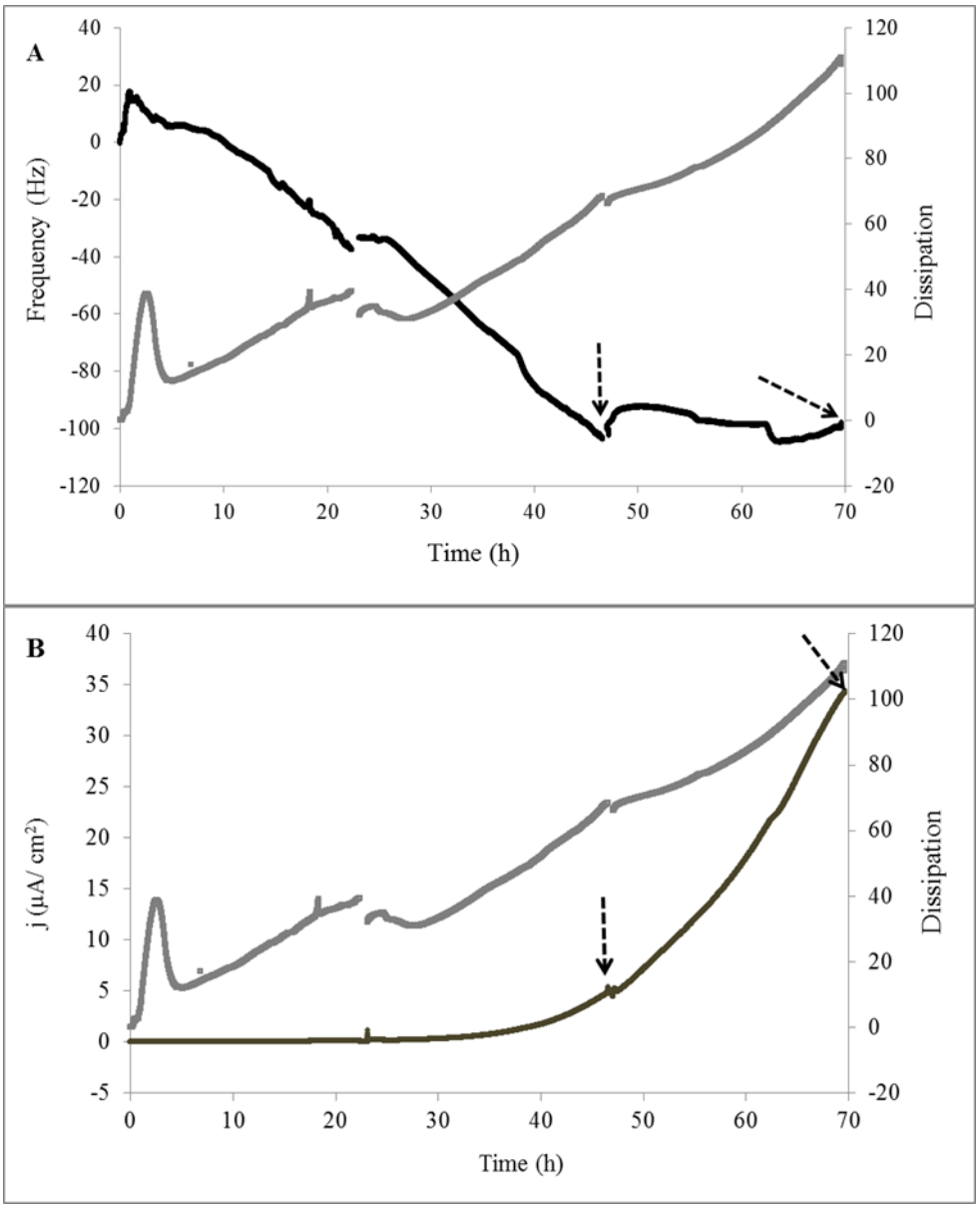

Figure 4.2 (A) Representative frequency Δ*f* (black) and dissipation Δ*D* (grey) shifts as a function of time. (B) Dissipation Δ*D* (grey) shifts as a function of time compared to current generation (black). Arrow indicates times when *in situ* cyclic voltammetry was performed. Flow rate of 100 µl/min, pH 7.0 - 7.2, temperature 30 °C and acetate media.

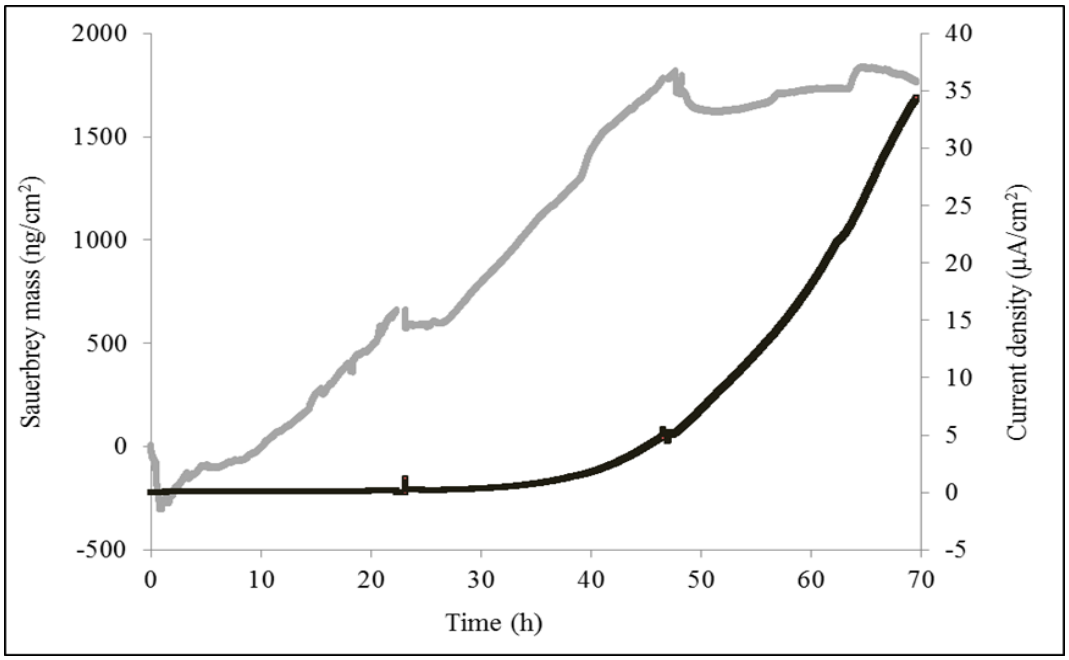

Figure 4.3 Sauerbrey mass (*Δm*-grey) and current density (black) as a function of time. Flow rate of 100 µl/min, pH 7.0 - 7.2, Temperature 30 °C and acetate media.

The Sauerbrey mass (*Δm*) attains a steady value of ~1800 ng/cm^2 after 47 h of operation that persists up to the 70 h shown in Figure 4.3. After 40 h of operation 1430 ng/cm^2 of Sauerbrey mass is observed, equivalent to 80 % of the steady value, but at this time only 1.7 µA/cm^2 of current output is measured, 4.8 % of the response at 70 h. The large increment in current generation, over a period with little Sauerbrey mass change, is because improved attachment between cell and electrode and/or improved cell to cell connection within an established biofilm may be required for current flow to occur. Babauta *et al* (2014) report that initial GS biofilm growth is limited by metabolic processes and not current generation and for current to increase the number of sites facilitating electron transfer increase with increasing cell density. Marsili *et al*. (2010) reported on the correlation between the mass of protein from GS developed on electrodes as a function of time and current, and they observe an increment in acetate oxidation, from 2 mA mg^{-1} protein initially to 8 mA mg^{-1} protein within 6 hours of bacterial growth. In this present study we also observed more current is produced with less biomass in in the exponential phase condition.

The ratio of Δf/ΔD can be used to measure the viscoelasticity of the biofilm formed on the gold surface with a value of Δf/ΔD above zero reported to correspond to higher elasticity nature of the layer whilst a negative value corresponds to a more viscous layer (Gutman *et al*., 2012).

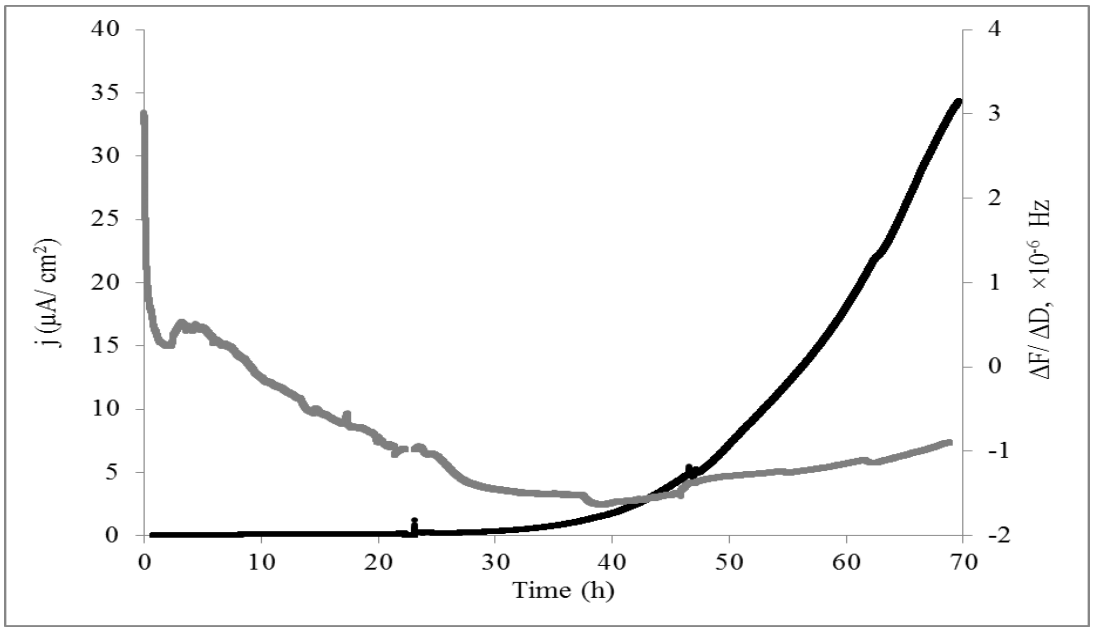

Figure 4.4 Ratio of Δf/ΔD (grey) as a function of time compared to current density (black) during experiment.

From Figure 4.4, the ratio Δf/ΔD indicates elastic property of the GS biofilm during initial stages of the cell attachment (up to 10 hours). The cost to bacterial cells in terms of elastic energy when adhering on the electrode surface and the thermal energy in the environment may result in an energetic barrier to bacterial adhesion (Anselme *et al* 2010). Between 10 h and 40 h post-inoculation the biofilm becomes more viscous. If the adhere layer become viscoelastic there will be a loss of energy due to internal friction in the film. Viscoelasticity allows biofilms to resist detachment due to increased fluid shear by deformation, while remaining attached to a surface. Recently Babauta *et al* also observed the viscoelastic nature of GS biofilms grown in gold QCM sensor after 115 hours of operation (Babauta *et al*., 2014) and also observed typical current response of *G. sulfurreducens* biofilm growth, consisting of a lag phase followed by an exponential phase. Initial GS biofilm growth

was not limited by current but limited by metabolic process. For current increment, higher redox site concentration must have increased with increasing cell density. They quantified the frequency shift during initial growth and exponential growth of electrode-respiring *G. sulfurreducens* biofilms. In the initial lag phase the frequency shift of the biofilm deposition process was linear with respect to current (slope, -0.52 Hz nA) but in log phase condition the biofilms are different from lag phase due to change in the physical structure of the biofilm resulting in a change in frequency shift (slope, -26-33 Hz µA). The second linear region of the frequency shift/current relationship for the biofilm corresponds with the exponential current increase (Babauta *et al*., 2014). In this study we also observed two different frequency shifts in relation to current generation during initial lag phase (slope -0.3 Hz nA) and the exponential growth phase (slope, -4.0 Hz µA).

The *in situ* voltammetric and EQCM-D behaviour of biofilms recorded at selected time intervals after inoculation, using slow-scan cyclic voltammetry and EQCM-D is presented in Fig 4.5 and 4.6. Sigmoidal cyclic voltammograms are observed at different time intervals and change in magnitude of the catalytic oxidation current observed in the slow scan cyclic voltammograms as a function of time (46:40 and 69:43 h). Figure 4.5 and 4.6 shows sigmoidal cyclic voltammograms recorded at the time intervals of 46:40 and 69:43 hrs after reactor initiation, using slow-scan cyclic voltammetry, permit estimation, from the first derivative of the voltammogram, of acetate oxidation centred at −0.42 V vs. Ag/AgCl is good agreement with that reported in chapter 3 and by others (Fricke *et al*., 2008; Liu *et al*., 2011; Torres *et al*., 2008). The sigmoidal voltammogram is indicative of catalytic oxidation of the acetate substrate by the biofilm with heterogeneous electron transfer to the electrode (Katuri *et al*., 2010). The catalytic oxidation current observed in the slow scan voltammograms as a function of time correlates with the amperometric current observed at same time period. For example amperometric current density of 5 and 35 μAcm^{-2} was obtained after 46 and 70 h of operation where CV catalytic current density was showing the same magnitude of current generation at same time interval (Fig 4.5 and 4.6).

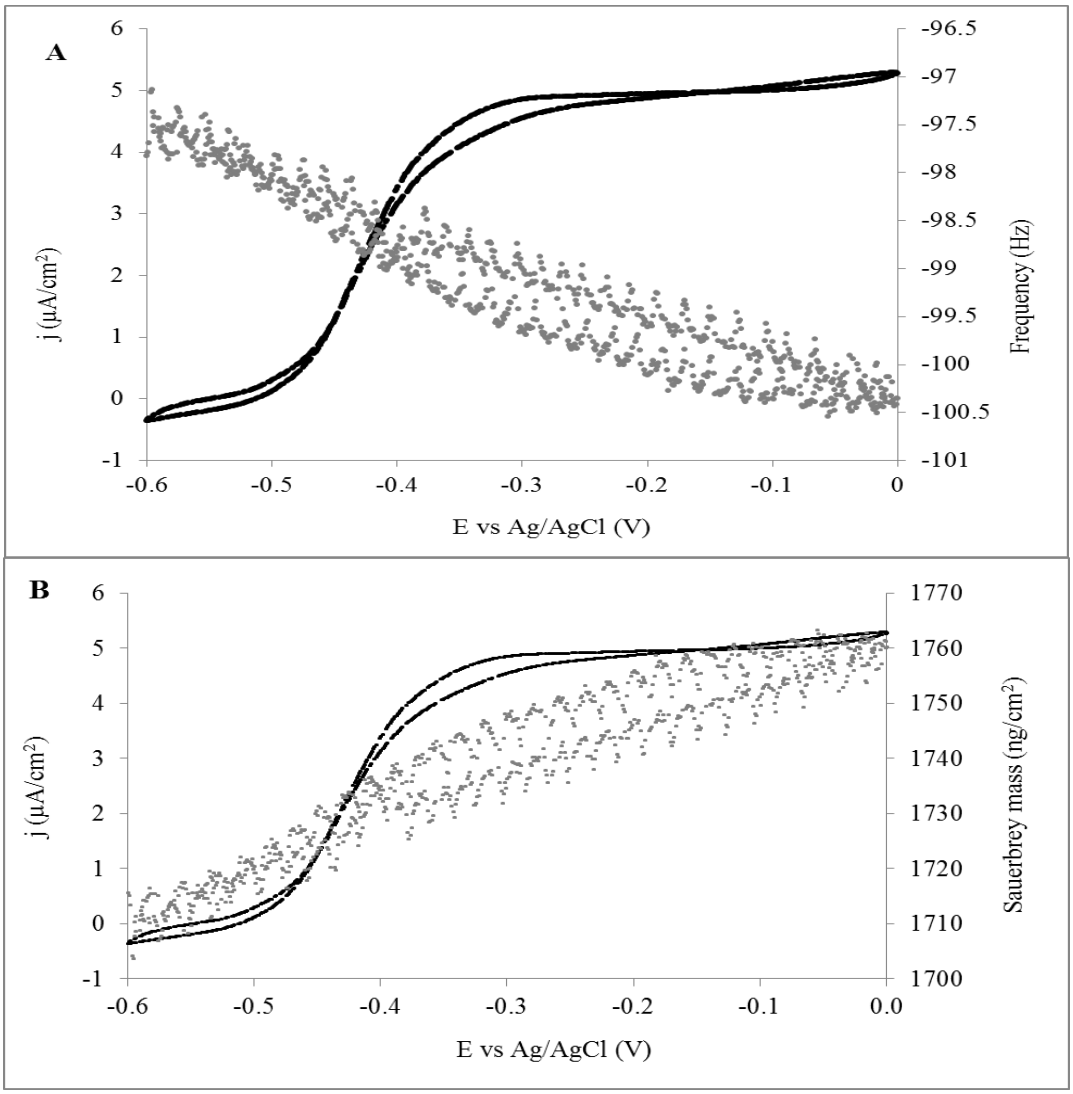

Figure 4.5 (A) Cyclic voltammogram at 1 mV/s vs frequency changes (*Δf*). (B) Mass changes (*Δm*) induced by cycling potential at 1 mV/s for GS, both recorded on biofilms grown for 46:40 h.

The plots also show that the oxidation of the biofilm is accompanied by a decrease in frequency, reversible upon reduction that can be related to an increase and subsequent decrease in mass during electrolysis assuming a simplified rigid layer model. Quantitative interpretation of EQCM data is based on the combination of the Sauerbrey equation and Faraday's Law. The former relates changes in frequency to changes in mass, whereas the latter (Q = nFN) relates charge passed in an electrochemical experiment (Q) to the number of moles of material electrolyzed (N)

(n = number of electrons involved in the electrochemical reaction). Therefore, frequency changes can be related to the total charge passed. By integration of the current in cyclic voltammetry a calculation of the mass change from the quantity of charge passed is obtained, and this can be compared with the observed mass change (QCM). The molar mass of sodium acetate was calculated to be 82 g mol^{-1}, (assuming n = 1), whereas the molar mass of the electrolyte anion (CH_3COO^-) is 59 g mol^{-1}.

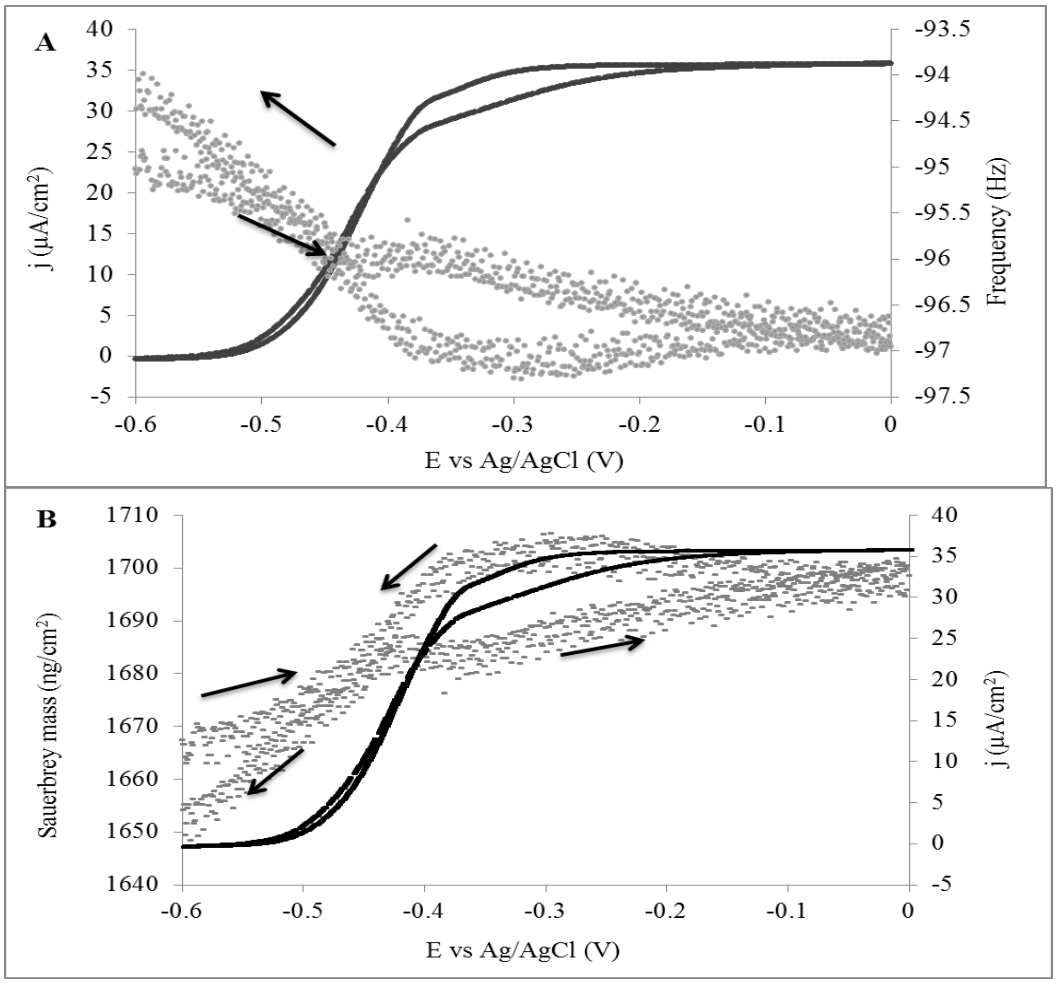

Figure 4.6 (A) Voltammogram at 1 mV/s vs frequency changes (Hz). (B) Mass changes (*Δm*) induced by cycling potential at 1 mV/s for GS, both recorded on biofilms grown for 69:43 h.

Anions are inserted and removed during the redox process up to the cyclic voltammetry peak region, and that the mass changes associated with this process are confirmed by QCM measurements. Simultaneous cyclic voltammetry and QCM measurements permitted the calculation of the mass change to be expected from the quantity of charge passed, and this was compared with the observed mass change (QCM). Comparison of this change in mass with the charge passed is consistent with incorporation of electrolyte anions into the film during oxidation, required to maintain the electro neutrality of the film (Bott, 1999). The cyclic voltammograms and associated frequency changes are shown in figure 4.5 and 4.6. Calculation of the mass change calculated from the charge (Mass [charge]) for this process was 42 ng and 147ng at the time interval of 46 and 70 hours. Calculation of the mass changes from frequency (mass [QCM]) for this process was 43 ng and 45 ng at the time interval of 46 and 70 h. The change in mass during CV of thicker *G.sulfurreducens* biofilms points to the importance of the flux not only of charge species but also of neutral species solvent as well. The movement of solvent in *G.sulfurreducens* biofilms plays an important role in the overall electron-transfer rates and the ionic composition of the electrolyte may have a strong influence. The viscoelasticity of the film due to the incorporation of water may contribute to the increase in mass. In case of CV there was a change in frequency of the biofilm which might be due to some cationic species that was ejected from the film in order to maintain the electro neutrality of the film. Babauta *et al*. 2014 also observe a negative frequency shift during oxidation of acetate by GS biofilms using CV and they conclude that the frequency shift response is predominately caused by ion flux through the biofilm.

4.4 Conclusion:

The initial interaction of electroactive bacteria with solid electrode surface is a crucial step in biofilm formation and electricity generation. The total mass and viscosity of the biofilm increased after inoculation, indicating that the decrease of frequency was associated with biofilm formation and activity. We used EQCM-D

technology to monitor *in situ* changes of the GS biofilms properties and their relation to electrochemical performance. A combination of cyclic voltammetry and QCM measurements permitted the calculation of the mass change from the quantity of charge passed, and this was compared with the observed mass change (Δm). During cyclic voltammograms, there was a negative increase in frequency shift at oxidizing potentials. This investigation led to evaluation of the EQCM-D measurement technique to monitor the *in situ* change of the biofilm properties and to correlate the response with the electrochemical performance. From this study we observed the viscoelastic properties of the biofilm increased as function of time, leading to the better current generation. In future the *in situ* changes of mass with combination of electrochemical response can be applied to evaluate the effects of the electrode modification, growth, and environmental factors which are crucial for the establishment of bacterial biofilm in microbial fuel cell technology.

References

Babauta, J.T., Beasley, C.A., Beyenal, H. 2014. Investigation of electron transfer by Geobacter sulfurreducens biofilms by using an electrochemical quartz crystal microbalance. *ChemElectroChem*, 1(11), 2007-2016

Bott, A. 1999. Characterization of films immobilized on an electrode surface using the electrochemical quartz crystal microbalance. *Current Separation*, **18**(3), 79-83.

Brown-Malker, S.T., Read, S., Rowlands, A., Cooper-White, J., Keller, J. 2010. Electrochemical quartz crystal microbalance to monitor biofilm browth and properties during bio-electrochemical system inoculation and load conditions. *ECS Transactions*, **28**(9), 11-22.

Chen, J.Y., Shahid, A., Garcia, M.P., Penn, L.S., Xi, J. 2012. Dissipation monitoring for assessing EGF-induced changes of cell adhesion. *Biosensors and Bioelectronics*, **38**(1), 375-381.

Fricke, K., Harnisch, F., Schröder, U. 2008. On the use of cyclic voltammetry for the study of anodic electron transfer in microbial fuel cells. *Energy and Environmental Science*, **1**(1), 144-147.

Gutman, J., Walker, S.L., Freger, V., Herzberg, M. 2012. Bacterial attachment and viscoelasticity: physicochemical and motility effects analyzed using quartz crystal microbalance with dissipation (QCM-D). *Environmental science and technology*, **47**(1), 398-404.

Jana, P.S., Katuri, K., Kavanagh, P., Kumar, A., Leech, D. 2014a. Charge transport in films of Geobacter sulfurreducens on graphite electrodes as a function of film thickness. *Physical Chemistry Chemical Physics*, **16**(19), 9039-9046.

Katuri, K.P., Kavanagh, P., Rengaraj, S., Leech, D. 2010. Geobacter sulfurreducens biofilms developed under different growth conditions on glassy carbon electrodes: insights using cyclic voltammetry. *Chemical Communications*, **46**(26), 4758-4760.

Kreth, J., Hagerman, E., Tam, K., Merritt, J., Wong, D., Wu, B., Myung, N., Shi, W., Qi, F. 2004. Quantitative analyses of Streptococcus mutans biofilms with quartz crystal microbalance, microjet impingement and confocal microscopy. *Biofilms*, **1**(4), 277-284.

Kwon, K., Evans, J.W. 2004. Comparison between cyclic voltammetry and chronoamperometry when coupled with EQCM for the study of the SEI on a carbon film electrode. *Electrochimica Acta*, **49**(6), 867-872.

Lau, P.C., Dutcher, J.R., Beveridge, T.J., Lam, J.S. 2009. Absolute quantitation of bacterial biofilm adhesion and viscoelasticity by microbead force spectroscopy. *Biophysical Journal*, **96**(7), 2935-2948.

Liu, Y., Harnisch, F., Fricke, K., Sietmann, R., Schröder, U. 2008. Improvement of the anodic bioelectrocatalytic activity of mixed culture biofilms by a simple consecutive electrochemical selection procedure. *Biosensors and Bioelectronics*, **24**(4), 1006-1011.

Liu, Y., Kim, H., Franklin, R.R., Bond, D.R. 2011. Linking spectral and electrochemical analysis to monitor c-type cytochrome redox status in living Geobacter sulfurreducens biofilms. *ChemPhysChem*, **12**(12), 2235-2241.

Malvankar, N.S., Vargas, M., Nevin, K.P., Franks, A.E., Leang, C., Kim, B.-C., Inoue, K., Mester, T., Covalla, S.F., Johnson, J.P., Rotello, V.M., Tuominen, M.T., Lovley, D.R. 2011. Tunable metallic-like conductivity in microbial nanowire networks. *Nature Nanotechnology*, **6**(9), 573-579.

Marcus, I.M., Herzberg, M., Walker, S.L., Freger, V. 2012. Pseudomonas aeruginosa attachment on QCM-D sensors: the role of cell and surface hydrophobicities. *Langmuir*, **28**(15), 6396-6402.

Marsili, E., Rollefson, J.B., Baron, D.B., Hozalski, R.M., Bond, D.R. 2008. Microbial biofilm voltammetry: Direct electrochemical characterization of catalytic electrode-attached biofilms. *Applied and Environmental Microbiology*, **74**(23), 7329-7337.

Marsili, E., Sun, J., Bond, D.R. 2010. Voltammetry and growth physiology of Geobacter sulfurreducens biofilms as a function of growth stage and imposed electrode potential. *Electroanalysis*, **22**(7-8), 865-874.

Nevin, K.P., Kim, B.C., Glaven, R.H., Johnson, J.P., Woodward, T.L., Methé, B.A., Didonato Jr, R.J., Covalla, S.F., Franks, A.E., Liu, A., Lovley, D.R. 2009. Anode biofilm transcriptomics reveals outer surface components essential for high density current production in Geobacter sulfurreducens fuel cells. *PLoS ONE*, **4**(5).

Nevin, K.P., Richter, H., Covalla, S.F., Johnson, J.P., Woodard, T.L., Orloff, A.L., Jia, H., Zhang, M., Lovley, D.R. 2008. Power output and columbic efficiencies from biofilms of Geobacter sulfurreducens comparable to mixed community microbial fuel cells. *Environmental Microbiology*, **10**(10), 2505-2514.

Olsson, A.L., van der Mei, H.C., Busscher, H.J., Sharma, P.K. 2008. Influence of cell surface appendages on the bacterium− substratum interface measured real-time using QCM-D. *Langmuir*, **25**(3), 1627-1632.

Otto, K., Silhavy, T.J. 2002. Surface sensing and adhesion of Escherichia coli controlled by the Cpx-signaling pathway. *Proceedings of the National Academy of Sciences*, **99**(4), 2287-2292.

Richter, H., McCarthy, K., Nevin, K.P., Johnson, J.P., Rotello, V.M., Lovley, D.R. 2008. Electricity generation by geobacter sulfurreducens attached to gold electrodes. *Langmuir*, **24**(8), 4376-4379.

Sauerbrey, G. 1959. Verwendung von schwingquarzen zur wägung dünner schichten und zur mikrowägung. *Zeitschrift für Physik*, **155**(2), 206-222.

Schofield, A.L., Rudd, T.R., Martin, D.S., Fernig, D.G., Edwards, C. 2007. Real-time monitoring of the development and stability of biofilms of Streptococcus

mutans using the quartz crystal microbalance with dissipation monitoring. *Biosensors and Bioelectronics*, **23**(3), 407-413.

Snider, R.M., Strycharz-Glaven, S.M., Tsoi, S.D., Erickson, J.S., Tender, L.M. 2012. Long-range electron transport in Geobacter sulfurreducens biofilms is redox gradient-driven. *Proceedings of the National Academy of Sciences*, **109**(38), 15467-15472.

Strycharz-Glaven, S.M., Snider, R.M., Guiseppi-Elie, A., Tender, L.M. 2011. On the electrical conductivity of microbial nanowires and biofilms. *Energy and Environmental Science*, **4**(11), 4366-4379.

Torres, C.I., Marcus, A.K., Parameswaran, P., Rittmann, B.E. 2008. Kinetic experiments for evaluating the nernst-monod model for anode-respiring bacteria (ARB) in a biofilm anode. *Environmental Science and Technology*, **42**(17), 6593-6597.

Wang, X., Feng, Y., Ren, N., Wang, H., Lee, H., Li, N., Zhao, Q. 2009. Accelerated start-up of two-chambered microbial fuel cells: Effect of anodic positive poised potential. *Electrochimica Acta*, **54**(3), 1109-1114.

Xie, X.-H., Li, E.L., Tang, Z.K. 2010. Real-time monitoring of induced adaptation of redox active Escherichia coli biofilm by EQCM-controlled extracellular redox environment. *Electrochemistry Communications*, **12**(4), 600-602.

Zhou, M., Chi, M., Luo, J., He, H., Jin, T. 2011. An overview of electrode materials in microbial fuel cells. *Journal of Power Sources*, **196**(10), 4427-4435.

Chapter-5

Quantitative proteomic analysis of *Geobacter sulfurreducens* grown with different electron acceptor

5.1 Introduction

Proteomics is the large-scale study of protein expression. The proteome is the entire complement of proteins produced by an organism or system. The bacterial proteome is therefore a dynamic set of proteins expressed in a specific cell, given a particular set of conditions. Proteomics is often considered the next step in the study of biological systems after genomics. The microbial degradation of organic substrate in the anode chamber is one of the key processes of electricity generation in MFCs. The most important biological factors affecting the performance of MFCs are the type and source of inoculums. Microorganisms as biocatalysts are a vital factor that affects the power output by contributing to electron transfer rates, biofilm thickness, conductance, substrate uptake rate and overall internal resistance of the cell (Borole *et al*., 2011). Pure cultures of bacteria are suitable for foundation studies because of high electrochemically activity of certain strains, such as those from *Geobacter* sp. (Bond & Lovley, 2003; Cao *et al*., 2009; Dumas *et al*.,2008; Zhou *et al*., 2005).

Geobacter is a gram-negative bacterium commonly found in soil, sediment and subsurface environment (Bond & Lovley, 2003) *Geobacter sp* has the capability to couple the reduction of soluble and insoluble oxidised metals to substrate oxidation. Several redox active outer membrane *c*-type cytochromes have been

identified as electron transfer components in anode-bound biofilm of *Geobacter sulfurreducens* (Mehta *et al*., 2005). C-type cytochromes function as electron transfer conduits connecting the cytoplasm with the cell membrane facilitating electron transfer to the terminal electron acceptor (Borole *et al*., 2011). In bacterial respiration electrons are removed from primary donor (carbon source) and transferred to the terminal electron acceptor through a series of electron carriers, such as NADH dehydrogenase, ubiquinone and cytochromes (Lovley, 2006). Electron carriers such as NAD^+ and $NADP^+$ transfer electrons and protons when reduced to NADH or NADPH. The energy released during the electron transport permits bacteria to push protons to the periplasm. Therefore a proton motive force is generated, enabling activity of ATP synthase and the formation of ATP. Genomic analysis of GS has identified coding sequences for periplasmic cytochromes, membrane cytochromes and other outer membrane proteins that can contribute to extracellular electron transport (Methé *et al*., 2003). For electrode-attached biofilms the anode acts as an inert electron acceptor, in the absence of any other soluble electron acceptor.

Two mechanisms for long range electron transfer through biofilms attached to an electrode surface have been suggested i) electron transfer through electron hopping via cytochromes present in the outer membrane of the bacterium and ii) metallic-like conductivity through pili (nanowires). Evidence has been presented to support (and oppose) both assumptions (Malvankar *et al*., 2011; Strycharz-Glaven *et al*., 2011) but so far no general agreement has been reached. The process of electron transfer from within the cell to the terminal electron acceptor is a complex mechanism. In *GS* periplasmic cytochromes, membrane bound cytochromes and pili have been identified as important in electron transfer to the electron acceptors using a combination of genomic, proteomic and electrochemical studies. For example, Mehta *et al*. identified c-type cytochrome OmcS localised on the type IV pili of GS as the terminal electron donator to Fe (III) oxide (Mehta *et al*., 2005). Nevin *et al*. report that the outer-membrane c-type cytochrome, OmcZ, is an important component contributing to electron transfer through thicker *GS* biofilms attached to electrode surfaces (Nevin *et al*., 2009). Methe *et al* report that *GS* encodes genes for

glycolysis, the tricarboxylic acid (TCA) cycle and the pentose phosphate pathway (Methé *et al*., 2003). However, *GS* contains many additional redox-active proteins that could potentially contribute to current production (Snider *et al*., 2012). A comparison of differential protein expression of *Geobacter sulfurreducens* grown on carbon cloth electrode versus that of planktonic cells using fumarate as electron acceptor is presented in this chapter. In this present study we used isobaric tags for relative and absolute quantitation (iTRAQ) technique to quantify the proteins to understand the electron transfer mechanism in *Geobacter sulfurreducens* bacteria during different electron acceptor. iTRAQ technique one of the most robust techniques to be applied in quantitative proteomics analysis and, the proteomics data gives better understanding of the electron transfer mechanisms in exoelectrogenic bacteria during the process of shuttling electrons outside the cell membrane (Pereira-Medrano *et al*., 2013). This technology employs amine-reactive isobaric tags to label peptides at the N-terminus and the lysine side chains, thereby labelling all peptides in a digest mixture. The main advantages of iTRAQ technique, 1) All peptides are labelled resulting in increased confidence and higher quality data, 2) up to 8 labels can be used for multiplexing experiments, 3) improved MS/MS fragmentation results in more confident peptide or protein identifications.

This study seeks to identify specific proteins which are important for respiration using a solid electrode acceptor compared to a soluble electron acceptor. A change in the nature of the electron acceptor (fumarate versus solid electrode) in the growth medium of *G. sulfurreducens* resulted in alteration of the expression pattern of proteins.

5.2 Material and methods

5.2.1 Experimental set-up

The study was carried out in two sets and each set containing five H-type fuel cells. Each fuel cell containing a carbon cloth (50 cm^2 E-TEK) anode and multiple graphite rod cathodes (65 cm^2) separated by Nafion117 proton-exchange membrane (PEM, Sigma Aldrich) 12 cm^2 in area. The volume of both the anode and cathode chambers was 125 mL. Each reactor used 125 mL of *Geobacter* feed solution in the anode chamber. Synthetic media contained 10 mM acetate used as a source of electron donor. The acetate medium also contained (per L): 0.1 g KCl, 0.15 g NH_4Cl, 0.6 g Na_2HPO_4, 2.5 g $NaHCO_3$, 10 mL trace element solution and 10 mL vitamin solution (Katuri *et al*. 2012b) prepared according to the protocol supplied by the culture centre (http://www.dsmz.de, medium no. 826). The cathode chamber consisted of 50 mM ferricyanide in 100 mM phosphate buffer (pH 7.0). Custom built Ag/AgCl (3M KCl) with a porous vycor frit (Advanced Glass and Ceramics) was used as a reference electrode.

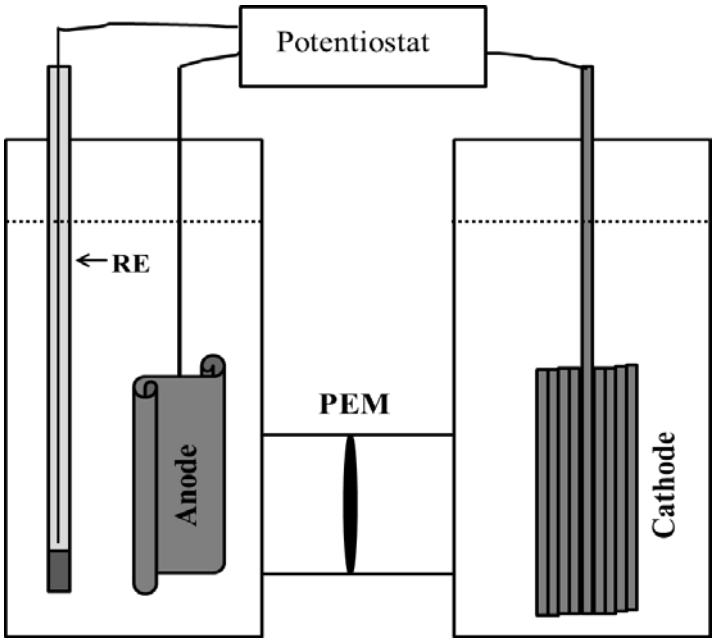

Figure 5.1 Schematic diagram of the MFCs used in the study

5.2.2 Pure culture and biofilm growth on electrode surface

Geobacter sulfurreducens (ATCC 51573) was used as a source of electro active bacteria. The strain was sub-cultured in 100 mL airtight, rubber septa-sealed anaerobic syringe bottles containing 90 mL of growth medium. After 90 ml of medium was added, each 100 ml vial was sealed with a butyl rubber bung and flushed with N_2/CO_2 (80:20, vol/vol) gas. Filter-sterilized electron acceptor sodium fumarate (50 mM) was added after autoclaving as per DSMZ guidelines. Vials were inoculated with 1 ml stock culture and incubated at 30 °C on a shaker. The subsequent growth on the fresh media constitutes a subculture. The same synthetic medium containing acetate as a source of electron donor, as that described for the fuel cell study above was used as feed. The bacteria were cultured in fumarate solution (50 mM) containing *Geobacter* growth medium for 2 weeks (three sub-culture) prior to inoculation in the electrochemical cell. A subculture is simply the transfer of established microorganism growth on media to fresh medium. In this present study we used 3rd subculture for inoculation to the electrochemical cell. Liquid batch cultures of *G. sulfurreducens* strain were in anaerobic serum bottles at 30 °C containing 10 mM acetate and 50 mM fumarate as the terminal electron acceptor. The culture bottles were kept like that thereafter with no further nutrient supplementation. Prior to inoculation, half of the bacteria were harvested by centrifugation (12 min at 12,000g) and re-suspended in sterilized medium without addition of fumarate as electron acceptor and half of the harvested bacteria was collected and stored at −80 °C until iTRAQ analysis. All culture manipulations were performed under strict anaerobic conditions in an anaerobic glove-box. Following inoculation biofilms were induced to grow on carbon cloth electrodes under a constant applied potential (0 V vs. Ag/AgCl) using a multichannel potentiostat (CHI-1030a, CH Instruments, Austin, TX). The pH of the feed was in the range of 7.2–7.5 throughout the experiment and the cell was operated at temperatures that varied from 28 to 32 °C. All inoculations were carried out in a sterile anaerobic glove box (Coy Laboratory Products, Grass Lake, MI), and incubations were performed at 30 °C in a controlled-temperature hot room. MFCs were allowed run for eight batches (1 batch

= 24 ± 1h) to ensure sufficient biomass formation. Every batch feed involved replacement of 25 mL of 25 mM acetate concentrated synthetic *G. sulfurreducens* medium without any additional inoculum.

5.2.3 Protein extraction and iTRAQ labelling

The iTRAQ experiment was carried out in order to examine the differences in protein expression in *G. sulfurreducens* cells cultured using fumarate as a soluble electron acceptor and cultured as biofilms grown on carbon cloth electrode as electron acceptor. To this end, protein extracts were prepared from four replicate planktonic cultures of *G. sulfurreducens* (two technical replicates for reproducibility of the results and two biological replicates from the difference sources under the same conditions) grown in acetate containing medium supplemented with fumarate (50 mM) as a soluble electron acceptor and from four replicate biofilm samples grown on carbon cloth electrodes in the absence of soluble fumarate as electron acceptor. Planktonic cells were harvested for differential proteomics analysis from two different sources called biological replicates. Biological replicates in particular are usually influenced by both technical and biological processes. At the time of sampling, 10µg ml^{-1} chloramphenicol was added to both planktonic cells and biofilms to block further protein expression. Chloramphenicol inhibits protein synthesis by interacting with the 50S portion of the 70S ribosome (Lin *et al,*. 1997). Biofilms were gently detached from the electrode surfaces by sonication and vortex and the cell suspension was placed in 50 ml tubes for centrifugation. Cells suspensions, isolated from biofilm and soluble fumarate cultures were collected by centrifugation at 8000 g for 8 min at 4°C. After centrifugation the pellets were washed with 2 ml of triethylammonium bicarbonate (TEAB) buffer. Protein extraction and quantification were conducted as previously described (Gunnigle *et al*., 2013) using a sonication protocol and the Calbiochem Non-Interfering Protein Assay kit (Merck KGaA, Darmstadt, Germany), respectively. After protein concentration normalization (100 µg in 20 µl), iTRAQ labelling was carried out following the manufacturer's recommendation (ABSciex, Foster City, CA). Reagents 113, 114, 115 and 116 were employed to label the fumarate cultured cells with 113

and 114 used for the technical replicates for reproducibility of the first biological replicate (source-1) and 115 and 116 for the technical replicates for reproducibility of the second biological replicate (source-2). Similarly, reagents 117, 118, 119 and 121 were used to label the biofilm samples (117 and 118 for the first biological replicate and 119 and 121 for the second biological replicate). Each label has a unique charged reporter group, a peptide reactive group and a balance neutral group to maintain an overall mass of 145Da. When a peptide is fragmented by MS/MS fragmentation, the iTRAQ reporter groups break off and produces distinct ions at m/z 114, 115, 116, 117, 118, 119, 121 and 122 (H. R. Fuller and G. E. Morris., 2012). Following iTRAQ labelling, the resulting eight samples were combined to be further fractionated and analysed by liquid chromatography-tandem mass spectrometry (LC-MS/MS) as previously described (Gunnigle *et al*., 2013). MS-MS is where the first MS quantifies the number of fragments and the second MS scan is used to identify the most abundant peaks (Wiese *et al*., 2007).

5.2.4 Protein identification and relative expression (work performed by Dr. Florence Abram).

The MS/MS data were processed using the Paragon search algorithm within the ProteinPilot software (version 4.0.8; ABSciex, Foster City, CA) (Gunnigle *et al*., 2013). The data were searched against the Trembl database with no species restriction. A threshold of unused Protscore (from ProteinPilot) of 2 (corresponding to protein detection with ≥99% confidence) was employed for protein identification. In addition, for each protein, a minimum of two unique peptides were detected. For relative protein quantification purpose each detected peptide was assigned an expression ratio based on the iTRAQ reagent (113 to 121) peak intensities in the MS/MS spectra. Protein ratios were then calculated by ProteinPilot from the ratios of the individual unique peptides derived from each protein. By default, ProteinPilot provides all the expression ratios using 113 as denominator. However, to access the expression ratio of each protein and particularly to determine the statistical significance of the differentially expressed proteins, it is necessary to take into consideration all the ratios using 113, 114, 115, 116, 117, 118, 119 and 121 as

denominators. For simplicity, the two independent biological replicates analysed in the present study were considered as separate. Consequently, each protein was associated with eight ratios: 117/113, 117/114, 118/113, 118/114 reflecting the relative protein expression in the biofilm versus planktonic cells in the first biological replicate and 119/115, 119/116, 121/115, 121/116 reflecting the relative protein expression in the samples in the second biological replicate. All the corresponding output protein and peptide summary files generated by ProteinPilot were exported to the ProteinPilot Descriptive Statistics Template (PDST; ABSciex, Foster City, CA) for data analysis. In order to determine the statistical significance of the differentially expressed proteins under the two conditions investigated (electrode biofilms and planktonic cells grown in the presence of fumarate as soluble electron acceptor) ratio channels (113 to 121) were selected alternatively as decoy or target within PDST. A total of eight analyses using PDST were carried out setting 113, 114, 115 and 116 first as decoy and then as target for the determination of differential expression. In all cases, the false discovery rate, as calculated by PDST was found to be < 5%. After extracting the differentially expressed proteins common to the eight output files (resulting from the eight PDST analyses), a threshold of >1.2 fold difference in expression between samples was applied for biological significance.

5.3 Results and discussion

5.3.1 Growth of G. sulfurreducens biofilms

In this study, we focus on biofilms of *G. sulfurreducens* induced to form on anodes during fed-batch-mode operation in a dual chambered electrochemical cell using acetate as the electron donor and carbon cloth anodes as the electron acceptor. After inoculation, an increase in the oxidation current production was observed over time. The feed solution was replaced every 24 ± 1 hours of batch operation to maintain sufficient carbon source in to the anode chamber (no further inoculum). Figure 5.2 shows the current generation as a function of time. In this present study we observed maximum current density (normalized to the geometric anode surface area) of 2.0 A m^{-2} (Figure-5.3) after 195 hours of operation. Marsili *et al*, 2010

reported a steady-state current density in 20 mM acetate of 4–7 A m $^{-2}$ achieved after 72 hours under an applied potential of 0.04 V vs. Ag/AgCl by GS biofilms at graphite or roughened glassy carbon electrodes. More recently Katuri *et al*, 2012 reported a steady-state amperometric current density for acetate oxidation by GS biofilm on carbon electrodes of 9.2 A m $^{-2}$ after 142 h of repeated batch mode experiments. In this present study we achieved less current density compared to others may be due to different electrode material.

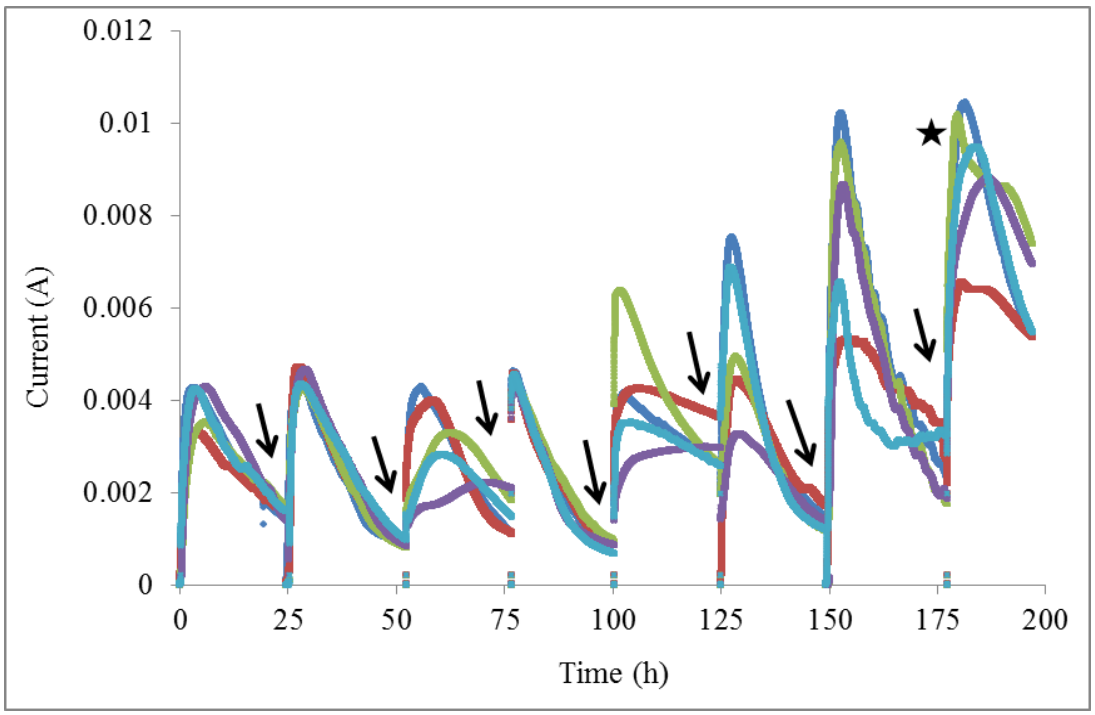

Figure 5.2 Amperometric responses of carbon cloth working electrodes, as a function of time, during *G. sulfurreducens* biofilm growth operation is shown (10 mM acetate) under 0 V vs. Ag/AgCl applied potential. Arrows (black) indicate a change feed and star indicates the *in-situ* CV analysis. Each of 5 reactors is shown individually.

To examine the catalytic activity of the anodic biofilm, slow scan cyclic voltammograms were recorded *in situ* in the cell culture medium. Sigmoidal voltammograms shown in figure 5.3 permit estimation from the first derivative of the CVs (not shown) of acetate oxidation centered at −0.42 vs. Ag/AgCl. The sigmoidal cyclic voltammograms is indicative of catalytic oxidation of the substrate by the

biofilm and heterogeneous electron transfer to the electrode, with similar responses reported on for acetate oxidation by anodic biofilms of *G. sulfurreducens* (Katuri *et al*., 2010; Katuri *et al*., 2012; Marsili *et al*., 2010).

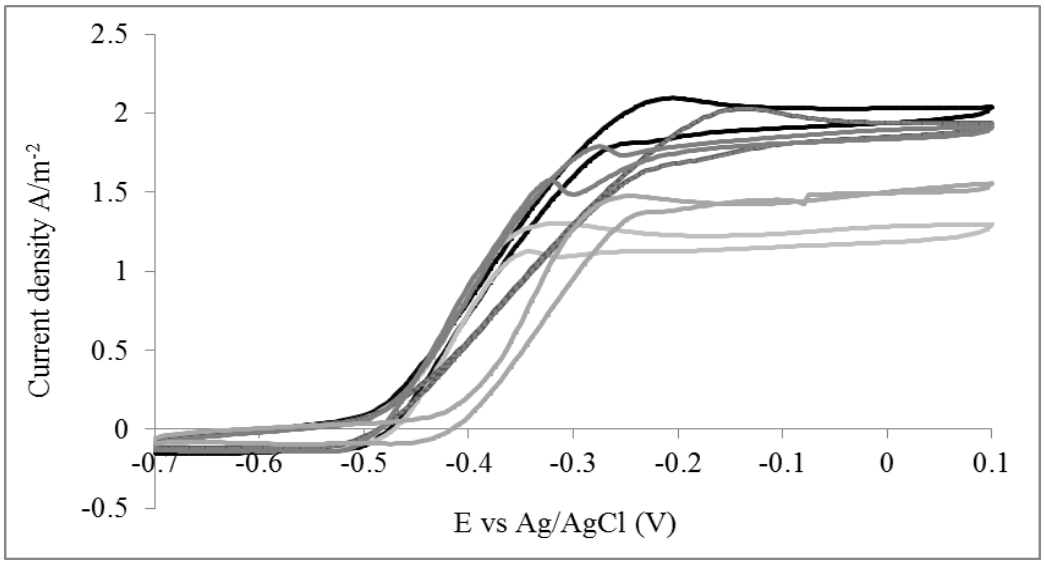

Figure 5.3 Slow-scan (1 mV/s) cyclic voltammetry of *G. sulfurreducens* biofilms grown on carbon cloth electrodes at 0 V vs Ag/AgCl (batch-8). Each of 5 reactors is shown individually.

5.3.3 Differential protein expression

The *G.sulfurreducens* genome is a single circular chromosome of 3,814,139 base pairs with a total of 3466 predicted protein encoding open reading frames (Methe *et al* 2003). A total of 1318 proteins were identified in both biofilm and planktonic *G. sulfurreducens* samples. This represents 38 % of the protein predicted to encode. Overall 77 proteins were found, within the level of significance chosen, to be differentially expressed, amongst these 40 were expressed at higher levels in the biofilm samples, (Table 1) and 37 were expressed at reduced levels in the biofilm samples (Table 2). In this paper we refer to probability scores to measure significance and only report quantitative results that are statistically significant thus requiring a score >1.3 (Pereira-Medrano *et al*., 2013).

Table 1, The proteins at a higher level over the biofilm sample

GSU number	Protein name	Fold change*	Suggested function	Predicted cellular location
GSU1239	Glutamate synthase, FMN-Fe(II)-binding domain protein	8.8	metal ion binding	Cytoplasmic
GSU1305	Glutamate dehydrogenase, GdhA	6.6	cellular amino acid metabolic process	Unknown
GSU1237	FAD-dependent pyridine nucleotide-disulfide oxidoreductase family protein	4.9	flavin adenine dinucleotide binding	Cytoplasmic
GSU0496	Efflux pump, RND family, membrane fusion protein	4.1	transmembrane transport	Cytoplasmic Membrane
GSU1778	Type II secretion system secretin lipoprotein PulQ	3.5	polysaccharide catabolic process	Outer Membrane
GSU3066	D-alanine--D-alanine ligase	3.1	peptidoglycan biosynthetic process	Cytoplasmic
GSU2823	Efflux pump, RND family, membrane fusion protein	3.0	Secretion protein	Cytoplasmic Membrane
GSU3366	Glutamine--tRNA ligase	3.0	ATP binding	Cytoplasmic
GSU2362	Winged helix-turn-helix transcriptional regulator, MarR family	2.8	DNA binding	Cytoplasmic
GSU2013	Phosphoglucomutase/phosphomannomutase family protein	2.8	phosphoglucomutase activity	Cytoplasmic
GSU0117	Amino acid aminotransferase, putative	2.8	biosynthetic process	Cytoplasmic

GSU number	Protein name	Fold change*	Suggested function	Predicted cellular location
GSU1783	Type II secretion system ATPase PulE	2.8	ATP binding	Cytoplasmic
GSU2028	Type IV pilus secretin lipoprotein PilQ	2.8	Transport	Outer Membrane
GSU1013	Peptidoglycan-binding lipoprotein, OmpA family	2.7	Transport. motor activity	Cytoplasmic Membrane
GSU3281	Thioredoxin	2.7	protein disulfide oxidoreductase activity	Cytoplasmic
GSU1700	Malate oxidoreductase, NADP-dependent, phosphate acetyltransferase-like domain-containing	2.6	NAD binding	Cytoplasmic
GSU2733	Uncharacterized protein	2.5	Hypothetical protein	Outer Membrane
GSU0317	Uncharacterized protein	2.5	Hypothetical protein	Unknown
GSU2090	Peptidylprolyl cis-trans isomerase, putative	2.5	peptidyl-prolyl cis-trans isomerase activity	Cytoplasmic Membrane
GSU2268	Outer membrane protein assembly factor BamA	2.3	protein insertion into membrane	Outer Membrane
GSU2429	Peptidylprolyl cis-trans isomerase, PpiC-type	2.2	protein folding	Unknown
GSU0328	Type II secretion system ATPase GspE	2.2	protein transporter activity	Cytoplasmic
GSU3293	Ferritin-like domain protein	2.2	metal ion binding	Cytoplasmic

GSU number	Protein name	Fold change*	Suggested function	Predicted cellular location
GSU0016	Peptidylprolyl cis-trans isomerase lipoprotein, PpiC-type	2.1	protein folding	Cytoplasmic Membrane
GSU0332	Probable cytosol aminopeptidase	2.0	Catalytic activityi	Cytoplasmic
GSU2617	Protein translocase subunit SecD	1.7	intracellular protein transmembrane transport	Cytoplasmic Membrane
GSU1894	2-dehydro-3-deoxyphosphooctonate aldolase	1.7	3-deoxy-8-phosphooctulonate synthase activity	Cytoplasmic
GSU3318	Uncharacterized protein	1.7	Hypothetical protein	Unknown
GSU2496	Uncharacterized protein	1.7	Hypothetical protein	Unknown
GSU2060	Zinc protease PmbA, putative	1.7	Proteolysis	Cytoplasmic
GSU2862	DNA-directed RNA polymerase subunit beta'	1.7	DNA-directed RNA polymerase activity	Cytoplasmic
GSU0927	Zinc-dependent peptidase, M16 family	1.6	metal ion binding	Unknown
GSU0800	Amino acid ABC transporter, periplasmic amino acid-binding protein	1.5	transporter activity	Periplasmic
GSU2831	DNA-directed RNA polymerase subunit alpha	1.5	DNA-directed RNA polymerase activity	Cytoplasmic

GSU number	Protein name	Fold change*	Suggested function	Predicted cellular location
GSU0658	Chaperone protein ClpB	1.4	nucleoside-triphosphatase activity	Cytoplasmic
GSU0028	Biopolymer transport membrane proton channel, TolQ-related protein	1.3	protein transporter activity	Cytoplasmic Membrane
GSU3380	Aspartyl/glutamyl-tRNA(Asn/Gln) amidotransferase subunit B	1.3	carbon-nitrogen ligase activity, with glutamine as amido-N-donor	Cytoplasmic
GSU3304	Outer membrane channel OmpJ	1.3	iron assimilation by reduction and transport	Unknown
GSU1177	Succinate dehydrogenase/fumarate reductase, flavoprotein subunit	1.3	anaerobic respiration	Cytoplasmic Membrane
GSU0810	Peptidoglycan-binding outer membrane protein, OMP_b-brl, OmpA and OmpA domain-containing	1.3	Transport protein	Outer Membrane

* Fold change indicates the average expression ratio for *G. sulfurreducens* grown in the absence (MFC- biofilm) and in the presence of a soluble electron acceptor (planktonic).

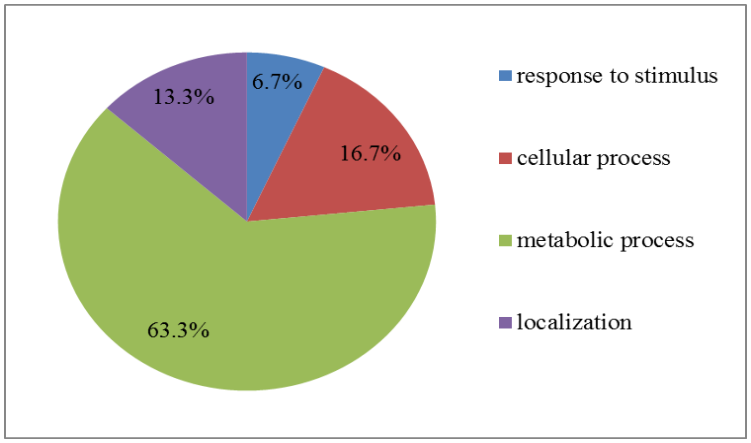

Figure 5.4 Proteins expressed at a higher level in the electrode biofilms (40 proteins) Proteins classified according to biological process.

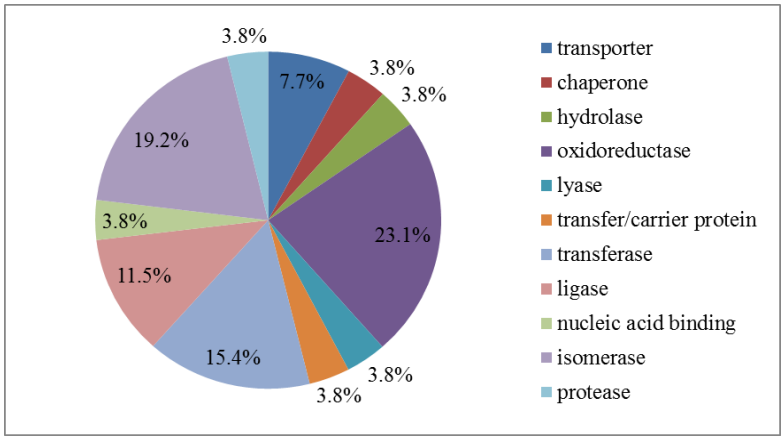

Figure5.5 Proteins expressed at a higher level in the electrode biofilms (40 proteins) Proteins classified according to protein class/function.

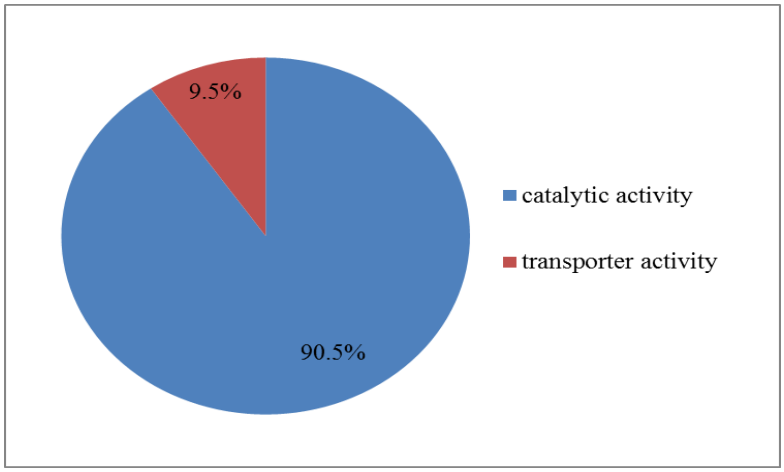

Figure5.6 Proteins expressed at a higher level in the electrode biofilms (40 proteins) Proteins classified according to molecular function of protein.

Table 2. 37 The protein at a lower level in the biofilm samples

GSU number	Protein name	Fold change*	Suggested function	Predicted cellular location
GSU3351	Uncharacterized protein	-1.3	Hypothetical protein	Unknown
GSU2053	Indolepyruvate:ferredoxin oxidoreductase, α subunit, IorA-2	-1.4	Carbohydrate metabolism	Cytoplasmic
GSU0113	ATP synthase subunit β, AtpD	-1.4	Energy metabolism	Cytoplasmic
GSU1736	ACT domain protein	-1.4	Amino acid metabolism	Cytoplasmic
GSU1793	Trigger factor, Tig	-1.5	Chaperone	Cytoplasmic
GSU0617	NHL repeat domain lipoprotein	-1.5	Lipoprotein	Unknown
GSU2433	ATP-dependent protease	-1.6	Proteolysis	Cytoplasmic
GSU1242	Amino acid aminotransferase	-1.6	Amino acid metabolism	Cytoplasmic
GSU2390	Chaperone protein, HtpG	-1.6	Chaperone	Cytoplasmic
GSU3092	Uncharacterized protein, YqeY	-1.7	Hypothetical protein	Cytoplasmic
GSU1469	2-oxoglutarate:ferredoxin oxidoreductase, KorB	-1.7	Carbohydrate metabolism	Cytoplasmic

GSU number	Protein name	Fold change*	Suggested function	Predicted cellular location
GSU3193	Lon protease, Lon-3	-1.8	Proteolysis	Cytoplasmic
GSU2675	C1 family peptidase domain protein	-1.9	Proteolysis	Cytoplasmic Membrane
GSU1909	Ketol-acid reductoisomerase, IlvC	-2.1	Amino acid metabolism	Cytoplasmic
GSU2193	Ferritin-like domain protein	-2.1	Iron storage protein	Cytoplasmic
GSU0331	Periplasmic trypsin-like serine protease, DegP	-2.1	Proteolysis	Unknown
GSU0674	Hydroxylamine reductase, Hcp	-2.2	Energy metabolism	Cytoplasmic
GSU1735	Branched-chain amino acid ABC transporter, LivK-2	-2.2	Amino acid transporter	Periplasmic
GSU2005	Branched-chain amino acid ABC transporter	-2.4	Amino acid transporter	Periplasmic
GSU2706	Phosphate acetyltransferase, Pta	-2.5	Carbohydrate metabolism	Cytoplasmic
GSU1442	Carbonic anhydrase	-2.7	Energy metabolism	Unknown
GSU3401	Branched-chain amino acid ABC transporter	-2.9	Amino acid transporter	Periplasmic
GSU1465	Isocitrate dehydrogenase, NADP-dependent, Icd	-3.0	Carbohydrate metabolism	Cytoplasmic

GSU number	Protein name	Fold change*	Suggested function	Predicted cellular location
GSU2055	TRAP proton/solute symporter	-3.0	Transport protein	Periplasmic
GSU1660	Aconitate hydratase 2, AcnB	-3.1	Carbohydrate metabolism	Cytoplasmic
GSU2539	Carboxynorspermidine/carboxyspermidine dehydrogenase	-3.1	Amino acid metabolism	Cytoplasmic
GSU3271	Outer membrane channel, OprB family	-3.4	Transport protein	Outer Membrane
GSU3289	Ferritin-like domain protein	-3.7	Iron storage protein	Cytoplasmic
GSU2286	Enolase, Eno	-3.8	Carbohydrate metabolism	Cytoplasmic
GSU1468	2-oxoglutarate:ferredoxin oxidoreductase, α-subunit, KorA	-4.0	Carbohydrate metabolism	Cytoplasmic
GSU2527	Nitrite/sulfite reductase domain protein	-4.1	Oxidation-reduction process	Cytoplasmic
GSU0945	Cystathionine γ-synthase/β-lyase, MetC-2	-4.7	Amino acid metabolism	Cytoplasmic
GSU0944	Cystathionine γ-synthase/β-lyase, MetC-1	-5.6	Amino acid metabolism	Cytoplasmic
GSU1183	O-acetyl-L-homoserine sulfhydrylase, MetY-1	-7.3	Amino acid metabolism	Cytoplasmic
GSU1346	Sulfate ABC transporter, CysP	-9.1	Energy metabolism	Periplasmic

GSU number	Protein name	Fold change*	Suggested function	Predicted cellular location
GSU2602	Integration host factor, β subunit, IhfB-2	-10.3	DNA binding protein	Cytoplasmic
GSU3132	Histone-like protein, Hup	-18.4	DNA binding protein	Cytoplasmic

* Fold change indicates the average expression ratio for *G. sulfurreducens* grown in the absence (MFC- biofilm) and in the presence of a soluble electron acceptor (planktonic).

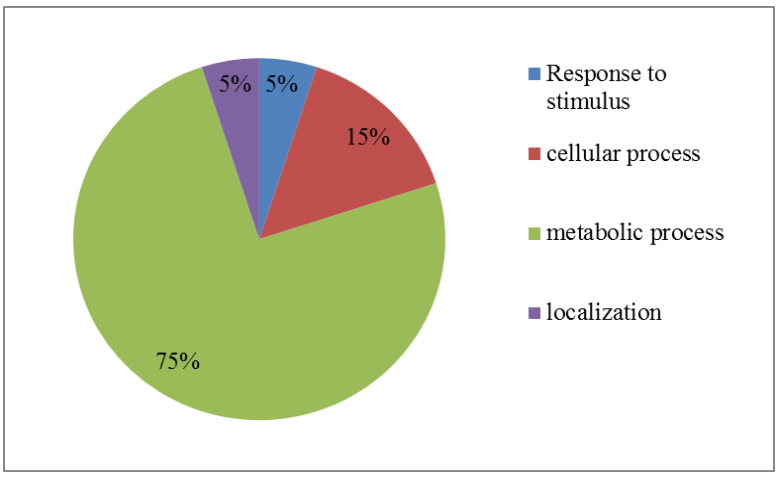

Figure 5.7 Proteins expressed at reduced level in the electrode biofilms (37 proteins) Proteins classified according to biological process.

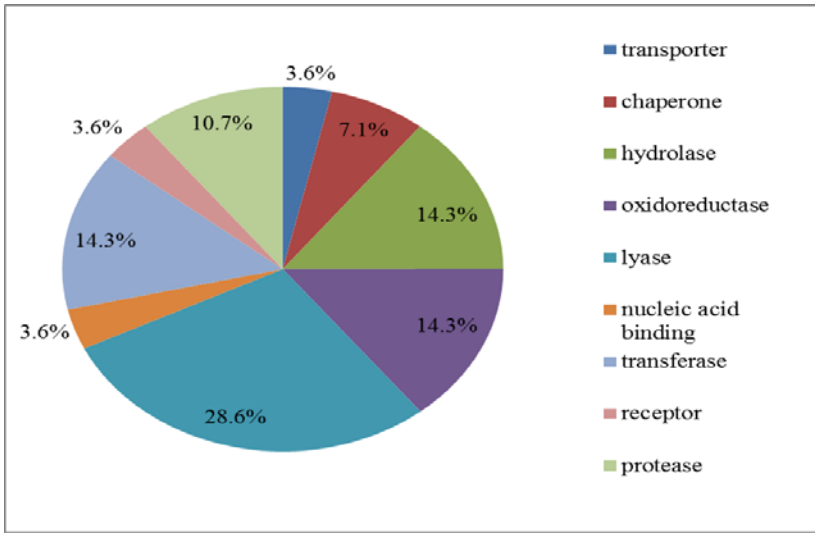

Figure 5.8 Proteins expressed at reduced level in the electrode biofilms (37 proteins) Proteins classified according to protein class/function.

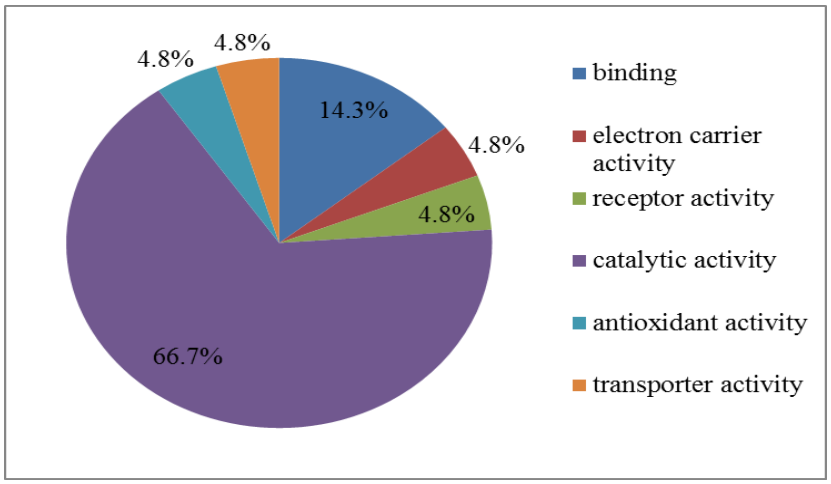

Figure 5.9 Proteins expressed at reduced level in the electrode biofilms (37 proteins) Proteins classified according to molecular function of protein.

A change in the nature of the electron acceptor (fumarate versus solid electrode) in the growth medium of *G. sulfurreducens* resulted in alteration of the expression pattern of proteins mainly located in the membrane (outer and cytoplasmic) and periplasm. The nature of the electron acceptor impacts particularly on the levels of proteins belonging to certain functional categories. In the present study we used expressed protein list from the experiments and panther mapper tools software to investigate the functional roles of the proteins identified. Using this method 63 % of *G. sulfurreducens* protein involved in metabolic process, 17 % protein involved in cellular process, 13 % protein involved in localization process and 7 % protein involved in stimulation process were found to be over expressed under the conditions of the present study (Figure 5.4). The metabolic process is a chemical reactions and pathways, including anabolism and catabolism, by which living organisms transform chemical substances.

Out of a total of 1318 protein, 77 proteins were differentially expressed when GS grown on solid electron acceptor versus soluble electro n acceptor. We observed differential over-expression of 40 proteins at higher level in solid electron acceptor of these 8 proteins were found to be over expressed at a level more than 3 fold higher for cell cultured using the electrode as electron acceptor. Most of the identified proteins were either outer membrane or cytoplasmic membrane bound. The most highly represented function of the more abundant protein is catalytic activity (90 %) (Figure 5.6) responsible for storage and release of energy other highly represented functions are those associated with transporter activity (10 %)(Figure 5.6). In the present study we identified 6 oxidoreductase family proteins involved in electron transfer (GSU1700, GSU1305, GSU3281, GSU1237, GSU1177, and GSU1239) (PANTHER software and tools). Our result (from Uniprot database) shows that membrane bound protein plays an important role in electricity generation. The outer membrane proteins (pilQ, pulQ) that are increased in the 3.5 fold which are involve in type-IV pilus biogenesis. Type IV pili are essential for attachment, colonization and biofilm formation (Bansal *et al.*, 2013) and type IV pili are implicated in improving current generation (Reardon & Mueller, 2013). The peptidoglycan binding proteins GSU 0810 and 0813 were detected in higher level in solid electron acceptor. These proteins are important for structural integrity and stability in GS cells OmpA family protein is known to play an important role in stress survival and movement of

substrate (molecule, ion) in to, out of or within the cell like a transporter or pore (Bansal *et al*., 2013). Proteins involved in acetate oxidation via citric acid cycle, electron/proton transport across cell membrane and ATP synthesis were also found to be over expressed in the electrode attached biofilms (GSU 1783,GSU 0328) (PANTHER mapper tools).

The cytoplasmic proteins glutamate dehydrogenase and glutamate synthase (GSU 1239 and GSU 1305) over expressed compare to soluble electron acceptor 6 and 8 fold in solid electron acceptor. Enzymatic activities of glutamate dehydrogenase and glutamine synthase were participating in the nitrogen metabolism and related ammonium absorption (De-Bashan *et al*., 2008). Glutamate dehydrogenase and glutamine synthase plays key role in maintaining the balance of carbon and nitrogen within the cell (De-Bashan *et al*., 2008). This study showed that the cytoplasmic DNA repair and recombination proteins GSU3132 and GSU2602 was down regulated compare to soluble electron acceptor 18 and 10 fold in solid electron acceptor. These results suggest that this protein might be more important for reduction of soluble fumarate than solid electrode. The majority of the proteins that were down-regulated in planktonic cells are involved in anabolic process. Most of the proteins expressed at reduced levels in planktonic cells were predicted to be localised in the cytoplasm, a total of 26 out of 37 proteins (Table-2). Sixty seven percent of the total down-regulated proteins are involved in catalytic activity and 14% decreased protein involved in cellular binding (Figure 5.9). Nevin *et al*. report that the outer-membrane protein plays an important role for high density current production in *Geobacter sulfurreducens* fuel cells (Nevin *et al*., 2009).

5.4 Conclusion

Our proteomics data shows that, in electrode attached biofilms the majority of the proteins expressed at higher levels are localized in the cellular membrane (Table-1). The proteins expressed at reduced levels are involved in anabolic processes localised in the cytoplasm. In solid electron acceptor biofilms, the functional categories of protein that are increased are those involved in catalytic activity and transporter activity. Data shown in figure 5.6 that 90 % proteins are active in catalytic activity and 10 % proteins are active in transporter activity in electrode

attached biofilms. In planktonic cell culture (Figure-5.9) 66 % proteins are involved in catalytic activity, 14 % proteins are active in binding activity and 4.8 % of proteins are active in electron carrier and transporter activity. Isomerase class protein expressions were observed only in attached biofilm cell and this class of protein responsible for cell replication. This was confirming by the proteomics results showing several outer membrane proteins were expressed at higher levels in solid electron acceptor plays important role for high density current production. Further studies with a broader range of electron acceptors are necessary to better understand the electron-acceptor pathways.

Acknowledgement

We thank the University of St. Andrews for the help with LCMS/ MS and iTRAQ analysis.

References:

Bansal, R., Helmus, R.A., Stanley, B.A., Zhu, J., Liermann, L.J., Brantley, S.L., Tien, M. 2013. Survival during long-term starvation: global proteomics analysis of geobacter sulfurreducens under prolonged electron-acceptor limitation. *Journal of Proteome Research*, **12**(10), 4316-4326.

Bond, D.R., Lovley, D.R. 2003. Electricity production by Geobacter sulfurreducens attached to electrodes. *Applied and Environmental Microbiology*, **69**(3), 1548-1555.

Borole, A.P., Reguera, G., Ringeisen, B., Wang, Z.W., Feng, Y., Kim, B.H. 2011. Electroactive biofilms: Current status and future research needs. *Energy and Environmental Science*, **4**(12), 4813-4834.

Cao, X.X., Fan, M.Z., Liang, P., Huang, X. 2009. Effects of anode potential on the electricity generation performance of geobacter sulfurreducens. *Gaodeng Xuexiao Huaxue Xuebao/Chemical Journal of Chinese Universities*, **30**(5), 983-987.

De-Bashan, L.E., Magallon, P., Antoun, H., Bashan, Y. 2008. Role of glutamete dehydrogenase and glutamine synthetase in chlorella vulgaris during assimilation of ammonium when jointly immobolized with the microalgae growth promoting bacterium azospirillum brasilense1. *Journal of Phycology*, **44**(5), 1188-1196.

Dumas, C., Basseguy, R., Bergel, A. 2008. Electrochemical activity of geobacter sulfurreducens biofilms on stainless steel anodes. *Electrochimica Acta*, **53**(16), 5235-5241.

Gunnigle, E., McCay, P., Fuszard, M., Botting, C.H., Abram, F., O'Flaherty, V. 2013. A functional approach to uncover the low-temperature adaptation strategies of the archaeon Methanosarcina barkeri. *Applied and Environmental Microbiology*, **79**(14), 4210-4219.

H. R. Fuller and G. E. Morris (2012). Quantitative proteomics using iTRAQ labeling and mass spectrometry, integrative proteomics, Dr. Hon-Chiu Leung (Ed.), ISBN: 978-953-51-0070-6, InTech, DOI: 10.5772/31469.

Katuri, K.P., Kavanagh, P., Rengaraj, S., Leech, D. 2010. Geobacter sulfurreducens biofilms developed under different growth conditions on glassy carbon electrodes: insights using cyclic voltammetry. *Chemical Communications*, **46**(26), 4758-4760.

Katuri, K.P., Rengaraj, S., Kavanagh, P., O'Flaherty, V., Leech, D. 2012. Charge transport through Geobacter sulfurreducens biofilms grown on graphite Rods. *Langmuir*, **28**(20), 7904-7913.

Lin, A. H., Murray, R. W., Vidmar, T. J., & Marotti, K. R. (1997). The oxazolidinone eperezolid binds to the 50S ribosomal subunit and competes with binding of chloramphenicol and lincomycin. *Antimicrobial Agents and Chemotherapy*, 41(10), 2127–2131.

Lovley, D.R. 2006. Bug juice: harvesting electricity with microorganisms. *Nature Reviews. Microbiology*, **4**(7), 497-508.

Malvankar, N.S., Vargas, M., Nevin, K.P., Franks, A.E., Leang, C., Kim, B.-C., Inoue, K., Mester, T., Covalla, S.F., Johnson, J.P., Rotello, V.M., Tuominen, M.T., Lovley, D.R. 2011. Tunable metallic-like conductivity in microbial nanowire networks. *Nature Nanotechnology*, **6**(9), 573-579.

Marsili, E., Sun, J., Bond, D.R. 2010. Voltammetry and growth physiology of geobacter sulfurreducens biofilms as a function of growth stage and imposed electrode potential. *Electroanalysis*, **22**(7-8), 865-874.

Mehta, T., Coppi, M.V., Childers, S.E., Lovley, D.R. 2005. Outer membrane c-type cytochromes required for Fe(III) and Mn(IV) oxide reduction in geobacter sulfurreducens. *Applied and Environmental Microbiology*, **71**(12), 8634-8641.

Methé, B.A., Nelson, K.E., Eisen, J.A., Paulsen, I.T., Nelson, W., Heidelberg, J.F., Wu, D., Wu, M., Ward, N., Beanan, M.J., Dodson, R.J., Madupu, R., Brinkac, L.M.,

Daugherty, S.C., DeBoy, R.T., Durkin, A.S., Gwinn, M., Kolonay, J.F., Sullivan, S.A., Haft, D.H., Selengut, J., Davidsen, T.M., Zafar, N., White, O., Tran, B., Romero, C., Forberger, H.A., Weidman, J., Khouri, H., Feldblyum, T.V., Utterback, T.R., Van Aken, S.E., Lovley, D.R., Fraser, C.M. 2003. Genome of geobacter sulfurreducens: metal reduction in subsurface environments. *Science*, **302**(5652), 1967-1969.

Nevin, K.P., Kim, B.C., Glaven, R.H., Johnson, J.P., Woodward, T.L., Methé, B.A., Didonato Jr, R.J., Covalla, S.F., Franks, A.E., Liu, A., Lovley, D.R. 2009. Anode biofilm transcriptomics reveals outer surface components essential for high density current production in Geobacter sulfurreducens fuel cells. *PLoS ONE*, **4**(5).

Pereira-Medrano, A.G., Knighton, M., Fowler, G.J.S., Ler, Z.Y., Pham, T.K., Ow, S.Y., Free, A., Ward, B., Wright, P.C. 2013. Quantitative proteomic analysis of the exoelectrogenic bacterium Arcobacter butzleri ED-1 reveals increased abundance of a flagellin protein under anaerobic growth on an insoluble electrode. *Journal of Proteomics*, 78(0), 197-210.

Reardon, P.N., Mueller, K.T. 2013. Structure of the type IVa major pilin from the electrically conductive bacterial nanowires of geobacter sulfurreducens. *Journal of Biological Chemistry*. 288, 29260-29266.

Snider, R.M., Strycharz-Glaven, S.M., Tsoi, S.D., Erickson, J.S., Tender, L.M. 2012. Long-range electron transport in Geobacter sulfurreducens biofilms is redox gradient-driven. *Proceedings of the National Academy of Sciences*, **109**(38), 15467-15472.

Strycharz-Glaven, S.M., Snider, R.M., Guiseppi-Elie, A., Tender, L.M. 2011. On the electrical conductivity of microbial nanowires and biofilms. *Energy & Environmental Science*, **4**(11), 4366-4379.

Zhou, L., Liu, Z., Lian, J., Li, F., Du, Z., Li, H. 2005. Microbial fuel cell used in study on dissimilatory ferric oxides reduction by Geobacter metallireducens. *Huagong Xuebao/Journal of Chemical Industry and Engineering (China)*, **56**(12), 2398-2403.

Chapter-6

Bioelectricity generation from dairy wastewaters in microbial fuel cells

6.1 Introduction

The escalating energy consumption in conjunction with declining conventional energy resources has triggered various research interests for development of sustainable renewable energy sources (Lovley, 2006, Schaetzle, 2008 ; Rabaey & Verstraete, 2005). Microbial fuel cell (MFC) technology has received a great deal of attention in recent years due to its potential advantages of sustainable electricity generation along with wastewater treatment (Allen & Bennetto, 1993; Gil *et al*., 2003; Kim *et al*., 1999). In MFCs, direct electricity is generated from organic matter through the catalytic activity of microorganisms. Conventionally, MFC consists of an anodic and a cathodic chamber separated by a proton exchange membrane (PEM) (Gil *et al*., 2003). Microbes in the anodic chamber of an MFC oxidize the organic matter which generates electrons and protons. The anode acts as an inert electron acceptor and these electrons are transported to the cathode through an external circuit. Protons that diffuse from the anodic chamber through the PEM reach the cathode where they combine with the electrons and oxygen (provided from air) to form water (Bond *et al*., 2002; Min & Logan, 2004). Electric current generation is made possible by keeping microbes separated from oxygen or any other end terminal soluble electron acceptor other than the anode which requires an anaerobic anodic chamber.

MFCs have been operated successfully on a variety of organic matter, ranging from pure synthetic to complex real wastewaters. Substrate type is an important factor affecting the performance of MFCs (Venkata Mohan *et al*., 2008). Different types of substrates can influence the bacterial biofilm growth and MFC power density and coulombic efficiency. Several organic compounds have been studied as fuels in MFCs: glucose (Rabaey *et al*., 2003), acetate, butyrate (Liu *et al*., 2005b), cysteine (Logan *et al*., 2005), proteins (Heilmann & Logan, 2006), lignocellulose (Rismani-Yazdi *et al*., 2007), xylose and humic acids (Huang *et al*., 2008). However, MFCs for real world applications must be tested with real wastewater, with reports appearing on use of complex waste streams in MFCs: domestic wastewater (Min & Logan, 2004; You *et al*., 2006), food processing wastewater (Oh & Logan, 2005), saline seafood wastewater (You *et al*., 2010), dairy wastewater (Venkata Mohan *et al*., 2010), molasses wastewater (Zhong *et al*., 2011), dye wastewater (Kalathil *et al*., 2011), slaughterhouse wastewater (Katuri *et al*., 2012), uric salt (You *et al*., 2014) and brewery wastewater (Feng *et al*., 2008). Wastewaters from different industrial operations contain high concentrations of organic and inorganic substances as well as soluble and insoluble materials (Tauseef *et al*., 2013). Power production in an MFC mainly depends on reactor configuration, electrode material, performance of proton exchange membrane (PEM), specific source of substrate, and operating conditions such as temperature. Temperature is an important parameter for MFCs performance. Temperature can influence the rate and path of carbon flow during electrogenesis by affecting the activity of electroactive bacteria. Most of the MFCs performance has been examined in temperature range of 20-35 ºC. Liu *et al* reported 9 % power density decrease when temperature was reduced from 32 ºC to 20 ºC in single chamber MFCs (Liu *et al*., 2005a). In another study Min *et al* 2008 reported similar phenomenon using a dual chamber MFC with a ferricyanide cathode wherein the power density was reduced by 39 % when the temperature was decreased from 30 ºC to 22 ºC, and no noticeable power generation at 15 ºC . Catal *et al*. reported using a single chamber MFCs with mixed carbon source as a substrate. They obtained maximum power density of 486 mW m^{-2} at 14 ºC compared to 602 mW m^{-2} at 30 ºC temperature for the same MFC (Catal *et al*., 2011), achieved by gradual adaptation of the MFC to decreasing temperatures.

The process of anaerobic digestion (AD) involves the complete breakdown of complex organic molecules by different consortia of microorganisms, in the absence of oxygen, and it results in the production of biogas as the end product (Schink, 1997). All conventional AD reactors are operated under mesophilic temperature condition to ensure optimum microbial activity. Temperature can affect the rate and path of carbon flow during methanogenesis by influence the activity of microorganism (McKeown *et al*., 2009). Low temperature AD has emerged as an economically attractive waste treatment strategy, which confers considerable advantages over conventional mesophilic temperature (Bialek *et al*., 2012). Failure of the bioreactors to retain granular sludge during low temperature AD may lead to severe hydraulic washout of psychro-active sludge (Lettinga *et al*., 1999).

Increased demand for milk and milk products caused large growth of dairy industries in Ireland. Increasing demand for dairy products will result in huge quantities of dairy waste water production. This increase of dairy wastewater production should be combined with more sustainable, energy-efficient wastewater treatment technologies. In the present study, the feasibility of using dairy wastewater as a substrate for an MFC for electricity generation with simultaneous accomplishment of wastewater treatment has been investigated. A novel MFC is designed for simultaneous wastewater treatment and electricity production. Two identical MFCs were used with high concentration substrate of synthetic and real dairy wastewater. The MFCs were operated at temperatures of 15 ºC, pertinent to the climate in the Republic of Ireland, and 30 ºC to evaluate the performance as a form of electricity generation and substrate degradation under these conditions.

6.2 Materials and Methods

6.2.1 MFC construction

The studies were carried out in up-flow dual chambered polyacrylic-based MFCs. The cylindrical MFCs consisted of an outer catholyte chamber separated from a rectangular polyacrylic inner anolyte chamber, with anode and cathode separated by Nafion117 proton-exchange membrane (PEM, Sigma Aldrich) inserted in

opposite faces of the inner chamber (Fig.1). Each membrane was of 20 cm^2 surface area, making the total exposed membrane surface area of 40 cm^2. The working volume of the anolyte chamber of both MFCs was 350 mL, whilst that of the catholyte chamber was 1200 mL. Graphite plates were used as anodes giving a total surface area of 140 cm^2. Carbon cloth (16 cm × 7.5 cm) coated in platinum (60 % HP Pt on Vulcan XC-72) was used as a cathode in all MFCs. The electrodes were connected externally with titanium wire through an external resistance of 100 Ω. The medium influent was supplied to the MFCs from the bottom of the anode chamber using a peristaltic pump (Gilson, France) with effluent exit from the anode chamber at the top of the reactor.

6.2.2 MFC operations

An initial study was undertaken to evaluate MFC operation at 15 ^oC using a high substrate concentration of synthetic dairy wastewater of 4 g/L COD. The MFCs inoculated with anaerobic sludge collected from an anaerobic digester (Mutton Island wastewater treatment center, Galway). The granular sludge was crushed in a grinder for 10 seconds and 220 mL of the resultant sludge was added to the anode chamber to establish a sludge loading at 0.75 kg COD kg VSS^{-1} (Behera & Ghangrekar, 2009). The VSS/L (volatile suspended solids/litre) was found to be 24.19 g/L. A known volume of well mixed sludge sample was taken in high silica glass crucible and dried over night at 103 to 105 ºC for sludge with high concentration. The increase in weight of crucible was represented as total solids. For measurement of VS, the crucible was kept in a muffle furnace at 550 ± 50 ºC after drying the crucible at 105 ºC and weighing. After ignition for 15 to 20 minutes, the crucible was cooled down at room temperature in a desiccators and weight was measured. The weight lost in ignition was expressed as VSS. Synthetic media contained milk powder, and 0.1 g KCl, 7.5 g $CaCl_2$, 0.25 g KH_2PO_4, 0.35 K_2HPO_4, 5 g $NaHCO_3$, 10 ml of mineral solution and 1 ml of trace element solution (per L) was used as feed, with the solution having COD of 4000 mg L^{-1}.

The feed pH was kept in the range of 7.2 - 7.5 throughout the experiments and the MFCs were operated at temperatures of14 ± 1 ºC. In initial stage MFCs were

operated under batch mode to encourage attachment of bacteria to anodes. The first batch consisted of 220 mL of the inoculum supplemented with 130 mL of the synthetic dairy wastewater. After one batch mode operation, the MFCs were subsequently operated in continuous mode at organic loading rate (OLR) of 2.5 kg COD m^{-3} d^{-1} maintaining a hydraulic retention time (HRT) of 12 h using the peristaltic pump. The effluent left the anode chamber at the top and was recirculated into the cathode chamber, to function as catholyte, with the chamber aerated to facilitate the supply of oxygen as oxidant. Upon reaching a steady state voltage output across the 100 Ω resistors, the performances of MFCs were evaluated by polarization experiments using a variable resistance box.

A subsequent study was carried out using the same MFC design but with sampled dairy wastewater as feed, and a higher temperature, to investigate COD removal efficiency with simultaneous electricity generation compared to a parallel anaerobic digestion study, conducted in the Microbial Ecology Laboratory using the same wastewater as feed, and to treatment of the outlet from the AD study using the MFC. As before, the two MFCs were inoculated initially with anaerobic sludge collected from an anaerobic digester (Mutton Island wastewater treatment center, Galway). The dairy wastewater was collected from a local dairy plant situated in Ballineen, Co. Cork, Ireland. The characteristics of the raw dairy wastewater were a pH of 8.5 – 9.0 and COD of 1900–2000 mg/L. The collected wastewater was stored at 4 ºC before feeding to the MFCs. The feed pH was maintained in the range of 7.2 - 7.5 throughout the experiments by acid addition and the MFCs were operated in the temperature range of 28 to 32 ^{o}C. In the initial stage both MFCs were operated under batch mode condition to encourage the attachment of bacteria to the graphite plate anodes, as before. After one batch mode operation dairy wastewater was introduced as feed with OLR of 1.4 kg COD $m^{-3}d^{-1}$ and a second MFC was operated with the dairy wastewater which was previously treated by conventional upflow anaerobic sludge blanket (UASB) anaerobic treatment process with OLR of 0.06 kg COD $m^{-3}d^{-1}$.

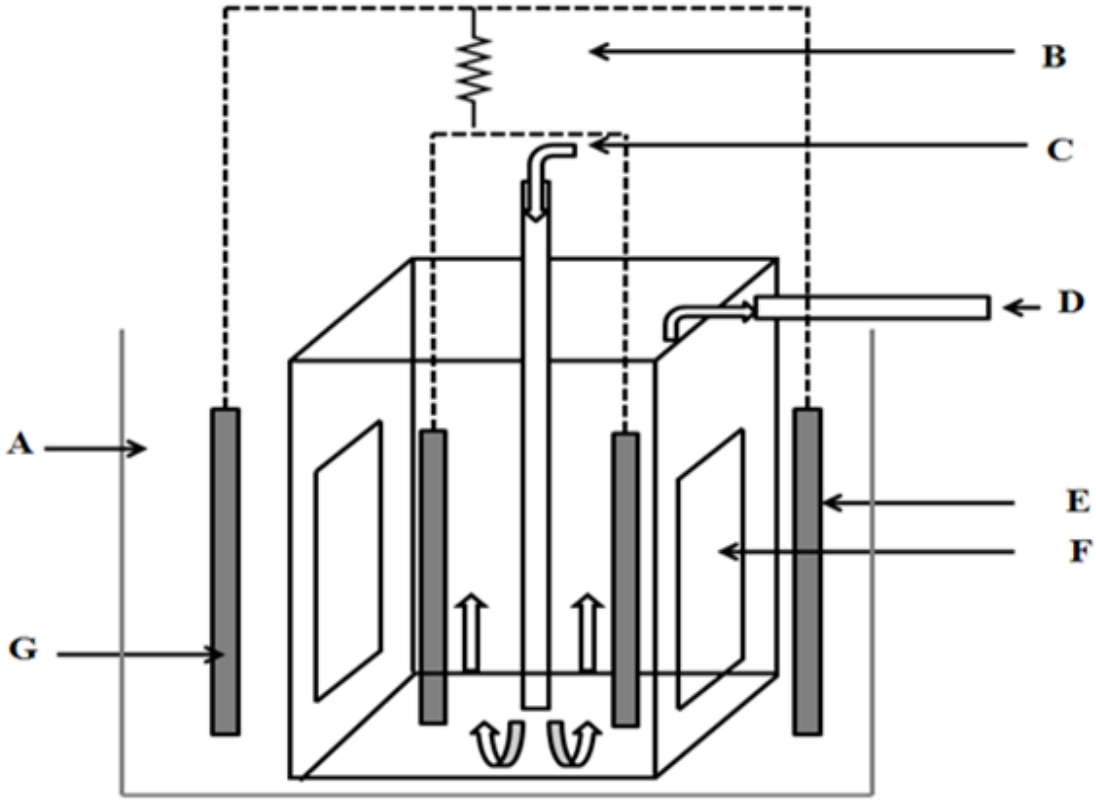

Figure 6.1 Schematic diagram of the MFCs used in the study: (A) catholyte (B) external resistance load (C) cell culture medium anolyte influent (D) anolyte effluent (E) cathode (F) membrane (G) anode.

6.2.3 MFC testing

For both studies, MFC cell voltages were recorded continuously using a digital multimeter with data acquisition unit (Pico data logger, UK) throughout the batch and continuous feed experiments by connecting anode and cathode across a 100 Ω external resistor. Current (*I)* was calculated using Ohm's law ($I = V/R$) with MFC power estimated by $P = IV$, where I is cell current and V is the cell voltage. Polarization studies were carried out by varying the external resistances from 10 kΩ to 10 Ω. Power density was normalized to the geometric anode surface area. Internal resistance of the MFCs was estimated from the slope of linear portion of the plot of voltage versus current (Picioreanu *et al*., 2007). The coulombic efficiency (*CE*) was

estimated using the ratio of charge produced (by integrating the measured current over time) to theoretical charge on the basis of consumed COD, with the theoretical charge production estimated as (F x n x w)/M, where F is Faraday's constant, n is the number of moles of electrons produced per mole of substrate (= 4 for wastewater COD), w is the daily COD load consumed in gram and M is molar mass of acetate (Logan *et al*., 2006).

For measurement of solids in the sludge inoculum, a known volume of sample was placed in a silica glass crucible and dried overnight at 103 - 105 ºC. The increase in weight of crucible was represented as total solids (APHA, 1998). For measurement of VS, the crucible was heated in a muffle furnace at 550 ± 50 °C. After ignition for 15 to 20 minutes, the crucible was cooled down to room temperature in a desiccator and weighed. The weight lost during ignition was expressed as VS (APHA, 1998).

The COD of samples was determined by the closed reflux colorimetric method (APHA, 1998). Briefly, the sample was placed in a capped glass tube which was heated at reflux for two hours in the presence of potassium dichromate as oxidant. The oxygen consumed was measured against standard ferrous ammonium sulphate solutions.

The specific methanogenic activity (SMA) test is used to detect changes in bacterial activity during operation. Bacterial populations were investigated against a variety of soluble substrates (ethanol, acetate, propionate and butyrate) and a gaseous substrate (H_2 / CO_2) according to the method described by (Coates *et al*., 1996; Collins *et al*., 2003).

6.2.4 Scanning electron microscopy (SEM)

Electrodes removed from the reactor were sectioned into pieces for scanning electron microscopy (SEM). Prior to SEM imaging, fixation was undertaken, using a series of primary and secondary fixatives as described in chapter 3 (Bond & Lovley, 2003; Kuo, 2007). The dried samples were mounted over SEM stubs with double-

sided conductivity tape and a thin layer of gold metal applied using an automated sputter coater (Emitech, K550) for 2 min and imaged using a model 4700 SEM instrument (Hitachi, Japan).

6.3 Results and discussion

Ireland is one of the largest producers of milk and dairy based products in the world. Dairy wastewater contains complex organics, such as polysaccharides, proteins and lipids (Venkata Mohan *et al*., 2010). Since dairy wastewaters are rich in biodegradable organic compounds one can ask whether they can be effectively used for renewable energy generation. This study seeks to determine whether synthetic dairy wastewater can be used, at temperatures pertinent to Ireland, to generate electric power, and subsequently compare electricity generation using dairy wastewaters to anaerobic digestion, at temperatures of 28-32 °C.

6.3.1 Operation using synthetic dairy wastewater

Initially MFCs were operated in batch mode to avoid washout of the sludge inoculum and to encourage attachment of bacteria to the anode surface (Jana *et al*., 2014). After ~2 days of operation in batch mode, MFC operation was switched to continuous mode at an OLR of 2.5 kg COD m^{-3} d^{-1} to maintain the hydraulic retention time (HRT) of 12 h to compare data with (Bialek *et al*., 2012). It was observed that the COD removal efficiency in the anode chamber increased with increase in time at ambient temperature (average temperature of 15 ºC) as is evident in figure 6.2. The COD removal efficiency after 25 days reached a steady value of 59 %. Bialek *et al* 2012 report that maximum 60 % COD removal efficiency when temperature was reduced from 25 ºC to 15 ºC in conventional expanded granular sludge bed reactor using similar type of synthetic dairy waste water.

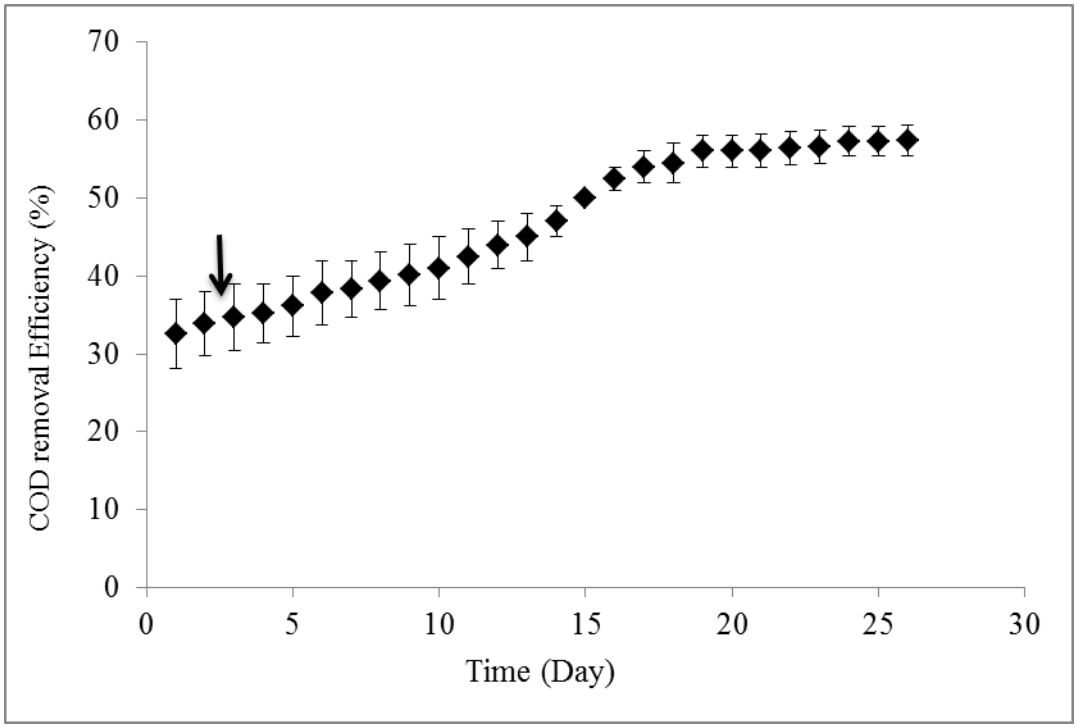

Figure 6.2 COD removal efficiency of MFCs at 15 ºC. Solid arrow indicates the time where the reactor was switched from batch to continuous mode operation.

6.3.2 Power generation

The voltage, produced across the 100 Ω external resistance load, shows an increase from ~350 mV, when the feed is switched to continuous mode, to a stable voltage of ~400 mV 12 days after inoculation. Maximum power density (normalized to the geometric anode surface area) and volumetric power (normalized to the working volume of anode chamber) of ~180 mW/m^2 and ~7150 mW/m^3, respectively, is estimated over this steady period across the 100 Ω external resistance. Catal *et al* reported maximum power density of 486 mW m^{-2} achieved by gradual adaptation of the MFC to decreasing temperatures at 14 ºC using a single chamber air breathing MFC (Catal *et al*., 2011). Acetate fed MFCs shifted from 30 ºC to 15 ºC showed the power density drop from 1260 mW/m^2 to 709 mW/m^2 (Cheng *et al*., 2011). Our results demonstrate the optimal operating condition is important to electricity production in MFCs at sub-ambient temperatures.

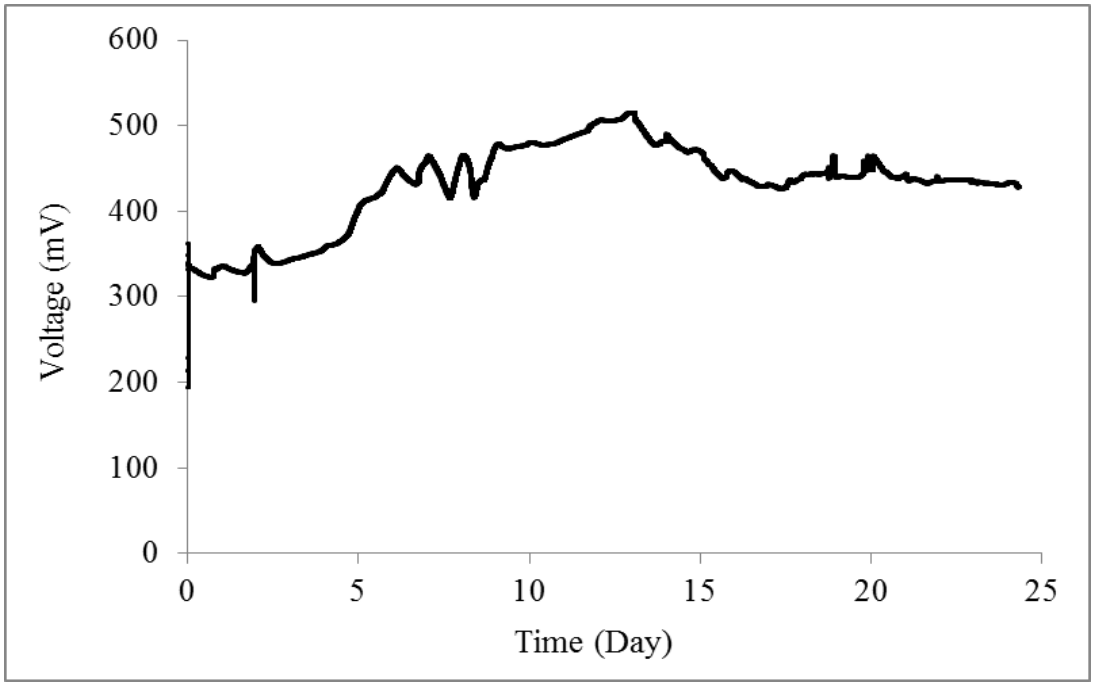

Figure 6.3 Voltage generation in the MFCs across 100 Ω external resistances. The operating feed pH was pH 7.2 -7.5, temperature 14 ± 1 ºC and HRT of 12 h.

Polarization studies were carried out for the MFCs by varying the external resistance from 5000 Ω to 10 Ω. The Polarization curve (Figure 6.4) showed a maximum power density of 206 mW m^{-2} at 50 Ω ± 10 Ω external resistances in both the MFCs. Internal resistance of the MFC was measured from the slope of line from the plot of voltage versus current. The mean internal resistance value of MFCs is 45.5 ± 3 Ω.

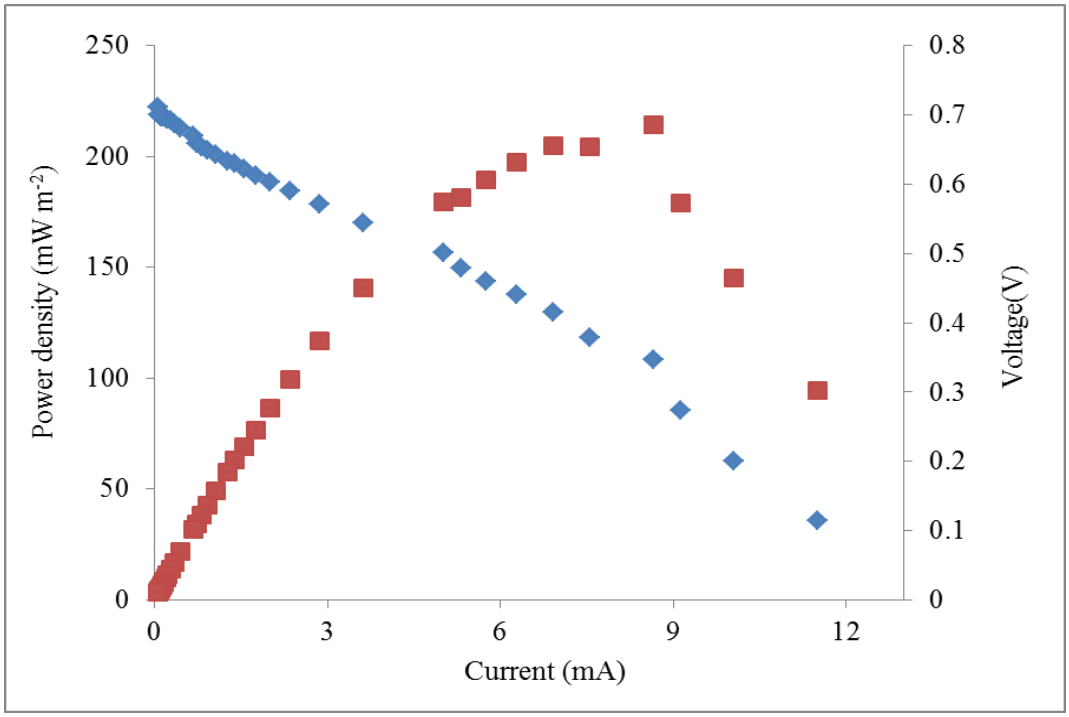

Figure 6.4 Polarization curves measured at various external resistances (10-5000 Ω) during stable performance of MFC. Cell voltage (blue) and power density (red) versus current density.

6.3.3 SMA and SEM

After completion of experiment sludge sample from MFCs and stored seed sludge was used for specific methanogenic activity test. As expected sludge samples yield high SMA values, with a maximum reading of 41 ml while MFC values were <5ml. After an initial lag phase methane production increased very slowly for the MFCs but much faster in the case of the original seed sludge in growth phase. We have observed maximum SMA of 24.29 g COD CH_4 g^{-1} VSS^{-1} day^{-1} in original seed sludge whereas only 4.83 g COD-CH_4 g^{-1} VSS^{-1} hr^{-1} in MFC. The results show that the presence of methanogenic bacteria in the original seed sludge was much higher and the sludge collected from MFCs after completion of experiment was much lower in methanogenic bacteria.

Electron microscopy is used to examine morphological structure, cell attachment, topography and bacterial cell distribution on the electrode surfaces. The

images in figure 6.5 show formation of a thick layer, with heterogeneous topography, of bacterial cells on the electrode surface, presumably responsible for electron transfer and thus current generation in the MFC as well as substrate degradation, as described in chapter 1 and by others (Biffinger *et al*., 2007; Reguera *et al*., 2006). The presence of characteristic 2 µm long rod-shaped bacteria in the SEM image is comparable to the dimensions reported for *Geobacter* sp, and the images are similar to those observed by others for biofilms grown on graphite electrodes (Bond & Lovley, 2003; Strycharz-Glaven *et al*., 2011; Torres *et al*., 2008).

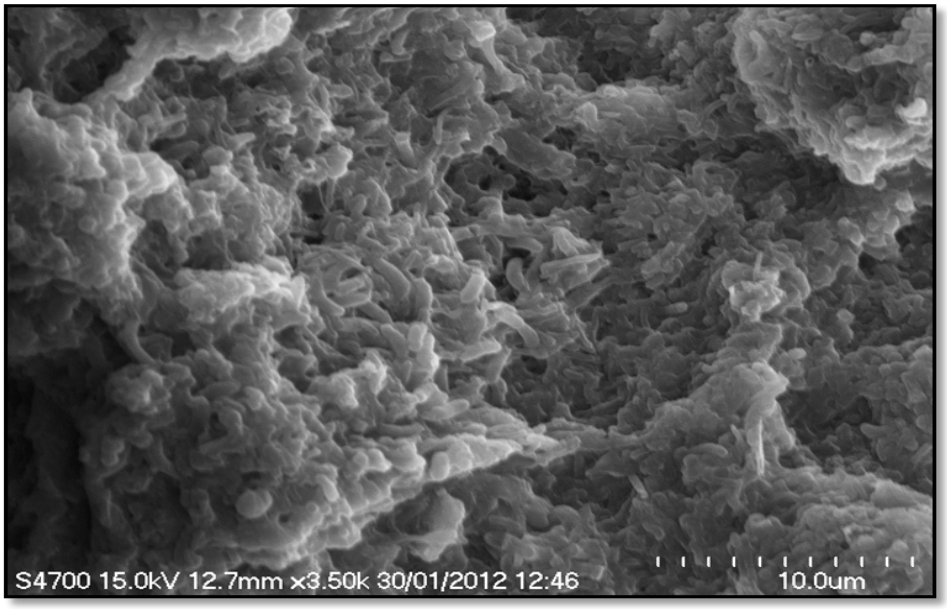

Figure 6.5 SEM of anode biofilm sampled from the reactor after completion of the experiment. The operating pH of the feed was pH 7.2 -7.5, temperature 14 ± 1 ºC and HRT of 12 h.

This study demonstrates the successful complex synthetic dairy wastewater treatment and electricity generation in up-flow MFCs at sub-ambient temperatures.

6.3.4 Treatment of sampled dairy wastewater

In this study identical MFCs were fed with two different samples of dairy wastewater. One MFC was operated with dairy wastewater at COD of 2000 mg/L and a second MFC was operated by feeding it from the outlet stream of an anaerobic digester, fed with the dairy wastewater, with the outlet stream having a COD of 82

mg/L. After ~2 days of batch mode operation to encourage, the attachment of electrogenic bacteria to the graphite plate anodes, both the MFCs operation was switched to continuous mode at an OLR of 1.4 kg COD m^{-3} d^{-1} and 0.06 kg COD $m^{-3}d^{-1}$ by maintaining a hydraulic retention time of 12 h. The COD removal efficiency in the anode chamber increased with time but there was a negligible COD removal efficiency observed in MFC fed with AD-treated dairy wastewater, which could be due to less bio degradable compound present in treated wastewater MFC. After steady state condition untreated dairy wastewater MFC and treated wastewater MFC showed COD removal efficiency of 83 % and 7 % respectively (Fig. 6.6). Dhall *et al* report that the ratio of BOD: COD of dairy wastewater in-between 0.74- 0.91 dependent on BOD seed (Dhall *et al*. 2012).

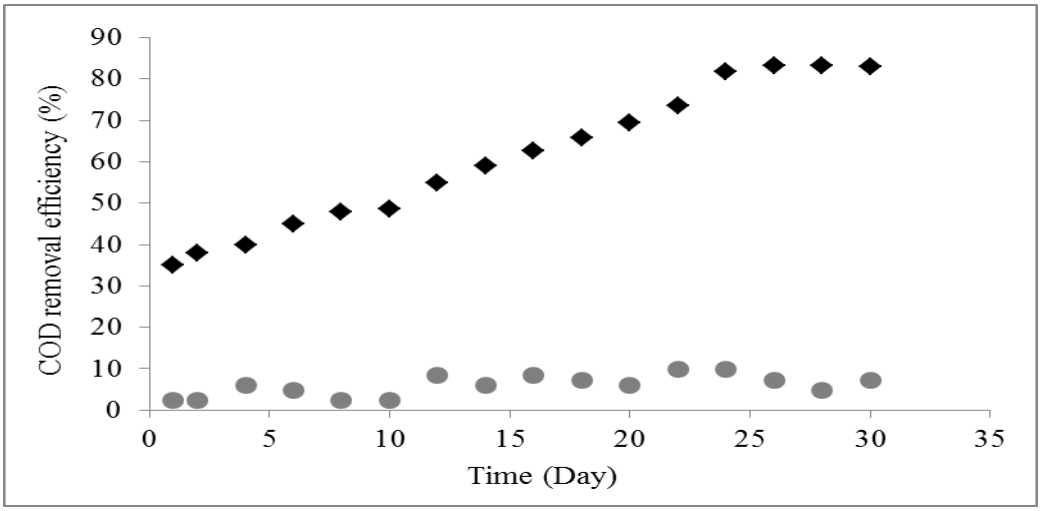

Figure 6.6 COD removal efficiency of both the MFCs at 32 °C. Untreated wastewater MFC (Black) and AD treated wastewater MFC (grey).

The anode effluent was brought to the cathode chamber to work as catholyte, where it was given further aerobic treatment. After further aerobic treatment in cathode chamber, the overall COD removal efficiency of 88.5 % was achieved in the MFC. Tawfik *et al* report that using a UASB reactor followed by activated sludge process for the treatment of dairy wastewater, they achieved maximum COD removal efficiency of 69 % and 79 % respectively. Bialek *et al*., 2012 report that maximum 80 % COD removal efficiency when conventional expanded granular sludge bed reactor operated at 37 ºC temperature with dairy waste water. Keily *et al*.,

2011 reported less than 1 mA of current production from a dairy manure wastewater-fed MFC and maximum COD removal efficiency of 70 %. Biocathodes have been successfully used in MFCs. Biocathodes have several advantages over abiotic cathodes such as the cost of operation of MFCs is lowered by eliminating the use of synthetic catholyte. Jana *et al.*, 2010 report a successful operation of biocathode in up flow microbial fuel cell operation. They observed maximum 90 % COD removal efficiency in different organic loading rate condition. This study demonstrated the effectiveness of this technology in wastewater treatment for dairy wastewater with simultaneous electricity generation.

6.3.5 Power generation

After inoculation, a gradual increase in the voltage production across the 100 Ω external resistance load was observed in dairy wastewater MFC but very little current generation observed in AD-treated dairy wastewater MFC. After 22 days of continuous mode operation a steady state current was observed in both MFCs. Dairy wastewater MFC generated maximum voltage of 0.412 V across 100 Ω external resistance but AD treated dairy wastewater MFC generated lower voltage (Figure 6.7).

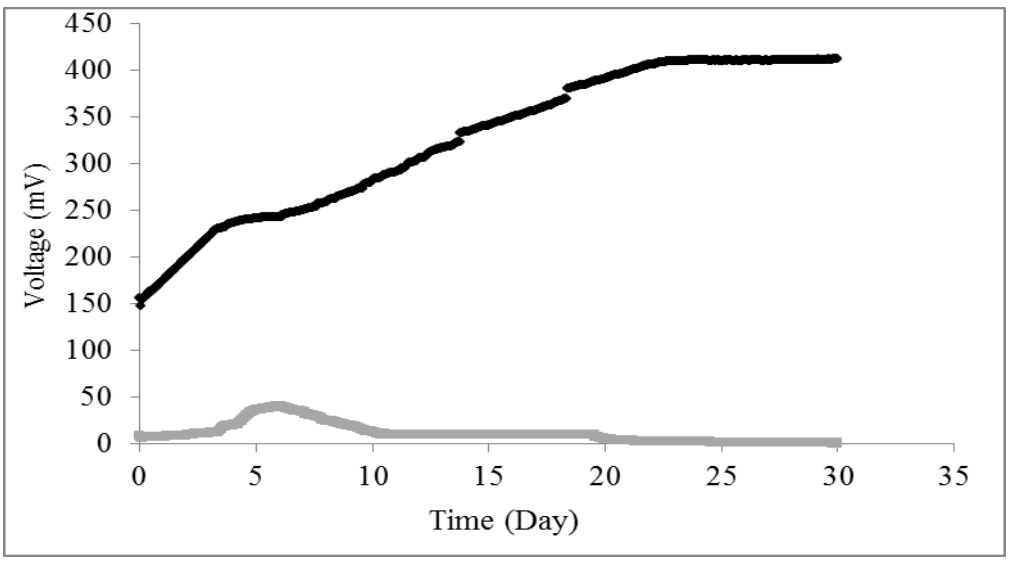

Figure 6.7 Voltage generations as a function of time for both the MFCs. Untreated dairy wastewater MFC (Black) and AD treated dairy wastewater MFC (grey). The operating feed pH was pH 7.2 -7.5, temperature 32 ºC and HRT of 12 hours

After steady state condition, polarization experiments were carried out for the by varying the external resistance from 5000 Ω to 10 Ω. Polarization curve (Figure 6.8) showed a maximum power density of 270 mW^{-2} m^{-2} at 10 Ω external resistance in dairy wastewater MFC.

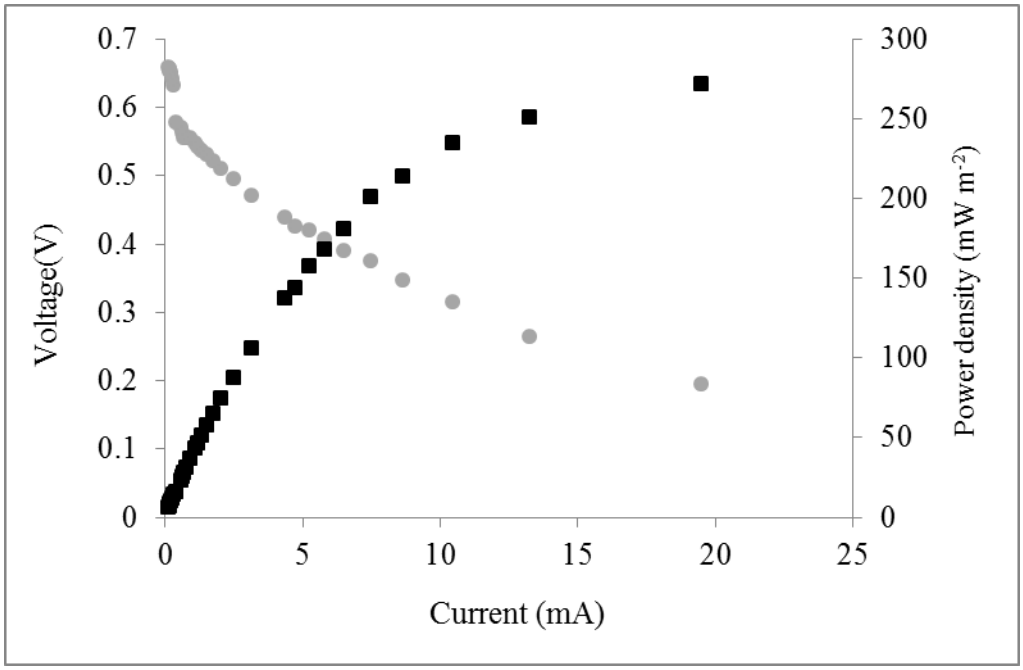

Figure 6.8 In-situ polarization curves, recorded on day 30, cell voltage and power density versus current density for untreated dairy wastewater MFC. Voltage (grey) and current density (black).

Internal resistance of the MFC was measured from the slope of line from the linear area of the plot of voltage versus current. The internal resistance of MFC was 25 Ω and generated maximum volumetric power (normalized to the working volume of anode chamber) of 10864 mW m^3 at 10 Ω external resistance. The very low internal resistance proves the effectiveness of new reactor design for simultaneous wastewater treatment and electricity generation. We observed an internal resistance of 45 Ω when treating with real synthetic wastewater in the same reactor configuration. Comprising with artificial dairy wastewater, a real dairy wastewater MFC showing less internal resistance may be due to the different organic loading rate or conductivity of the wastewater, because an increase in a solution's temperature will cause an increase in the mobility of the ions in solution.

Power generation is one of the main goals of MFC operation. We also seek to capture as many of the electrons stored in the biomass as possible as current and to recover as much energy as possible from the system. The recovery of electrons is measured as coulombic efficiency. Coulombic efficiency of 2.5 % at 100 Ω was obtained when MFC operated with real dairy wastewater, where coulombic efficiency of 2.3 % at 100 Ω was obtained when MFCs were operated with synthetic wastewater. Nimje *et al.*, 2012 reported coulombic efficiency of 2.9 % for the single chamber MFC operating on food and dairy wastewater. Orta *et al* reported coulombic efficiency of 2 % for the single chamber MFC operating on dairy wastewater (Orta *et al* 2011).

The COD removal efficiency and current generation results demonstrate the feasibility of this configuration of MFC as an effective wastewater treatment technology which ensures reliable effluent quality. This has implications for the upscale of MFCs to industrial scale.

6.4 Conclusions

This study has demonstrated effective treatment of synthetic and real dairy wastewater in a microbial fuel cell, simultaneously generating bioelectricity. The new design MFC demonstrated very good performance in terms of electricity harvesting and organic matter removal at all operating temperatures. The MFCs were operated at sub-ambient temperatures (15 ºC), achieved 65 % COD removal efficiency and the MFCs operated at controlled 30-32 °C achieved 88 % COD removal efficiency. Higher COD removal efficiency and power production observed in this study has demonstrated utility of MFCs as a dairy wastewater treatment process, simultaneously harvesting direct electricity for onsite applications. Although, MFCs are reported to be successful for wastewater treatment and electricity recovery, many aspects need further investigation. There is no consistency in the type of reactors, material of reactor and electrodes, geometry and size of the reactor, area of the electrode required with respect to reactor volume. Microbial fuel cell technology can be useful in low strength wastewater treatment and at low temperature where conventional anaerobic treatment processes does not function well. MFC technology holds great promise towards sustainable energy generation along with application within a broad range in near future.

References

Allen, R.M., Bennetto, H.P. 1993. Microbial fuel-cells - Electricity production from carbohydrates. *Applied Biochemistry and Biotechnology*, **39-40**(1), 27-40.

APHA. 1998. Standard methods for the examination of water and wastewater. 20th edn, American public health association/american water works association/water environment federation, washington DC,USA.

Behera, M., Ghangrekar, M.M. 2009. Performance of microbial fuel cell in response to change in sludge loading rate at different anodic feed pH. *Bioresource Technology*, **100**(21), 5114-5121.

Bialek, K., Kumar, A., Mahony, T., Lens, P.N.L., O' Flaherty, V. 2012. Microbial community structure and dynamics in anaerobic fluidized-bed and granular sludge-bed reactors: influence of operational temperature and reactor configuration. *Microbial Biotechnology*, **5**(6), 738-752.

Biffinger, J.C., Pietron, J., Ray, R., Little, B., Ringeisen, B.R. 2007. A biofilm enhanced miniature microbial fuel cell using Shewanella oneidensis DSP10 and oxygen reduction cathodes. *Biosensors and Bioelectronics*, **22**(8), 1672-1679.

Bond, D.R., Holmes, D.E., Tender, L.M., Lovley, D.R. 2002. Electrode-reducing microorganisms that harvest energy from marine sediments. *Science*, **295**(5554), 483-485.

Bond, D.R., Lovley, D.R. 2003. Electricity production by geobacter sulfurreducens attached to electrodes. *Applied and Environmental Microbiology*, **69**(3), 1548-1555.

Catal, T., Kavanagh, P., O'Flaherty, V., Leech, D. 2011. Generation of electricity in microbial fuel cells at sub-ambient temperatures. *Journal of Power Sources*, **196**(5), 2676-2681.

Cheng, S., Xing, D., Logan, B.E. 2011. Electricity generation of single-chamber microbial fuel cells at low temperatures. *Biosensors and Bioelectronics*, **26**(5), 1913-1917.

Coates, J.D., Coughlan, M.F., Colleran, E. 1996. Simple method for the measurement of the hydrogenotrophic methanogenic activity of anaerobic sludges. *Journal of Microbiological Methods*, **26**(3), 237-246.

Collins, G., Woods, A., McHugh, S., Carton, M.W., O'Flaherty, V. 2003. Microbial community structure and methanogenic activity during start-up of psychrophilic

anaerobic digesters treating synthetic industrial wastewaters. *FEMS Microbiology Ecology*, **46**(2), 159-170.

Feng, Y., Wang, X., Logan, B.E., Lee, H. 2008. Brewery wastewater treatment using air-cathode microbial fuel cells. *Applied Microbiology and Biotechnology*, **78**(5), 873-880.

Gil, G.-C., Chang, I.-S., Kim, B.H., Kim, M., Jang, J.-K., Park, H.S., Kim, H.J. 2003. Operational parameters affecting the performannce of a mediator-less microbial fuel cell. *Biosensors and Bioelectronics*, **18**(4), 327-334.

Heilmann, J., Logan, B.E. 2006. Production of electricity from proteins using a microbial fuel cell. *Water Environment Research*, **78**(5), 531-537.

Huang, L., Zeng, R.J., Angelidaki, I. 2008. Electricity production from xylose using a mediator-less microbial fuel cell. *Bioresource Technology*, **99**(10), 4178-4184.

Jana, P.S., Katuri, K., Kavanagh, P., Kumar, A., Leech, D. 2014. Charge transport in films of Geobacter sulfurreducens on graphite electrodes as a function of film thickness. *Physical Chemistry Chemical Physics*, 16(19), 9039-9046.

Kalathil, S., Lee, J., Cho, M.H. 2011. Granular activated carbon based microbial fuel cell for simultaneous decolorization of real dye wastewater and electricity generation. *New Biotechnology*, **29**(1), 32-37.

Katuri, K.P., Enright, A.M., O'Flaherty, V., Leech, D. 2012. Microbial analysis of anodic biofilm in a microbial fuel cell using slaughterhouse wastewater. *Bioelectrochemistry*, **87**, 164-171.

Kiely, P.D., Cusick, R., Call, D.F., Selembo, P.A., Regan, J.M., Logan, B.E. 2011. Anode microbial communities produced by changing from microbial fuel cell to microbial electrolysis cell operation using two different wastewaters. *Bioresource Technology*, **102**(1), 388-394.

Kim, B.H., Ikeda, T., Park, H.S., Kim, H.J., Hyun, M.S., Kano, K., Takagi, K., Tatsumi, H. 1999. Electrochemical activity of an Fe(III)-reducing bacterium, shewanella putrefaciens IR-1, in the presence of alternative electron acceptors. *Biotechnology Techniques*, **13**(7), 475-478.

Kuo, J. 2007. Electron microscopy: Methods and protocols. Humana press,Totowa, New jersey.

Liu, H., Cheng, S., Logan, B.E. 2005a. Power generation in fed-batch microbial fuel cells as a function of ionic strength, temperature, and reactor configuration. *Environmental Science and Technology*, **39**(14), 5488-5493.

Liu, H., Grot, S., Logan, B.E. 2005b. Electrochemically assisted microbial production of hydrogen from acetate. *Environmental Science and Technology*, **39**(11), 4317-4320.

Logan, B.E., Hamelers, B., Rozendal, R., Schröder, U., Keller, J., Freguia, S., Aelterman, P., Verstraete, W., Rabaey, K. 2006. Microbial fuel cells: Methodology and technology. *Environmental Science and Technology*, **40**(17), 5181-5192.

Logan, B.E., Murano, C., Scott, K., Gray, N.D., Head, I.M. 2005. Electricity generation from cysteine in a microbial fuel cell. *Water Research*, **39**(5), 942-952.

Lovley, D.R. 2006. Bug juice: Harvesting electricity with microorganisms. *Nature Reviews Microbiology*, **4**(7), 497-508.

Min, B., Logan, B.E. 2004. Continuous electricity generation from domestic wastewater and organic substrates in a flat plate microbial fuel cell. *Environmental Science and Technology*, **38**(21), 5809-5814.

Min, B., Román, Ó.B., Angelidaki, I. 2008. Importance of temperature and anodic medium composition on microbial fuel cell (MFC) performance. *Biotechnology Letters*, **30**(7), 1213-1218.

Nimje, V.R., Chen, C.-Y., Chen, H.-R., Chen, C.-C., Huang, Y.M., Tseng, M.-J., Cheng, K.-C., Chang, Y.-F. 2012. Comparative bioelectricity production from various wastewaters in microbial fuel cells using mixed cultures and a pure strain of Shewanella oneidensis. *Bioresource Technology*, **104**(0), 315-323.

Oh, S., Logan, B.E. 2005. Hydrogen and electricity production from a food processing wastewater using fermentation and microbial fuel cell technologies. *Water Research*, **39**(19), 4673-4682.

Picioreanu, C., Head, I.M., Katuri, K.P., van Loosdrecht, M.C.M., Scott, K. 2007. A computational model for biofilm-based microbial fuel cells. *Water Research*, **41**(13), 2921-2940.

Rabaey, K., Lissens, G., Siciliano, S.D., Verstraete, W. 2003. A microbial fuel cell capable of converting glucose to electricity at high rate and efficiency. *Biotechnology Letters*, **25**(18), 1531-1535.

Rabaey, K., Verstraete, W. 2005. Microbial fuel cells: novel biotechnology for energy generation. *Trends in Biotechnology*, **23**(6), 291-298.

Reguera, G., Nevin, K.P., Nicoll, J.S., Covalla, S.F., Woodard, T.L., Lovley, D.R. 2006. Biofilm and nanowire production leads to increased current in Geobacter

sulfurreducens fuel cells. *Applied and Environmental Microbiology*, **72**(11), 7345-7348.

Rismani-Yazdi, H., Christy, A.D., Dehority, B.A., Morrison, M., Yu, Z., Tuovinen, O.H. 2007. Electricity generation from cellulose by rumen microorganisms in microbial fuel cells. *Biotechnology and Bioengineering*, **97**(6), 1398-1407.

Tauseef, S.M., Abbasi, T., Abbasi, S.A. 2013. Energy recovery from wastewaters with high-rate anaerobic digesters. *Renewable and Sustainable Energy Reviews*, **19**(0), 704-741.

Venkata Mohan, S., Mohanakrishna, G., Sarma, P.N. 2008. Effect of anodic metabolic function on bioelectricity generation and substrate degradation in single chambered microbial fuel cell. *Environmental Science and Technology*, **42**(21), 8088-8094.

Venkata Mohan, S., Mohanakrishna, G., Velvizhi, G., Babu, V.L., Sarma, P.N. 2010. Bio-catalyzed electrochemical treatment of real field dairy wastewater with simultaneous power generation. *Biochemical Engineering Journal*, **51**(1-2), 32-39.

You, J., Greenman, J., Melhuish, C., Ieropoulos, I. 2014. Small-scale microbial fuel cells utilising uric salts. *Sustainable Energy Technologies and Assessments*, **6**(0), 60-63.

You, S.J., Zhang, J.N., Yuan, Y.X., Ren, N.Q., Wang, X.H. 2010. Development of microbial fuel cell with anoxic/oxic design for treatment of saline seafood wastewater and biological electricity generation. *Journal of Chemical Technology and Biotechnology*, **85**(8), 1077-1083.

You, S.J., Zhao, Q.L., Jiang, J.Q., Zhang, J.N. 2006. Treatment of domestic wastewater with simultaneous electricity generation in microbial fuel cell under continuous operation. *Chemical and Biochemical Engineering Quarterly*, **20**(4), 407-412.

Zhong, C., Zhang, B., Kong, L., Xue, A., Ni, J. 2011. Electricity generation from molasses wastewater by an anaerobic baffled stacking microbial fuel cell. *Journal of Chemical Technology and Biotechnology*, **86**(3), 406-413.

Chapter 7

Modified electrode for anode in microbial fuel cell

The initial bacterial attachment is an important step for biofilm formation. In microbial fuel cell technology, biofilm development is beneficial for better electricity generation. In microbial fuel cell, bacterial biofilm transfer the electron to solid electrode, which may involve at least one of the following mechanisms (i) electron shuttling mediating molecules (Marsili *et al*., 2008) (ii) redox active membrane-bound proteins (cytochromes) (Busalmen *et al*., 2008) (iii) via conductive nanowires (pili) (Gorby *et al*., 2006). The power outputs of microbial fuel cells are very less compare to a chemical fuel cell. Thus, there is a need to improve the electrode materials for microbial fuel cell performance. Regarding the interface between biofilms and electrodes, recent research has focused on modifying graphite anodes in order to increase microbial fuel cell performance. Modification of electrode surfaces provides a route to understand electron exchange mechanisms between bacteria and electrode (Kumar *et al*., 2013). This knowledge may lead to enhanced microbial fuel cell performance, for example ammonia gas treatment of carbon cloth electrodes results in rapid bacterial adhesion and improved performance of electrodes in a single-chamber microbial fuel cell (Wang *et al* 2009, Feng *et al.,* 2010). The nitric acid treatment of carbon fibre-based electrodes can increase MFC power output (Zhu *et al* 2011). Recently Saito *et al* reported 4-(N,N-dimethylamino) aryl groups at electrodes through diazonium reduction and concluded on the basis of X-ray

photoelectron spectroscopy studies that a low extent of modification was necessary to improve microbial fuel cell performance (Saito *et al.*, 2011).

Electrochemical reduction of aryl diazonium salts is a versatile technique for modification of graphitic electrode. Recently other researchers have used this technique for improvement of microbial fuel cell performance (Kumar *et al*., 2013; Picot *et al*.). We here report the initial findings of the controlled modification of graphite anodes with electrochemical reduction of aryl diazonium salts and the subsequent effect of the modified electrodes on the power output in microbial fuel cells.

7.4 Material and methods

7.4.1 Experimental set-up

The study was carried out in three H-type fuel cells separated by a proton exchange membrane. Two graphite rods (3 mm diameter, Graphite Store) with exposed area of 5.2 cm^2 each were used as working electrodes and carbon cloths were used as counter electrode. The working volumes of the anolyte and catholyte chamber of all the MFCs were 125 mL. Each reactor used 125 mL of *Geobacter* feed solution in the anolyte and the catholyte consisted of 50 mM ferricyanide in 100 mM phosphate buffer (pH 7.0). Custom built Ag/AgCl (3 M KCl) with a porous vycor frit (Advanced Glass and Ceramics) used as reference electrode. In this configuration, influent was supplied to the cell from the bottom of the chamber using a peristaltic pump (Gilson, France), with effluent exiting the chamber at the top of the reactor, as shown in Figure 1. Following inoculation biofilms were induced to grow on graphite rod electrodes under a constant applied potential (0 V vs. Ag/AgCl) using a multichannel potentiostat (CHI-1030a, CH Instruments, Austin, TX).

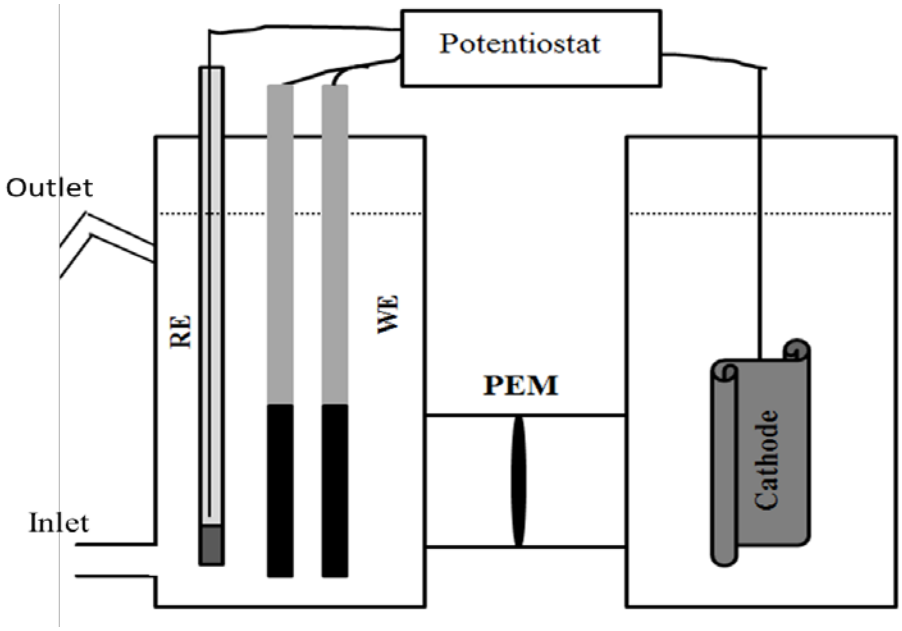

Figure 7.1 Schematic diagram of the MFCs used in the study

7.4.2 Electrode modification procedure

Diazonium salts were generated *in situ* in acid media (0.1 M HCl) containing 10 mM of the starting aryl amine followed by addition of 20 mM sodium nitrite (Baranton & Bélanger, 2005; Picot *et al*. 2011). This solution was then directly used as the electrolyte for the modification procedure of the graphite working electrode by electrochemical reduction of the diazonium salts using a potentiostat (Metrohm Autolab).

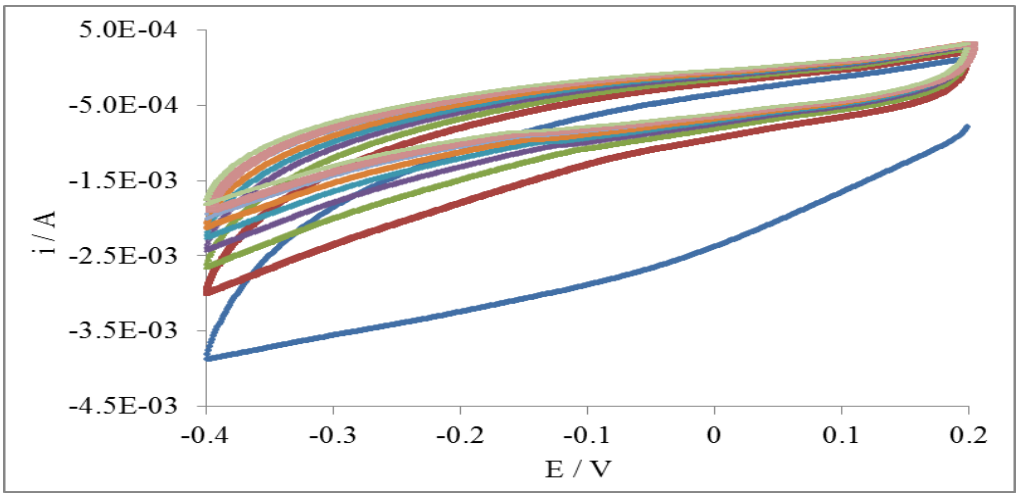

Figure 7.2 Cyclic voltammograms for a triphenylphosphonium modified graphite electrode

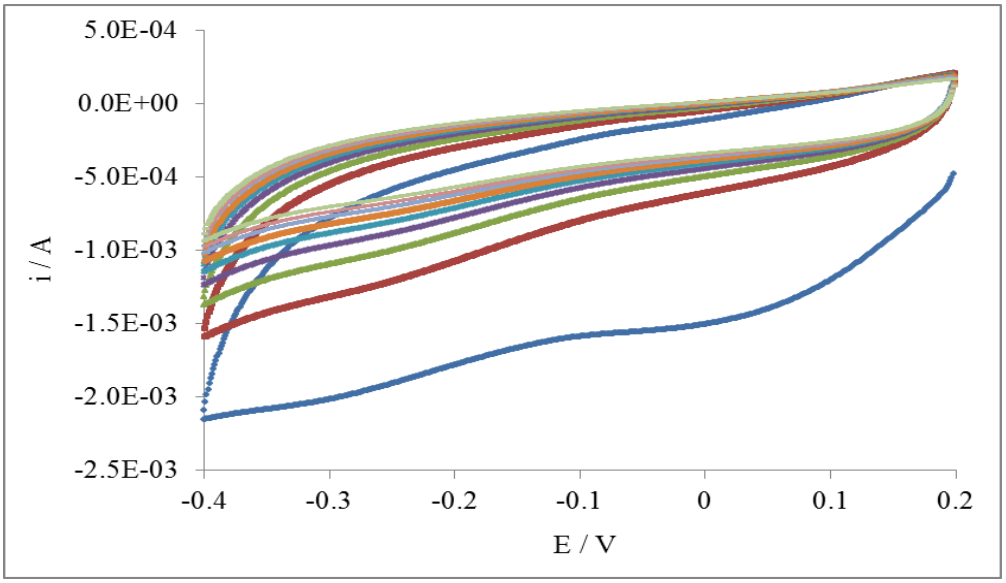

Figure 7.3 Cyclic voltammograms for a 4-benzyltriphenylphosphonium modified graphite electrode

A three-electrode cell configuration was used with an Ag/AgCl reference electrode and a carbon cloth as a counter electrode. Electrochemical reduction of the diazonium salts was carried out by recurrent cyclic voltammetry sweeps between +0.2 and −0.4 V (9 cycles) vs Ag/AgCl in the presence of either 4-phenylacetic acid diazonium or 4-benzyltriphenylphosphonium diazonium. Under continuous cycling, the magnitude of peak current decreased as shown in figure 7.2 and 7.3. This is proposed to be as a result of a decrease in availability of surface area for coupling once the first scan and coupling process is undertaken, thus indicating coupling reaction at electrode surfaces (Kumar and Leech, 2014). In the present study we used three H type reactor, for each three reactors, 2 working electrodes were employed. Two different modifications were performed by electrochemical reduction of aryl diazonium salts. The two electrodes were modified with 4-benzyltriphenylphosphonium diazonium displaying a positively charge group (R = NH_2, CH_2PPh^{3+}) and two others were modified with 4-phenylacetic acid diazonium displaying a negatively charge group (R = NH_2, CH_2COO^-). The two remaining working electrodes were left unmodified that served for the blank.

7.4.3 Biofilm growth on electrode surface

Geobacter sulfurreducens (ATCC 51573) was used as a source of electro active bacteria. Growth media containing acetate as a source of electron donor (20 mM) was used as feed. The feed pH was maintained in the range of 7.2–7.5

throughout the experiment and the cell was operated at temperature range of 28 to 32 ºC. Initially the reactor was operated over a single batch feed, by inoculation with GS directly from the culture bottles to encourage the attachment of electro genic bacteria to the graphite rode anodes. Thereafter, the electrochemical cell was operated using continuous delivery of acetate-containing medium only (no further inoculum) with a peristaltic pump using a flow rate of 5.0 mL h^{-1}.

7.4.4 Scanning electron microscopy (SEM)

Upon completion, the electrodes were removed from the reactor and sectioned into pieces for scanning electron microscopy (SEM). Prior to SEM imaging, fixation was undertaken, using a series of primary and secondary fixatives (Bond & Lovley, 2003; Kuo, 2007).

7.5 Results and discussion

After inoculation, an increase in the oxidation current production was observed over time (Figure 2). In case of triphenylphosphonium modified electrode a longer lag-phase for production of current was observed. In batch mode condition as shown in Figure 7.4, the CH_2COO^- modified anode recorded higher current, reaching 0.6 mA over this first batch feed cycle in comparison to the unmodified and triphenylphosphonium modified electrodes which attained maximum current of 0.13 and 0.00777 mA only compared to CH_2COO^- . After one batch cycle, represented by the arrows in Figure 7.2 the feed was switched to continuous mode on the 10^{th} day of operation providing a flow of 20 mM acetate to the anode to prevent electron donor depletion to biofilms. In continuous mode operation a rapid increase in current generation recorded for biofilms developed on both the modified and unmodified electrode. We observed the long term effects of the electrode modification to the MFCs performance. After 23 days of continuous mode operation CH_2COO^- modified and unmodified electrode reached maximum current of 1.53 and 1.6 mA current whereas triphenylphosphonium modified electrodes reached maximum current of 0.87 mA. In previous study we observed 45 hours of lag phase (chapter-3) prior to start continuous current generation but in this present study we observed early

response of CH_2COO^- modified electrode comparison to unmodified electrode and triphenylphosphonium modified electrode.

In this set-up, it is presumed that the cathode does not limit the current, as the ferricyanide catholyte was supplemented periodically over the time course of the experiments resulting in a constant electron acceptor concentration close to 50 mM, as reported previously (Katuri *et al*., 2012a; Katuri *et al*.; Kong *et al*., 2010).

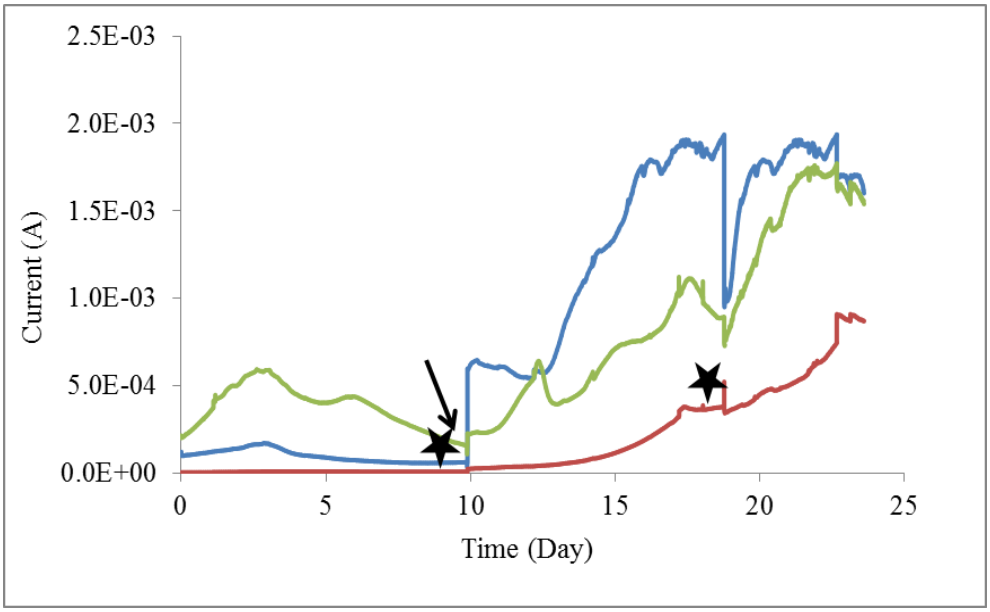

Figure 7.4 Amperometric responses of graphite rod working electrodes, as a function of time during GS biofilm growth operation (20 mM acetate) under 0 V vs. Ag/AgCl applied potential. Arrow indicates the region where the reactor was switched from batch to continuous mode operation and star indicates the time point of *in-situ* CV analysis. (Blue- Unmodified electrode, Red- Triphenyl phosphonium modified and Green- CH_2COO^- modified)

To examine the catalytic activity of the anodic biofilm slow scan cyclic voltammograms were recorded *in-situ* in the anode chamber in batch mode as well as continuous mode of operation. Sigmoidal voltammograms shown in figure 7.6 permit estimation from the first derivative of the CVs (not shown) of acetate oxidation centered at −0.41 vs. Ag/AgCl. The sigmoidal CV is indicative of catalytic oxidation of the substrate by the biofilm and heterogeneous electron transfer to the electrode, with similar responses reported on for acetate oxidation by anodic biofilms of *Geobacter sulfurreducens* (Katuri *et al*., 2010; Katuri *et al*., 2012b; Marsili *et al*., 2010).

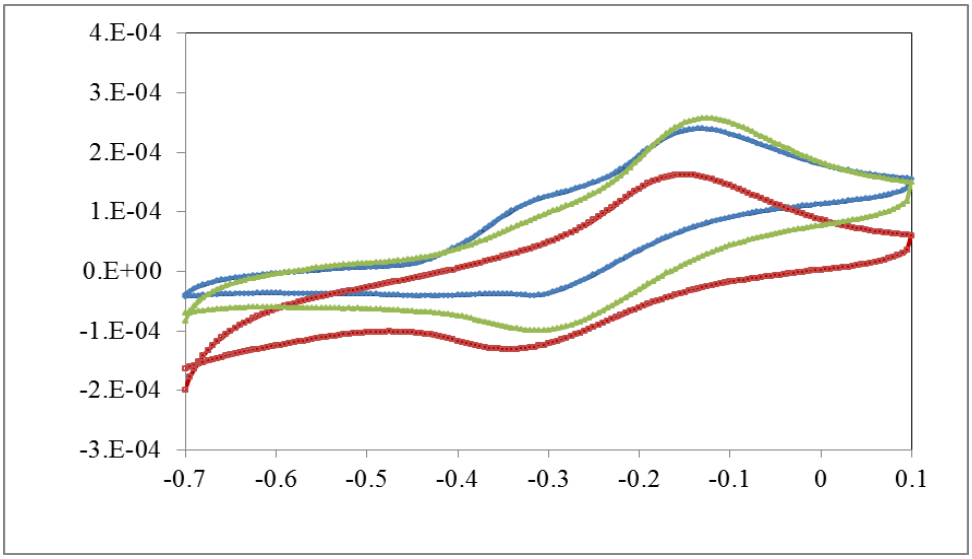

Figure 7.5 Cyclic voltammograms (5mV/s) of anodic biofilm, recorded in- situ on the initial batch mode operation. (Blue- Unmodified electrode, Red- Triphenyl phosphonium modified and Green- CH_2COO^- modified)

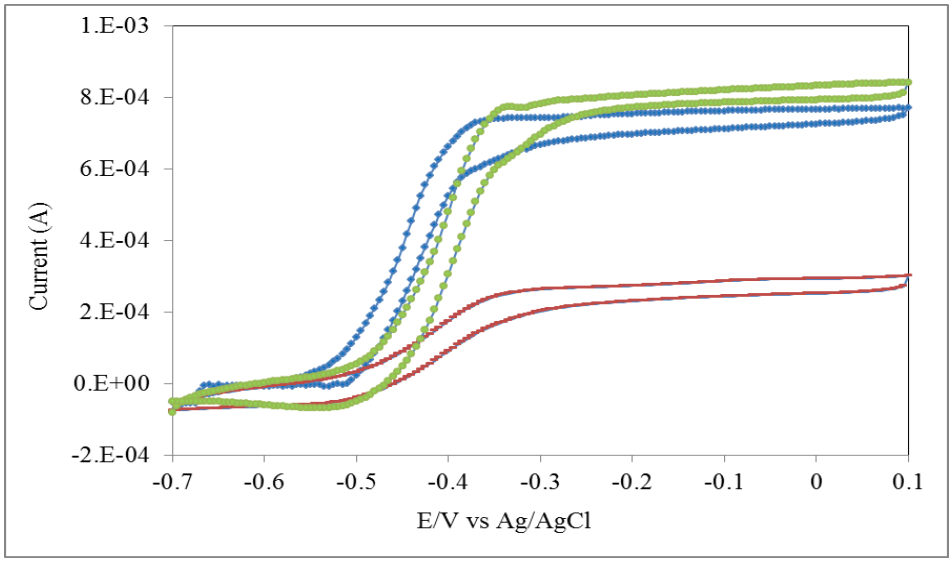

Figure 7.6 Cyclic voltammograms (5mV/s) of anodic biofilm, recorded *in-situ* on the continuous mode operation. (Blue- Unmodified electrode, Red- Triphenyl phosphonium modified and Green- CH_2COO^- modified)

Electron microscopy was used to examine the morphological structure, cell attachment, topography and bacterial cell distribution on the electrode surfaces. The images show the presence of rod-shaped cells closely associated with graphite surfaces, which were responsible for electron transfer, and thus current in the microbial fuel cell.

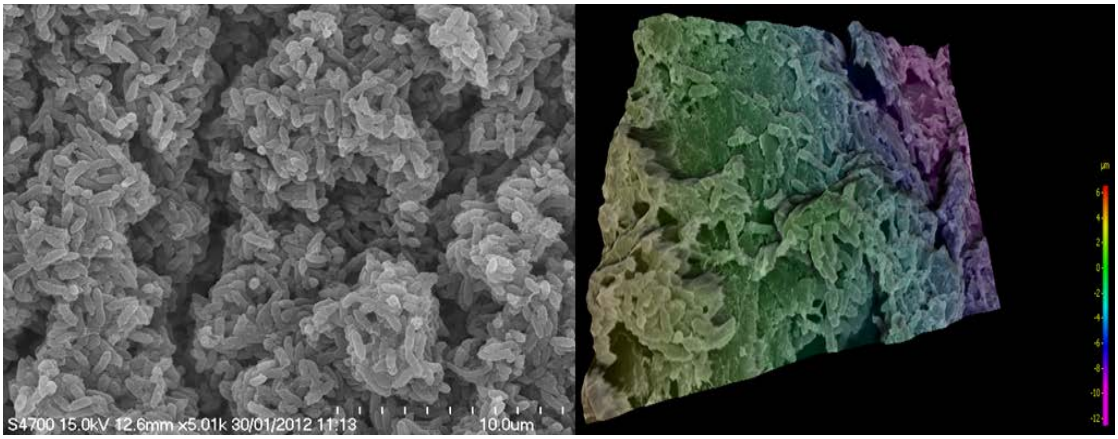

Figure 7.7 SEM images of unmodified electrodes sampled from the reactor after the end of the experiments.

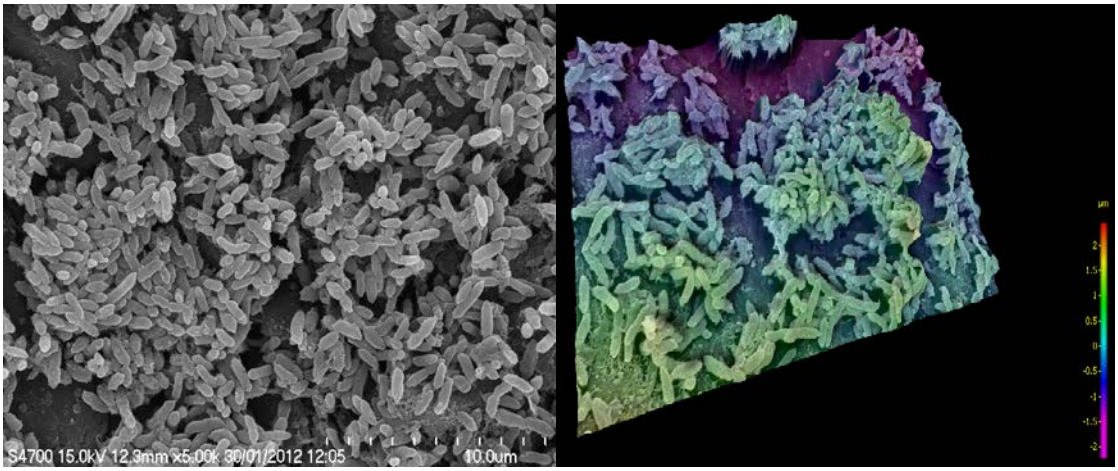

Figure 7.8 SEM images of CH_2COO^- modified electrode sampled from the reactor after the end of the experiments.

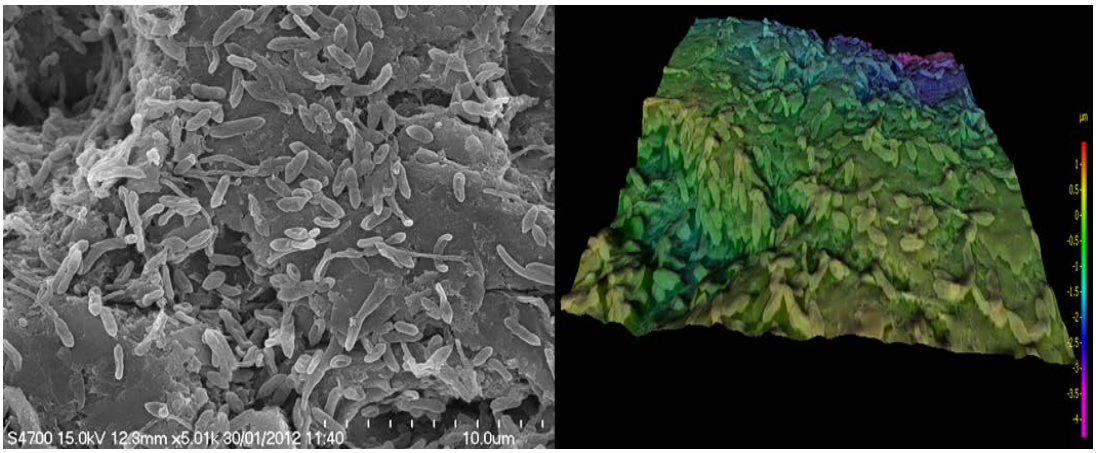

Figure 7.9 SEM images of triphenylphosphonium modified electrode sampled from the reactor after the end of the experiments.

The presence of characteristic 2 µm long rod-shaped bacteria in all the SEM images is comparable to the dimensions reported for GS cells, and the images are similar to those observed by others for biofilms grown on graphite electrodes. It should be noted that the biofilms, as evident from Figure 7.7, 7.8 and 7.9 present higher biofilm density with CH_2COO^- and an unmodified electrode as compared to triphenylphosphonium modified electrode (figure 7.9). Mathu *et al*, 2011 report the controlled modification of graphite anodes with the electrochemical reduction of aryl diazonium salts, and the subsequent effect of the modified electrodes on the power output of microbial fuel cells. They observed the negatively charged groups at the electrode surface (carboxylate) decreased microbial fuel cell power output while the introduction of positively charged groups doubled the power output. They conclude that, the improvement of the microbial fuel cell performance both to electrostatic attraction between the negatively charged bacteria outer environment and the positively charged anode surface and to the local physicochemical compatibility between the electroactive bacteria outer membrane cytochromes and the nature of the modifier. Here we report the preliminary findings of the controlled modification and its subsequent effect on the power output of microbial fuel cells. In this present study opposite trend of results were observed in microbial fuel cell performance. Initial results show that the introduction of chemical functional groups to anodes can enhance initial current density but the response of both modified and unmodified electrode is similar over long-term continuous feeding operation. The use of chemically modified electrodes to modulate reactor start-up and current output of microbial electrochemical cells provides an additional, key, tool to improve the understanding of bacterial attachment, colonization and growth at electrode surfaces (Kumar *et al*., 2013).

7.6 Conclusion

In the present study we report preliminary results on a comparison of biofilm response at positively and negatively charge group modified electrodes to that of un-modified electrodes. The response of both CH_2COO^- modified and unmodified anodes is similar over long-term continuous mode operation but triphenylphosphonium modified electrode shows less current generation throughout the experiment. Advanced research on the details of electron transfer mechanism for

biofilms growth on a different range of functionalized carbon electrodes is important to investigative the extracellular electron transfer mechanism in microbial fuel cell operation.

References

Baranton, S., Bélanger, D. 2005. Electrochemical derivatization of carbon Surface by reduction of *in situ* generated diazonium cations. *The Journal of Physical Chemistry*, **109**(51), 24401-24410.

Bond, D.R., Lovley, D.R. 2003. Electricity production by geobacter sulfurreducens attached to electrodes. *Applied and Environmental Microbiology*, **69**(3), 1548-1555.

Feng, Y., Yang, Q., Wang, X., Logan, B.E. 2010. Treatment of carbon fiber brush anodes for improving power generation in air–cathode microbial fuel cells. *Journal of Power Sources*, **195**(7), 1841-1844.

Katuri, K.P., Enright, A.-M., O'Flaherty, V., Leech, D. 2012a. Microbial analysis of anodic biofilm in a microbial fuel cell using slaughterhouse wastewater. *Bioelectrochemistry*, **87**(0), 164-171.

Katuri, K.P., Kavanagh, P., Rengaraj, S., Leech, D. 2010. Geobacter sulfurreducens biofilms developed under different growth conditions on glassy carbon electrodes: insights using cyclic voltammetry. *Chemical Communications*, **46**(26), 4758-4760.

Katuri, K.P., Rengaraj, S., Kavanagh, P., O'Flaherty, V., Leech, D. 2012b. Charge transport through Geobacter sulfurreducens biofilms grown on graphite rods. *Langmuir*, **28**(20), 7904-7913.

Kong, X., Sun, Y., Yuan, Z., Li, D., Li, L., Li, Y. 2010. Effect of cathode electron-receiver on the performance of microbial fuel cells. *International Journal of Hydrogen Energy*, **35**(13), 7224-7227.

Kumar, R., Leech, D. 2014. Immobilisation of alkylamine-functionalised osmium redox complex on glassy carbon using electrochemical oxidation. *Electrochimica Acta*, 140(0), 209-216.

Marsili, E., Sun, J., Bond, D.R. 2010. Voltammetry and growth physiology of geobacter sulfurreducens biofilms as a function of growth stage and imposed electrode potential. *Electroanalysis*, **22**(7-8), 865-874.

Picot, M., Lapinsonnière, L., Rothballer, M., Barrière, F. Graphite anode surface modification with controlled reduction of specific aryl diazonium salts for improved microbial fuel cells power output. *Biosensors and Bioelectronics.* **28**(1), 181-188.

Saito, T., Mehanna, M., Wang, X., Cusick, R.D., Feng, Y., Hickner, M.A., Logan, B.E. 2011. Effect of nitrogen addition on the performance of microbial fuel cell anodes. *Bioresource Technology,* **102**(1), 395-398.

Saito, T., Mehanna, M., Wang, X., Cusick, R.D., Feng, Y., Hickner, M.A., Logan, B.E. 2011. Effect of nitrogen addition on the performance of microbial fuel cell anodes. *Bioresource Technology,* **102**(1), 395-398.

Wang, X., Feng, Y., Wang, H., Qu, Y., Yu, Y., Ren, N., Li, N., Wang, E., Lee, H., Logan, B.E. 2009. Bioaugmentation for electricity generation from corn stover biomass using microbial fuel cells. *Environmental Science and Technology*, **43**(15), 6088-6093.

Zhu, F., Wang, W., Zhang, X., Tao, G. 2011. Electricity generation in a membrane-less microbial fuel cell with down-flow feeding onto the cathode. *Bioresource Technology,* **102**(15), 7324-7328.

Chapter 8

Conclusions and future scope of the studies

Significant conclusions from the experimental results are summarized in this chapter. The future scopes of the studies are listed.

8.1 Conclusions

Comparison of performance of an earthen plate and Nafion as membrane separators in dual chamber microbial fuel cells

This study demonstrated by comparison to Nafion, that an earthen plate membrane may provide a low-cost, more durable, alternative to Nafion in continuous flow MFCs but Nafion membrane as separator showed slightly better performance in terms of organic matter removal and electricity generation than the MFC based on earthen plate membrane separators. The 40 cm^2 Nafion 117 membranes used in the present experiment costs approximately €30.0 whilst the same area of the earthen plate costs approximately €0.025, making it 99 % cheaper. Utilization of such low cost separators may contribute to further development of economical MFC technology.

Charge transport in films of Geobacter sulfurreducens on graphite electrodes as a function of film thickness

In this study we report, the comparison of biofilm thickness as a function of time to the voltammetric responses in the presence and absence of acetate as electron donor. Here we are probing the charge transport in films of *Geobacter*

sulfurreducens on graphite electrodes as a function of film thickness. We observed that Acetate oxidation current generated from biofilms of an electroactive bacteria (EAB), *Geobacter sulfurreducens*, on graphite electrodes as a function of time does not correlate with film thickness. The thicker biofilms, of 50 ± 9 μm, display higher charge transport diffusion co-efficient than that in thinner films, as increased film porosity of these films improves ion transport required to maintain electro-neutrality upon electrolysis.

Monitoring Geobacter sulfurreducens biofilm formation and response using electrochemistry coupled to a quartz crystal microbalance

This study is focused on the effect of initial electro active bacterial attachment and deposition using a quartz crystal microbalance. In this present study we report the combined effect of *Geobacter sulfurreducens* adhesion to the QCM gold sensor and electricity generation. A combination of cyclic voltammetry and QCM measurements permitted the calculation of the mass change to be expected from the quantity of charge passed, and this was compared with the observed mass change (Δm). From this study we observed the viscoelastic properties of the biofilm increased as function of time which indicates better connectivity between the cell and the electrode surface leading to higher currents.

Quantitative proteomic analysis of Geobacter sulfurreducens grown with different electron acceptor

In this present study we report the different protein expression of *Geobacter sulfurreducens* grown on carbon cloth electrode and pure culture. A total of 1318 proteins were identified with a minimum of 99 % confidence in both biofilm and planktonic *G. sulfurreducens* samples. Overall 77 proteins were found to be common, amongst which 40 and 37 were expressed at higher and reduced levels in the biofilm samples. Data show that 90 % proteins are active in catalytic activity and 10 % proteins are active in transporter activity in attached biofilms. This was confirming by the proteomics results which showed several outer membrane proteins were expressed at higher levels in solid electron acceptor, playing an important role for high current density.

Bioelectricity generation from dairy wastewaters in microbial fuel cells

The study demonstrated effective treatment of synthetic and real dairy wastewater in microbial fuel cell, simultaneously generating bioelectricity**.** The MFCs were operated at sub-ambient temperatures (15 ^{o}C) achieved 65 % COD removal efficiency and the MFCs operated at controlled 30-32 ^{O}C achieved 88 % COD removal efficiency. Although, MFCs are reported to be successful for wastewater treatment and electricity recovery, many aspects need further investigation.

Modified electrode for anode in microbial fuel cell

Here we report the preliminary findings of the controlled modification of graphite anodes with the electrochemical reduction of aryl diazonium salts, and its subsequent effect on the power output of microbial fuel cells.

8.2 Synopsis

Microbial fuel cell (MFC) is a promising technology for electricity generation along with sustainable wastewater treatment. In MFC, the microorganisms act as catalyst which converts the chemical energy stored in the organic matter directly into electricity. The performance of MFC is affected by several factors, such as electrode material (Park and Zeikus, 2003), electrode surface area (Oh and Logan, 2006), reactor configuration, temperature (Liu *et al*., 2005, Catal *et al*., 2011)), proton exchange membrane (PEM) (Min *et al*., 2005), and pH (Gil *et al*., 2003). This thesis focuses on studies of microbial fuel cells (MFC). MFC utilize electro active bacteria to oxidize organic substrates degrading wastes and generating electricity. Microbial fuel cell studies dealt with the electrochemical characterization of model organism *Geobacter sulfurreducens* biofilms on electrodes that are induced to grow under fixed applied potential. Application of microbial fuel cell for wastewater treatment could be an attractive alternative to reduce the cost of treatment with simultaneous generation of electricity. This novel technology can be operated at temperatures below 20 °C and at low substrate concentration levels conditions where performance of conventional anaerobic treatment process is compromised. Proton exchange membrane influences the power output of the MFC. Nafion is the most popular PEM

because of its highly selective permeability of protons, but is expensive (Liu and Logan, 2004) and also subjected to fouling in long run process. Ultrex (Rabaey *et al*., 2004) and salt bridge (Min *et al*., 2005) have been used as alternatives to Nafion, but with low power production. Replacement of membrane with alternative cheaper material, ensuring similar or better performance, could improve the economic feasibility of the process by reducing not only the capital investment but also the operational cost for the membrane maintenance. The present study demonstrated the comparison of Nafion, to an earthen plate membrane which may provide a low-cost, more durable, alternative to Nafion in continuous flow MFCs.

Harnessing and understanding the mechanisms of growth and activity of biofilms of electroactive bacteria (EAB) on solid electrodes is of increasing interest, for application to microbial fuel and electrolysis cells. Microbial electrochemical cell technology can be used to generate electricity and/or higher value chemicals from organic wastes. In MFCs, bacterial biofilm transfer the electron to solid electrode, which may involve at least one of the following mechanisms (i) electron shuttling mediating molecules (Marsili *et al*., 2008) (ii) redox active membrane-bound proteins (cytochromes) (Busalmen *et al*., 2008) (iii) via conductive nanowires (pili) (Gorby *et al*., 2006). The capability of biofilms of electroactive bacteria to transfer electrons to solid anodes is a key feature of this emerging technology, yet the electron transfer mechanism is not hitherto fully characterized. Here we report electroactive biofilm production on graphite rod electrodes under continuous mode operation and provide an insight into the factors that may affect current generation by microbial fuel cell anodes.

Electrode active bacteria *Geobacter sulfurreducens* biofilms are widely used as a model electrochemical system to gain a mechanical understanding of electrons transfer to the extracellular space within a biofilm. Researchers have used various combined electrochemical techniques to study electrochemically active bacteria (Babauta *et al*, 2014). The quartz crystal microbalance with dissipation (QCM-D) monitoring is an attractive technique for monitoring cell adhesion processes. The QCM technology can be used to measure label-free biomolecules and macrostructures such as antibodies, proteins, carbohydrates, cells, DNA and bacteria. Recently this technology has been used to understand the electron transfer mechanism in microbial fuel cell system. The main aim of this study is to get an

insight into the process of initial bacterial adhesion to the electrode surface and to study the viscoelastic properties of *Geobacter sulfurreducens* bacteria-surface interaction.

Exoelectrogens have the ability to generate electricity in mediator-less microbial fuel cells (MFCs) through extracellular electron transfer to the anode (Pereira-Medrano *et al*, 2012). Earlier studies have proposed different mechanisms of direct electron transfer, typically involving at least a series of periplasmic and outer membrane complexes in these species (Lovley *et al.,* 1008). It has also been suggested that electrically conductive pilus-like appendages called nanowires can facilitate electron transport between different microorganisms in electroactive biofilms (Gorby *et al*., 2006). Although recent advances have been made in the understanding of the electron transfer mechanisms of electroactive bacteria but proper mechanisms are poorly understood. Quantitative proteomics analysis is still to play a major role in the characterization of the extracellular electron transfer pathways (Medrano *et al*, 2012). The proteomics analysis of *Geobacter sulfurreducens* grown in carbon cloth electrode versus planktonic cells revealed different protein expression. The availability of terminal electron acceptor effects the functional protein expression. The work describe here aim to understand differential protein expression under varied electron acceptor conditions.

MFCs have been operated successfully on a variety of substrates, from pure chemicals to complex wastes (Liu *et al*., 2004). Previous studies have proved that the energy-efficient treatment of wastewater is one of the most promising applications of MFCs. Generally, COD removal efficiency greater than 60 % is reported for MFCs, and most of the MFC configurations are reported to be capable to give COD removal efficiency ranging from 80 to 95 % while treating different wastewaters (Duteanu *et al.*, 2010). This efficiency is comparable with the high rate anaerobic processes. In present study, the feasibility of using dairy wastewater as a substrate to the MFC for electricity generation with simultaneous accomplishment of wastewater treatment has been investigated. Higher COD removal efficiency and power production observed under all operating temperatures in this study demonstrate utility of MFCs as wastewater treatment process, simultaneously harvesting direct electricity for onsite applications.

This study also provides preliminary examination for modifying the carbon surface chemistry and the effect of altering the surface chemistry on electroactive biofilm adhesion, growth and electrical power production. Mathu *et al*, 2011 report the controlled modification of graphite anodes with the electrochemical reduction of aryl diazonium salts, and the subsequent effect of the modified electrodes on the power output of microbial fuel cells. In present study we observed both modified and unmodified anodes are similar over long-term continuous mode operation. Advanced research on the details of electron transfer mechanism for biofilms growth on a different range of functionalized carbon electrodes is important to investigative the extracellular electron transfer mechanism in microbial fuel cell operation.

8.3 Future scope of the studies

Microbial fuel cells (MFCs) are one of the emerging technologies which treat wastewater and directly convert the biochemical energy stored in organic matter into electricity, making its operation sustainable. Although, MFCs are reported to be successful for wastewater treatment and electricity recovery, many aspects need further investigations. Continuous development for MFCs and bio-electrochemical research will be both fundamental and applied. Based on the findings of the present investigations, following suggestions are made for future studies.

The present study demonstrates the practicality of using earthen plate as an alternative separator in MFCs removing the use of expensive proton exchange membrane, making scope for construction of cost effective MFCs. The basic properties of the earthen plate membrane have been investigated. But complete specification of the material is to be determined before commercialization. In depth study of the material properties of the earthenware is required to understand the ion exchange mechanism. Proper modification in this material can be made in order to increase proton permeability and decrease oxygen diffusion.

From a fundamental perspective, using QCM technology, *in situ* changes of mass with combination of electrochemical response can be applied to evaluate the effects of the electrode modification, growth, and environmental factors which are crucial for the establishment of bacterial biofilm in microbial fuel cell technology.

From a fundamental aspect using proteomics to see the concentration of proteins being expressed during various stages of biofilm formation would be important. These studies may be able to give better understanding of initial biofilm colonization during anode respiration including the functions of these proteins. These studies could provide a deeper insight into the rate of colonization and the rate of biofilm growth on solid electrodes.

One in every three protein is requiring a metal cofactor, usually a transition metal, e.g. Cu, Fe, or Zn and control up and down-regulation of protein expression in cells (Mounicou *et al*., 2009). A systematic approach to the study of metal content and use within organisms is very important. A protein must bind with a metal for its function like catalytic activity or implication in electron-transfer reaction of redox-active metal ions. The understanding of functional connections of metal ions and their species with genes, proteins and other biomolecules within organisms is dependent on the information of the total of metal present in a cell. A systematic approach to the study of metal content in electro active biofilm is very important to understand the proper electron transfer mechanism in microbial fuel cell.

At present, the power densities of MFCs are too low for most envisioned applications and its fabrication cost is very high for commercial applications. Graphite was used as terminal electron acceptor in most of the MFCs. However due to slow kinetics of the oxygen reduction at plain carbon, and the resulting large over-potential, the use of such cathodes may limit the use of this material (Logan *et al*., 2006). Thus, there is need to improve electrode materials for better performance of the microbial fuel cell. Electrode material significantly affect the MFCs power output.

Life cycle assessment of a scaled up MFC needs to be done and performance, cost and environmental impacts should be compared with established wastewater treatment technologies. For example Foley *et al* compared the life cycle assessments for a high-rate anaerobic wastewater treatment plant, a MFC wastewater treatment plant and a MEC wastewater treatment plant producing dilute hydrogen peroxide. They report that a microbial fuel cell does not provide a significant environmental benefit relative to the conventional anaerobic treatment option. However a microbial

electrolysis cell provides significant environmental benefits through the displacement of chemical production by conventional method (Foley *et al.*, 2010).

References

Babauta, J.T., Beasley, C.A., Beyenal, H. 2014. Investigation of electron transfer by Geobacter sulfurreducens biofilms by using an electrochemical quartz crystal microbalance. *ChemElectroChem*, **1**(11), 2007-2016.

Busalmen, J.P., Esteve-Núñez, A., Berná, A., Feliu, J.M. 2008. C-type cytochromes wire electricity-producing bacteria to electrodes. *Angewandte Chemie - International Edition*, **47**(26), 4874-4877.

Catal, T., Kavanagh, P., O'Flaherty, V., Leech, D. 2011. Generation of electricity in microbial fuel cells at sub-ambient temperatures. *Journal of Power Sources*, ***196***(5), 2676-2681.

Duteanu N.M., Ghangrekar M.M., Erable B., Scott K. Microbial fuel cells – An option for wastewater treatment. 2010. *Environmental engineering and management journal*, 9, 1069-1087.

Foley, J.M., Rozendal, R.A., Hertle, C.K., Lant, P.A., Rabaey, K. 2010. Life cycle assessment of high-rate anaerobic treatment, microbial fuel cells, and microbial electrolysis eells. *Environmental science and technology*, 44(9), 3629-3637.

Gil, G.-C., Chang, I.-S., Kim, B.H., Kim, M., Jang, J.-K., Park, H.S., Kim, H.J. 2003. Operational parameters affecting the performannce of a mediator-less microbial fuel cell. *Biosensors and Bioelectronics*, **18**(4), 327-334.

Gorby, Y.A., Yanina, S., McLean, J.S., Rosso, K.M., Moyles, D., Dohnalkova, A., Beveridge, T.J., Chang, I.S., Kim, B.H., Kim, K.S., Culley, D.E., Reed, S.B., Romine, M.F., Saffarini, D.A., Hill, E.A., Shi, L., Elias, D.A., Kennedy, D.W., Pinchuk, G., Watanabe, K., Ishii, S., Logan, B., Nealson, K.H., Fredrickson, J.K. 2006. Electrically conductive bacterial nanowires produced by Shewanella oneidensis strain MR-1 and other microorganisms. *Proceedings of the National Academy of Sciences of the United States of America*, **103**(30), 11358-11363.

Liu, H., Logan, B.E. 2004. Electricity generation using an air-cathode single chamber microbial fuel cell in the presence and absence of a proton exchange membrane. *Environmental Science and Technology*, **38**(14), 4040-4046.

Liu, H., Cheng, S., Logan, B.E. 2005. Power generation in fed-batch microbial fuel cells as a function of ionic strength, temperature, and reactor configuration. Environmental Science and Technology, 39(14), 5488-5493.

Logan, B.E., Hamelers, B., Rozendal, R., Schröder, U., Keller, J., Freguia, S., Aelterman, P., Verstraete, W., Rabaey, K. 2006. Microbial fuel cells: methodology and technology. *Environmental science and technology*, 40(17), 5181-5192.

Lovley, D.R. 2008. The microbe electric: conversion of organic matter to electricity. *Current Opinion in Biotechnology*, **19**(6), 564-571.

Marsili, E., Baron, D.B., Shikhare, I.D., Coursolle, D., Gralnick, J.A., Bond, D.R. 2008. Shewanella secretes flavins that mediate extracellular electron transfer. *Proceedings of the National Academy of Sciences*, **105**(10), 3968-3973.

Min, B., Cheng, S., Logan, B.E. 2005. Electricity generation using membrane and salt bridge microbial fuel cells. *Water Research*, **39**(9), 1675-1686.

Mounicou, S., Szpunar, J., Lobinski, R. 2009. Metallomics: the concept and methodology. *Chemical Society Reviews*, 38(4), 1119-1138.

Oh, S.E., Logan, B.E. 2006. Proton exchange membrane and electrode surface areas as factors that affect power generation in microbial fuel cells. *Applied Microbiology and Biotechnology*, **70**(2), 162-169.

Park, D.H., Zeikus, J.G. 2003. Improved fuel cell and electrode designs for producing electricity from microbial degradation. *Biotechnology and Bioengineering*, **81**(3), 348-355.

Pereira-Medrano, A.G., Knighton, M., Fowler, G.J.S., Ler, Z.Y., Pham, T.K., Ow, S.Y., Free, A., Ward, B., Wright, P.C. 2013. Quantitative proteomic analysis of the exoelectrogenic bacterium Arcobacter butzleri ED-1 reveals increased abundance of a flagellin protein under anaerobic growth on an insoluble electrode. *Journal of Proteomics*, **78**(0), 197-210.

Picot, M., Lapinsonnière, L., Rothballer, M., Barrière, F. 2011. Graphite anode surface modification with controlled reduction of specific aryl diazonium salts for improved microbial fuel cells power output. *Biosensors and Bioelectronics*, **28**(1), 181-188.